

Chiral Perturbation Theory and Baryon Properties

Véronique Bernard

Lab. de Physique Théorique, Université Louis Pasteur, F67084, Strasbourg, France
E-mail: bernard@lpt6.u-strasbg.fr

February 8, 2022

Abstract

Theoretical as well as experimental progress has been made in the last decade in describing the properties of baryons. In this review I will mostly report on the theoretical issues. Two non-perturbative methods are privileged frameworks for studying these properties in the low energy domain: chiral perturbation theory, the effective field theory of the Standard Model at energies below 1 GeV and lattice QCD. I will mainly concentrate here on the first one but I will also discuss the complementarity of the two methods. Chiral extrapolations for lattice simulations of some nucleon properties will be investigated. I will then concentrate on processes involving at most two nucleons, describing for example pion-nucleon and pion-deuteron scattering, pion photo- and electroproduction off the nucleon and the deuteron and doubly virtual Compton scattering. Three flavor calculations will also be reviewed.

Contents

1	Introduction	2
2	Effective Field Theory	3
2.1	<i>Chiral Symmetry</i>	4
2.2	<i>Effective Chiral Meson Lagrangian</i>	4
2.2.1	Power counting	5
2.3	<i>Baryon Chiral Perturbation Theory</i>	7
2.3.1	Lagrangian	7
2.3.2	Low-energy constants	8
2.3.3	HBCHPT	13
2.3.4	Infrared regularization	15
2.3.5	Other regularizations	17
2.3.6	Summary	19
2.4	<i>Effective theory with Δ's</i>	20
2.5	<i>Lattice QCD and CHPT</i>	22

3	Chiral extrapolations	24
3.1	<i>Nucleon mass</i>	25
3.2	<i>axial-vector coupling</i>	27
3.3	<i>magnetic moment</i>	30
3.4	<i>Δ and Roper masses</i>	31
3.4.1	infinite volume limit	31
3.4.2	finite volume	32
4	Pion-nucleon and Pion-deuteron scattering	33
4.1	<i>πN scattering</i>	33
4.1.1	isospin symmetric case	34
4.1.2	isospin violating case	37
4.2	<i>πd scattering</i>	41
5	Electromagnetic properties	43
5.1	<i>Form Factors</i>	43
5.2	<i>Compton Scattering</i>	44
5.2.1	Real and Virtual Compton Scattering	44
5.2.2	V ² CS: spin structure functions and sum rules	46
5.3	<i>Photo-and Electroproduction</i>	48
5.3.1	off the nucleon	48
5.3.2	off deuterium	51
5.4	<i>Two-pion production</i>	52
6	Axial properties	53
7	Three flavors	54
7.1	<i>Chiral dynamics with strange quarks: General remarks</i>	54
7.2	<i>Baryon masses and Chiral Extrapolation</i>	56
7.3	<i>Baryon Electromagnetic Properties</i>	57
7.4	<i>Strange form factors of the nucleon</i>	58
7.5	<i>Kaon-Nucleon scattering</i>	60
7.6	<i>Kaon-Photoproduction</i>	61
7.7	<i>Proposals for improved chiral expansion</i>	61
7.7.1	Heavy kaon CHPT	62
7.7.2	long distance regularization	62
8	Conclusion	63

1 Introduction

Quantum chromodynamics (QCD) has emerged at the end of the sixties as the theory of strong interaction, for a brief history see [1]. At high energies it is perturbative, i.e. observables can be expanded in terms of the strong coupling constant α_s . However the theory becomes highly non-perturbative at low energies since α_s becomes large. At those low energies a central role is played by the spontaneously and explicitly broken chiral symmetry. Taking advantage of that one can formulate an effective field theory equivalent to QCD at low energy. This is the model-independent framework, Chiral Perturbation Theory (CHPT), which will be the topic of this review. Another model-independent way to solve QCD is the lattice approach. As we will see lots of progress has been made in that framework, however,

most calculations involve pion masses which are still far from their physical value. It is also limited in the lattice spacing and in the volume used in the calculations due to computational costs. There has thus been in the last decade a whole development of chiral extrapolations within CHPT as well as techniques to try to get a handle on the systematic errors inherent to the lattice calculations. There is thus nowadays a nice interplay between lattice and CHPT which will be reported here.

Testing QCD in the low energy domain has been and still is the subject of lots of work from the theoretical as well as experimental side. I will report here on some of these in the framework of CHPT restricting myself to the case when nucleons are present and especially to processes with one nucleon in the initial and mostly one nucleon in the final states. The ideas underlying CHPT have been generalized to the few nucleon sector where one has to deal with a nonperturbative problem. I will touch upon it while discussing processes involving two bound nucleons, namely the deuteron. For more details on chiral EFTs in the few-nucleon sector see [2].

In Section 2 after briefly reviewing what is an effective field theory and defining chiral symmetry, I will give some general properties of CHPT. I will then concentrate on Baryon Chiral Perturbation theory without and with explicit Δ degrees of freedom, Sections 2.3 and 2.4 respectively, discussing different regularizations of the theory. I will then show the complementarity of the two frameworks, lattice QCD and CHPT. In Section 3 I will report on chiral extrapolations of some baryon properties. In the two next sections I will discuss a few applications within $SU(2)$, namely πN and πd scattering and different electromagnetic properties of the nucleon. The last section will be devoted to the case of three flavors.

Baryon CHPT is a very active field. A great amount of studies have been done with and without the Δ degrees of freedom. I will unfortunately not be able to review all of what has been done and I apologize to those whose work I did not include.

2 Effective Field Theory

Many reviews and lectures concerning effective field theories and ChPT are at present available [3]- [14]. I will thus be rather brief here and refer the interested reader to these reviews for more details.

Effective field theories (EFTs) date back to the 70's and have become a popular tool ever since. Wilson, Fisher and Kadanoff first studied critical phenomena in condensed matter systems within an EFT. These were then developed in this context and enlarged to other fields. EFTs are powerful techniques when the relevant degrees of freedom depend on the typical energy of the problem. For energies beyond a certain scale Λ the fundamental theory is applicable while for energies below it can be more practical to use an effective theory. One has to keep in mind that a fundamental theory can in turn become an effective theory of some other fundamental theory at higher energies. There are different types of EFTs depending on the structure of the transition between the fundamental and the effective level.

- decoupling

In that case one integrates out the heavy degrees of freedom (heavy with respect to Λ). One is left with the light degrees of freedom described by a Lagrangian which contains a renormalizable part and non-renormalizable couplings suppressed by inverse powers of Λ . The coupling constants of the low-energy EFT can be obtained by perturbative matching to the underlying theory. The best known example is the Standard Model.

- non-decoupling

In that case the relevant degrees of freedom are different from the one of the fundamental theory due to a phase transition. This is the type we are interested in here, the phase transition being, as we will see, the spontaneous breakdown of chiral symmetry. Renormalizability is not a meaningful concept anymore and in general EFTs in this category are nonrenormalizable. Thus an infinite numbers of

counterterms have to be added to make it finite. However in an EFT where the range of applicability is below the scale Λ , the number of counterterms needed at each level of the expansion is finite though at increasing expansion powers, it increases drastically.

2.1 Chiral Symmetry

In the Standard Model the degrees of freedom are the gluons described by the non-abelian field strength tensor $G_{\mu\nu}$ and N_f flavors of quarks q . The QCD Lagrangian is given by:

$$\mathcal{L}_{QCD} = -\frac{1}{4}G_{\mu\nu}^a G^{\mu\nu a} + \sum_{N_f} \bar{q}(i\gamma^\mu D_\mu - m_q)q . \quad (1)$$

In what follows we will consider only the light quark sector (u, d, s) for which the masses m_q are much smaller than the hadronic scale of the order of 1 GeV. Typically the up and down mass are a few MeV and the strange mass is ~ 100 MeV. Therefore \mathcal{L}_{QCD} can very well be approximated by a Lagrangian \mathcal{L}_{QCD}^0 with no mass term. In that case left and right handed quarks live their own lives and the symmetry group of the Lagrangian, apart from the discrete symmetries of parity, charge conjugation and time reversal, is $SU(N_f)_L \times SU(N_f)_R \times U(1)_V$. $U(1)_V$ generates conserved baryon number while the remaining group $SU(N_f)_L \times SU(N_f)_R$ is the chiral symmetry group G we are mostly interested in this review. We will not discuss here the chiral anomalies and CP violation. A classical theory can be realized in quantum field theory in two different ways, the so-called Wigner-Weyl mode and the Nambu-Goldstone one, depending on how the vacuum responds to the symmetry transformation. In fact there are indications from experiment and theory that chiral symmetry is spontaneously broken in nature. Chiral symmetry is a symmetry of \mathcal{L}_{QCD}^0 but not of the vacuum which is invariant only under $SU(3)_V \times U(1)_V$, where $SU(3)_V$ is the subgroup of vector rotations. Evidences are for example the non-existence of degenerate parity doublets in the hadron spectrum, the existence of the triplet of unnaturally light pseudoscalar particles and the very different behaviour of the correlators of axial and vector currents. It is also supported by lattice simulations (for a recent study, see [15] and references therein). To a spontaneously broken symmetry corresponds non-vanishing order parameters and the appearance of Goldstone bosons. I will come back to that below. A typical model which describes spontaneous symmetry breaking is the linear sigma-model. However it has a few drawbacks. First it involves a σ particle, the chiral partner of the pion which is not observed. Second its renormalizability requires specific relations between various couplings which are not in agreement with experiment [16].

As we have seen the masses are in fact not exactly zero. The quark mass term leads to the so-called explicit chiral symmetry breaking: the vector and axial-vector currents are no longer conserved. In the limit of equal quark masses, QCD possesses an additional $SU(3)$ flavor symmetry. Restricting to the up and down quarks this is the well known isospin symmetry. However this symmetry is again broken, slightly in $SU(2)$ and more strongly within $SU(3)$. The difference in the quark masses as well as electromagnetic effects explains for example the splittings in mass for the hadrons appearing in the same multiplet. In the following I will mostly restrict to the equal mass case. Isospin violations will be discussed in Section 4.1.2.

2.2 Effective Chiral Meson Lagrangian

Chiral symmetry and its spontaneous symmetry breaking thus leads to:

- the existence of $N_f^2 - 1$ Goldstone particles, massless excitation of the vacuum corresponding to the $N_f^2 - 1$ axial generators of the chiral group as stated by the Goldstone theorem [17]: these are identified with the three (eight) lightest hadronic states, the pseudoscalar mesons π in $SU(2)$ (π, K, η in $SU(3)$).

- the Goldstone theorem also predicts that the interaction between these particles is weak. Thus a Lagrangian describing them must be of the derivative type. This allows for an *expansion in the external momentum* p as long as one stays below a certain scale. This scale corresponds in fact to the occurrence of other hadrons in the spectrum, $\Lambda_\chi \sim 1$ GeV, usually called the scale of chiral symmetry breaking.
- the quark masses being small one does not expect much changes while going from \mathcal{L}_{QCD}^0 to \mathcal{L}_{QCD} . An *expansion in m_q* around the chiral limit can be performed again below the scale Λ_χ . These small masses generate the physical values of the pseudoscalar mesons, typically to leading order in these quark masses one has:

$$M_\pi^2 = 2Bm_q \quad (2)$$

where the constant of proportionality B will be discussed below.

These features are best realized writing an effective theory in terms of the Goldstone bosons which will be valid up to the scale Λ_χ . This effective field theory is known as *Chiral Perturbation Theory (CHPT)* and has been first worked out by [18] and developed by [16, 19]. The idea underlying effective field theories is to write down the *most general* Lagrangian in terms of the observed asymptotic fields in agreement with the symmetries of the system:

$$\mathcal{L}_{QCD}[\bar{q}, q, G_{\mu\nu}] \rightarrow \mathcal{L}_{\text{eff}}[U, \partial U, \dots \mathcal{M}, v_\mu, a_\mu] . \quad (3)$$

In this equation U is a unitary matrix field representing the Goldstone bosons and transforming under a chiral transformation as $U \xrightarrow{G} g_R U g_L^{-1}$, $(g_R, g_L) \in G$. In order to be able to generate Green functions of quark currents, locally chiral invariant external fields, that is non-propagating objects, are introduced. \mathcal{M} which contains scalar and pseudoscalar fields enables one to describe the mass matrix while v_μ , a_μ , vector and axial fields, respectively, allow to describe the couplings to external photons and W bosons. The equivalence between the two Lagrangians has been shown in [20, 21].

The heavy fields not included in the theory can be seen through virtual effects included via low-energy constants (LECs) connected to the light fields, i.e the pseudo-Goldstone bosons. Indeed, the decoupling theorem [22] states that all effects from heavy fields will reveal themselves through renormalization of coupling constants.

2.2.1 Power counting

CHPT is thus a two-fold expansion in external momentum and quark masses and can be written as:

$$\mathcal{L}_{\text{eff}} = \sum_{i,j} \mathcal{L}_{i,j} , \quad \mathcal{L}_{i,j} = \mathcal{O}(p^i m_q^j) . \quad (4)$$

It is based on chiral countings rules: the field U counts as a quantity $\mathcal{O}(1)$, $\partial_\mu U$, v_μ and a_μ are thus $\mathcal{O}(p)$ (v_μ and a_μ appear in the covariant derivative at the same level as ∂_μ). In order to relate the two expansions one assigns a chiral counting to the quark masses through Eq. (2) where M_π^2 should be counted as a quantity of order p^2 .

As we have seen the spontaneous breaking of a symmetry is also related to the existence of non-vanishing order parameters. The simplest one is the quark condensate connecting the left and right handed quarks. It also plays a special role being related to the density of small eigenvalues of the QCD Dirac operator [23–25]. The question is: how big is the value of this condensate? The notion of big is related to another order parameter which is the pion decay constant F which will be defined below and can be expressed as an integral:

$$F^2 = \frac{1}{6} \int d^4x \langle 0 | \bar{u}_L(x) \gamma_\mu d_L(x) \bar{d}_R(0) \gamma^\mu u_R(0) | 0 \rangle . \quad (5)$$

There exists two scenarios the so-called standard one and Generalized CHPT [26] depending on the answer to that question. The standard scenario assumes that this condensate is large meaning that the quantity $B/F \equiv -\langle 0|\bar{q}q|0\rangle/F^3$ is much bigger than one while the Generalized one allows for a value comparable or even much smaller than one. These two scenarios lead to a different chiral counting, in the first case B is $\mathcal{O}(1)$ and thus m_q is $\mathcal{O}(p^2)$, see Eq. (2), while in the second case B is $\mathcal{O}(p)$ and thus m_q is also $\mathcal{O}(p)$. One thus has:

$$\mathcal{L}_{eff}^{std} = \sum_{i+2j=d} \mathcal{L}_{ij}, \quad \mathcal{L}_{eff}^{gchpt} = \sum_{i+j+k=d} B^k \mathcal{L}_{ij}. \quad (6)$$

How can one decide between the two cases?

- the Gell-Mann Okubo relation which relates the π , K and η masses which is well verified experimentally and holds naturally in standard CHPT is modified in Generalized CHPT.
- lattice simulations give values for $-\langle 0|\bar{q}q|0\rangle^{1/3} \sim 200 - 370$ MeV in agreement with standard CHPT, for a summary of recent results see [15].
- QCD like theories are expected to undergo a number of phase transitions at zero temperature upon varying N_f at fixed number of colours. It has been discussed in [27] that $N_f = 3$ could be not far from a chiral phase transition suggesting that in $SU(3)$ the quark condensate might be much smaller than in $SU(2)$. The different behaviour between the $SU(2)$ and the $SU(3)$ case could come from large vacuum fluctuations of strange $q\bar{q}$ pairs related to a large OZI-rule violation in the scalar channel [28]. I will come back to this in more detail in Section 7.1. In this context it has been pointed out [29] that it might not be necessary to introduce a different counting when the condensate is small, a non perturbative resummation of the vacuum fluctuations encoded in some LECs might in fact be sufficient. This is called Resummed Chiral Perturbation Theory.

At first sight the standard picture seems to be privileged at least within $SU(2)$. However one has certainly to await for better lattice results as well as more precise experimental results to really settle this issue definitively. For example the $\pi\pi$ scattering lengths are actually under debate since the preliminary analysis of K_{e4} data from NA48/2 [30] seems to be in conflict with the very precise determination [31,32] combining CHPT and dispersion relations.

In the rest of the review I will only discuss the standard case. Note that there has been only one attempt to apply the Generalized picture to the nucleons [33].

At tree level one can reconstruct the current algebra predictions of the 1960's as well as low energy theorems. With a hermitian Lagrangian tree amplitudes are necessarily real. Unitarity and analyticity however lead to complex amplitudes. A systematic low energy expansion thus requires a loop expansion. To do this in a consistent fashion one has to introduce a *counting scheme*. In fact it has been shown by Weinberg in the meson sector [18] that there is a one to one correspondence between loop and chiral order, that is diagrams with L meson loops are suppressed by powers of $(p^2)^L$. The power counting formula of Weinberg orders the various contributions to any S-matrix element for the pion interaction according to the chiral dimension D ,

$$D = 2 + \sum_d N_d(d-2) + 2L \quad (7)$$

with N_d the number of vertices with dimension d (derivatives and/or pion mass insertions). Chiral symmetry gives a lower bound for D , $D \geq 2$. The experimental precision reached in the meson sector makes it necessary to include corrections of $\mathcal{O}(p^6)$, for a review on two-loop calculations see [34]. At that order one has, according to the formula to include tree graphs ($L=0$) from $\mathcal{L}_{\pi\pi}^{(2,4,6)}$, one loop graphs ($L=1$) with insertion from $\mathcal{L}_{\pi\pi}^{(2,4)}$ and finally two loop graphs ($L=2$) with insertion from $\mathcal{L}_{\pi\pi}^{(2)}$.

2.3 Baryon Chiral Perturbation Theory

I will now extend the discussion to include matter fields. In this section I will concentrate on nucleons and pions coupled to external sources. The Δ degree of freedom will be discussed in Section 2.4. Couplings to photons will be given in Section 4.1.2. As we will see some problems arise concerning the power counting when matter fields are introduced. In order to solve these, different regularization have been introduced which will be discussed in Sections 2.3.4, 2.3.5.

2.3.1 Lagrangian

The minimal relativistic effective πN Lagrangian [35] up to $\mathcal{O}(p^4)$ is given below. For the heavy baryon case and the relation between the LECs in the two framework see that reference. Only the terms which will be needed in the review are shown explicitly:

$$\begin{aligned}
\mathcal{L}_{\text{eff}} &= \mathcal{L}_{\pi N}^{(1)} + \mathcal{L}_{\pi N}^{(2)} + \mathcal{L}_{\pi N}^{(3)} + \mathcal{L}_{\pi N}^{(4)} + \mathcal{L}_{\pi N}^{(5)} + \mathcal{L}_{\pi N}^{(6)} + \mathcal{L}_{\pi\pi}^{(2)} + \mathcal{L}_{\pi\pi}^{(4)} + \dots, \\
\mathcal{L}_{\pi N}^{(1)} &= \bar{\psi}(i \not{D} - m_0 + \frac{1}{2}g_0 \not{u}\gamma_5)\psi, \\
\mathcal{L}_{\pi N}^{(2)} &= \sum_{i=1}^7 c_i \bar{\psi} \mathcal{O}_i^{(2)} \psi = \bar{\psi}_N \left[c_1 \langle \chi_+ \rangle - c_2 \frac{1}{8m_0^2} \{ \langle u_\mu u_\nu \rangle \{ D^\mu, D^\nu \} + \text{h.c.} \} + c_3 \frac{1}{2} \langle u^2 \rangle \right. \\
&\quad \left. + c_4 \frac{i}{4} [u_\mu, u_\nu] \sigma^{\mu\nu} + \dots \right] \psi_N, \\
\mathcal{L}_{\pi N}^{(3)} &= \sum_{i=1}^{23} d_i \bar{\psi} \mathcal{O}_i^{(3)} \psi = \dots \frac{d_{16}}{2} \gamma_\mu \gamma_5 \langle \chi_+ \rangle u_\mu + \frac{id_{18}}{2} \gamma^\mu \gamma_5 [D_\mu, \chi_-] + \dots, \\
\mathcal{L}_{\pi N}^{(4)} &= \sum_{i=1}^{118} e_i \bar{\psi} \mathcal{O}_i^{(4)} \psi, \\
\mathcal{L}_{\pi\pi}^{(2)} &= \frac{F^2}{4} \langle \nabla_\mu U \nabla_\mu U^\dagger \rangle + \langle \chi_+ \rangle, \\
\mathcal{L}_{\pi\pi}^{(4)} &= \sum_{i=1}^7 l_i \tilde{\mathcal{O}}_i^{(4)} = \dots \frac{l_3}{16} \langle \chi_+ \rangle^2 + \frac{l_4}{16} \left\{ 2[\langle \nabla_\mu U \nabla^\mu U^\dagger \rangle \langle \chi_+ \rangle \right. \\
&\quad \left. + \langle \chi^+ U \chi^+ U + \chi U^+ \chi U^+ \rangle - 4\langle \chi^+ \chi \rangle - \langle \chi_- \rangle^2 \right\} + \dots,
\end{aligned} \tag{8}$$

where the following standard notations have been used:

$$\begin{aligned}
U &= u^2, \quad u_\mu = iu^\dagger \partial_\mu U u^\dagger \\
\nabla_\mu U &= \partial_\mu U - i(v_\mu + a_\mu)U + iU(v_\mu - a_\mu), \quad D_\mu = \partial_\mu + \frac{1}{2}[u^\dagger, \partial_\mu u] \\
\chi_\pm &= u^\dagger \chi u^\dagger \pm u \chi^\dagger u, \quad \chi = 2B(s + ip).
\end{aligned} \tag{9}$$

At lowest order the Lagrangian is given by the non-linear σ model. One recovers in $\mathcal{L}_{\pi\pi}^{(2)}$ the two parameters B and F discussed previously. F is the chiral limit value of the pion decay constant:

$$\langle 0 | A_\mu^a(0) | \pi^b(p) \rangle = i\delta^{ab} F p_\mu. \tag{10}$$

In Eq. (8) m_0 is the chiral limit of the nucleon mass m and g_0 the one of the axial vector coupling constant g_A defined by:

$$\langle N(p') | A_\mu^a | N(p) \rangle = \bar{u}(p') \left[\gamma_\mu G_A(t) + \frac{(p' - p)_\mu}{2m} G_P(t) \right] \gamma_5 \frac{\tau^a}{2} u(p) \tag{11}$$

with $t = (p' - p)^2$ the invariant momentum transfer and $g_A \equiv G_A(0)$. The form of Eq. (11) follows from Lorentz invariance, isospin conservation, the discrete symmetries C, P and T and the absence of second class currents [36] which is consistent with experimental information, see e.g. [37]. F , m_0 and g_0 differ from their physical values by terms proportional to the quark masses, e.g.

$$F_\pi = F(1 + \mathcal{O}(\mathcal{M})) = F \left(1 + \frac{M^2}{16\pi^2 F^2} (16\pi^2 l_4^r(\lambda) - \ln \frac{M^2}{\lambda^2}) + \mathcal{O}(M^4) \right). \quad (12)$$

The next-to-next-to-leading order contributions to F_π can be found in [38] (see also [39] and references therein). The expression for the nucleon mass and the axial vector coupling will be given in Section 3 and discussed in detail there.

The coefficients of the monomials $\mathcal{O}^{(n)}$ are the so-called LECs. The numbers of counterterms in $\mathcal{L}_{\pi N}^{(3),(4)}$ correspond to [35]. In that reference, terms in $\mathcal{L}_{\pi N}$ are included which could be eliminated by using equation of motion (EOM) for the classical fields as done in [40]. In fact the knowledge of both these physically equivalent Lagrangians allows for a non-trivial test of the calculations performed. In the case of $\mathcal{L}_{\pi\pi}^{(4)}$ we have used the expression given in [41] which also differs from the original one [16] by EOM terms though in that case the number of terms are the same. Clearly, the number of counterterms increases fastly with the order one is working. However, as we will see in the applications Sections 3, 4 and 5, only few of them appear in each process. We will be mostly concerned in this review with the order 2 and two of the order 3 counterterms for which we will give numerical values in the next section.

2.3.2 Low-energy constants

i) some general comments

The general properties of the LECs are the following:

- as we have seen they describe the influence of “heavy” degrees of freedom not contained explicitly in chiral Lagrangians.
- their values are *not constrained by symmetries*.
- most of them are *scale-dependent*, see Eq. (12). Indeed the Goldstone loops are in general divergent and need to be renormalized. Since by construction the full effective Lagrangian contains all terms permitted by the symmetries, the divergences can be absorbed in a renormalization of the coupling constants occuring in the Lagrangian. Thus one has for a generic LEC b_i in the modified \overline{MS} scheme

$$b_i = b_i^r(\lambda) + \kappa_i L \quad , \quad L = (4\pi)^{-2} \lambda^{d-4} \left\{ \frac{1}{d-4} - \frac{1}{2} (\ln 4\pi + \Gamma'(1) + 1) \right\}. \quad (13)$$

Of course the scale dependence thus introduced cancels with the one from the loops so that physical quantities are scale-independent. Since loops starts at order three in the nucleon sector the LECs of order two are scale-independent. The κ_i , Eq.(13) have been obtained in [16] for the mesons and [35, 40, 42] for the nucleons in HBCHPT from an explicit calculation of the one-loop generating functional (note that there is a misprint in [40] concerning the LEC d_{11} which was corrected in [43]). The complete divergence structure of the one-loop generating functional corresponding to the heavy baryon Lagrangian in the presence of virtual photons has been worked out in [43] using a super-heat-kernel method [44]. For the LECs which specifically enter this review the κ_i are given in Tables 1 and 2. Care has to be taken to the exact definition of the Lagrangian, for relations between the κ_i 's for different forms of the Lagrangian with or without EOM terms see [35, 40, 43].

- A very important property is that *they relate different observables*. This is illustrated in Table 1 where different sources from which the l'_i s can be obtained are given (in Table 2 only the sources from which the c 's have been determined are shown). This severely constrains the result of the calculation performed.
- They are assumed to fulfil the criteria of *naturalness* based on a dimensional analysis. Comparing the Lagrangian $\mathcal{L}_{\pi\pi}^{(2)}$ and $\mathcal{L}_{\pi\pi}^{(4)}$ for example one can make an estimate of the expected size of the couplings l_i in terms of the symmetry breaking scale $\Lambda_\chi \sim 4\pi F_\pi$. One has:

$$|l_i| \sim \frac{16F_\pi^2/4}{\Lambda_\chi^2} \sim \frac{4}{(4\pi)^2} \sim 0.025. \quad (14)$$

For the nucleon the c 's should be typically of the order $g_A/\Lambda_\chi \sim 1 \text{ GeV}^{-1}$.

One can distinguish between two different classes of LECs, the so-called dynamical LECs and the symmetry breakers. The first ones are proportional to ∂_μ^{2n} while the second are proportional to quark masses $m_q^{2n+1}, m_q \partial^{2n}, \dots$. The mixed LECs parametrizing operators with quark mass insertions and derivatives enter the second class since at fixed pion mass they can be absorbed in the values of certain dynamical LECs. $L_{\pi N}^{(2)}$ has, for example, two symmetry breakers and five dynamical LECs, see Eq. (8).

Determining the LECs from QCD is a difficult non-perturbative problem. Thus either one makes phenomenological evaluations based on experimental information at low energies or one uses additional inputs from theory in order to pin them down. The most commonly used approach is resonance saturation but sum rules [45–47] as well as matching to dispersion theory are also considered. Example of such a matching will be given in Section 7.4. These are the best candidates in the case of the dynamical LECs. The progress of lattice calculations in the last years has however opened the possibility to determine the LECs directly from QCD. These calculations are best suited in the case of the symmetry breakers since these can be obtained through variation of the quark masses. There has also been a lot of activity to determine the LECs from models and especially the Nambu–Jona-Lasinio (NJL) model, for reviews see for example [48]. These will not be discussed here. At present most attempts concern the meson sector. In the nucleon sector as we will see the LECs have been evaluated mostly by fitting the experiments, though some resonance saturation estimates exist for the LECs of order 2 [49, 50]. Let us look in more detail in two of these approaches:

I) ROLE OF RESONANCES and RESONANCE SATURATION

LECs correspond to coefficients of the Taylor expansion, with respect to the momenta, of some QCD correlation functions, once the singularities (poles and discontinuities) associated with the contributions of low-momentum pseudoscalar intermediate states have been subtracted. The Green's function involved being order parameters of the spontaneous breaking of chiral symmetry do not receive contributions from perturbative QCD at large momentum transfers, thus the LECs are expected to be sensitive to the physics in the intermediate regions, that is to the spectrum of mesonic resonances in the mass region around the hadronic scale. Most attempts up to date to estimate the values of the LECs from resonance data are thus based on the so-called principle of *resonance saturation which states that the LECs are largely saturated by resonance exchange*. This is also known as chiral duality.

The procedure relies on the construction of an effective Lagrangian with resonance degrees of freedom. Determining the LECs amounts to decoupling these resonances from the effective field theory. The traces of these frozen particles are then encoded in the numerical values of certain LECs. A first systematic analysis of the role of resonances in the CHPT Lagrangian was performed in the meson sector, [51–53] the couplings of meson resonances of the type $V(1^{--})$, $A(1^{--})$, $S(0^{++})$ and $P(0^{-+})$ being studied. In fact inclusion of vector particles follows many years of phenomenological analysis in

both nuclear and particle physics. They have therefore been considered in chiral Lagrangians from the early days on, usually with the assumption that vector and axial vector mesons are gauge bosons of local chiral symmetry (for reviews see [54]). Note that in the baryon sector the role played by the ρ meson is, in that case, the $\Delta(1232)$. We will discuss this later. In order to determine local operators from the resonance Lagrangian one lets the resonance masses M_R become very large with fixed ratios of coupling constants to masses. Typically the resonance propagator is replaced by its corresponding momentum expansion in t/M_R^2 where t is a typical momentum transfer squared. Thus the exchange of virtual resonances generates pseudo-Goldstone boson couplings proportional to powers of $1/M_R^2$. Clearly the lowest lying resonance will thus be the most important one, a fact which is supported by phenomenology. In [52, 53] the $\mathcal{O}(p^4)$ couplings of $\mathcal{L}_{\pi\pi}$ have been determined this way. It is found that whenever the vector meson contributes it almost saturates the LECs which is in agreement with the vector meson dominance principle.

Recently this analysis has been generalized and Lagrangians of this resonance chiral theory ($R\chi T$) have been constructed following the ideas of Weinberg [55], however having no power counting. They enlarge the range of validity of the effective field theory in the region $M_\rho < E < 2$ GeV and aim at determining the LECs up to $\mathcal{O}(p^6)$ in the meson sector. They are guided by the following principles:

(a) they use large N_c arguments which say that the correlators of colour-singlet quark-antiquark currents are given by tree-level exchanges of infinite towers of narrow resonances [56].

(b) the appropriate QCD short-distance constraints whose importance has been stressed in [57] and recognized since then, are implemented in the calculation. This additional input leads to the so called Minimal Hadron Ansatz which states that only those resonances which are needed to fulfil the constraints are taken into account.

Integration of the resonance fields then leads to LECs parametrized in terms of resonance masses and couplings. Information on those couplings and on the LECs have been extracted analysing QCD Green functions of currents both for large and small momenta, for example $\langle VAP \rangle$ and $\langle SPP \rangle$ Green functions [55]. Note that though it has some advantages one could work without a Lagrangian formulation and only use Green's functions [57–59].

Most calculations have at present only considered the large N_c limit. Incorporating next-to-leading contributions in the $1/N_c$ counting is not straightforward. Indeed quantum loops including virtual resonance propagators constitute a major technical challenge. Some studies have been done but mostly within models. In order to gain some understanding it seems worth to perform some explicit one-loop calculations of well chosen amplitudes. A first detailed investigation of the pion vector form factor at next-to-leading order in the $1/N_c$ expansion has thus been done in [60].

One problem has to be raised, namely the scale dependence of the LECs which is absent in this resonance picture at leading order. It has however been shown [52] that if one decomposes the LECs into a resonance part and a remainder which takes the scale dependence μ into account there is a region in μ where the LECs are almost entirely given by the resonance part, $\mu \sim M_R$. Recently this problem has been considered within the $R\chi T$ theory at order $1/N_c$ and first determinations of the scale dependence of certain LECs have been obtained [61, 62].

Resonance saturation has proven very successful in determining the values of certain LECs in the meson sector at one loop. However, the validity of the resonance saturation from the light resonance sector for the $\mathcal{O}(p^6)$ LECs [63] has been recently examined with the conclusion that some of these couplings are in fact not dominated by resonance contributions. In the nucleon sector only the LECs of order two have been studied so far. As an example, let us look at c_3 . The dominant contribution comes from the $\Delta(1232)$, there are additional smaller corrections from the $N^*(1440)$ resonance and also contributions from a scalar meson exchange. The Δ contributes $-2.54 \dots -3.18$ GeV $^{-1}$, the N^* $-0.06 \dots -0.22$ GeV $^{-1}$ and the scalar -1.33 GeV $^{-1}$ leading to c_3 varying between -3.6 and -5.0 GeV $^{-1}$ in the range of the empirical value quoted in Table 2. In view of its success, extension of the idea of resonance saturation has also been done in the two-nucleon sector [64]. Clearly more studies are needed

Table 1: Two LECs of $\mathcal{L}_{\pi\pi}^{(4)}$. r_π^S is the scalar pion radius. Values determined as explained in the text.

		\bar{l}_3	\bar{l}_4
		$\kappa_3 = -1/2$	$\kappa_4 = 2$
sources		mass ratios, $\pi\pi$ scat.	$r_\pi^S, F_\pi, \pi\pi$ scat.
standard CHPT		2.9 ± 2.4 [16]	4.4 ± 0.2 [32]
lattice	[65]	3.65 ± 0.12	4.52 ± 0.06
	[66]	$3.5 \pm 0.5 \pm 0.1$	
	[67]	0.6 ± 1.2	3.9 ± 0.5

on the role of resonances in the determination of the LECs, especially in the nucleon sector.

II) LATTICE

As will be stressed in Section 2.5 there exists today some lattice evaluation of the $\mathcal{O}(p^4)$ LECs in the meson sector, mostly the SU(3) ones. Let me give here the results for the SU(2) LECs l_3 and l_4 which belongs to the symmetry breakers' class. These are the ones of most concern in the baryon sector since they enter the pion mass and decay constant at next-to-leading order, respectively. They are also of particular importance since they contribute to fundamental quantities as the $\pi\pi$ scattering lengths. As can be seen from Table 1 where the scale-independent bar quantities related to the b_i^r by

$$b_i^r = \frac{\kappa_i}{32\pi^2} (\bar{b}_i + \ln \frac{M^2}{\lambda^2}) \quad (15)$$

are given, there is a rather good agreement between the SU(2) lattice results [65, 66] and the one obtained in standard CHPT. Note that the latter are in good agreement with the expected size of the LECs. One can also infer values for these LECs from SU(3) calculations using the relations derived in [19]. The MILC collaboration [67] found smaller value for \bar{l}_3 from such a calculation. Two remarks are in order here. First the lattice values are obtained for large values of the strange mass and what is really needed are the values for $m_s = 0$ or m_s physical. Second OZI-rule violating vacuum fluctuations would strongly affect the standard CHPT values [29], especially \bar{l}_3 whose value could be pushed towards larger negative value, as much as -17.8 [29]. In the following the CHPT values quoted in the table will be used.

ii) **leading order LECs and their determination** (F_π, F_K, g_A)

The most accurate experimental information on F_π and F_K come from the semi-leptonic transition $P \rightarrow \mu\nu$ while the axial-vector coupling constant g_A is measured in (polarized) neutron beta-decay [68]. Unfortunately the result of these measurements do depend on (a priori unknown) axial electroweak (EW) couplings of the u and d/s quarks to the W . In turn these EW couplings require a knowledge on these QCD quantities as well as others like transition form factors which are also measured in semi leptonic transitions of the type $P' \rightarrow Pl\nu$ where $P = \pi, K, D, B$. At present the only well known EW quantity is the vector coupling \mathcal{V}_{ud} of the u and d quarks to W . It is very accurately determined from $0^+ \rightarrow 0^+$ transitions in nuclei assuming conservation of the vector current, $\mathcal{V}_{ud} = 0.97377(26)$ [69]. What can presently be given very precisely are the values of the three LECs F_π, F_K and g_A within the Standard Model. Indeed in this framework the axial and vector couplings are equal and the CKM matrix V_{ij}^{CKM} is unitary ($\mathcal{V}_{ud} = V_{ud}^{CKM}$ in the SM). All over this review I will use the Standard Model result for the $SU(2)$ quantities F_π and g_A namely:

$$F_\pi \equiv F_\pi|_{SM} = 92.4(3) \text{ MeV}, \quad g_A \equiv g_A|_{SM} = 1.2695 \pm 0.0029$$

but the reader should keep in mind that physics beyond the Standard Model such as non standard EW couplings to quarks (for example RHCs [70]) would modify these values. It turns out that the meson sector would be more affected than the nucleon one since in that case the loops are proportional to g_A/F_π , quantity which is independent of the axial effective couplings to W. Note that in the standard model the ratio

$$F_K/F_\pi|_{SM} = 1.182(7) \quad (16)$$

(obtained from the experimental ratio of the radiative inclusive decay rates for $K \rightarrow \mu\nu(\gamma)$ and $\pi \rightarrow \mu\nu(\gamma)$ [71]) is considerably smaller than the value which has been used up to now in CHPT, namely 1.22 (obtained by taking the ratio of the central values of the experimental results for F_K and F_π [72]). There, as stressed above values for the axial EW couplings had to be inferred). Apart from CP-PACS/JLQCD [73] recent SU(3) lattice determinations of this ratio [67, 74, 75] lead to central values larger than the SM one, between 1.20 and 1.24 with rather small error bars. For a comparison of different lattice results see [76]. In Section 7 the exact value of this ratio will be irrelevant for the applications discussed. Indeed, an average value between F_π and F_K has usually been taken, the differences between these two quantities being in those particular cases of higher order.

iii) higher order LECs of $\mathcal{L}_{\pi N}$

Essentially two processes have been used to pin them down: $\pi N \rightarrow \pi N$ and $\pi N \rightarrow \pi\pi N$. These two processes will be discussed in more detail in Section 4. Here I will restrict the discussion to what is directly related to the determination of the counterterms.

Several works have concentrated their efforts in determining the counterterms of order two and three in πN scattering. Different methods have been used:

- a) fit to the data in the physical region [77].
- b) use of subthreshold coefficients [50, 78, 79]. Note that in [78, 79] they use the tree level formula which give the LECs in terms of the subthreshold coefficients whereas in [50] the next order terms are taken into account. It turns out that the corrections are not that small leading to somewhat different values for the counterterms.
- c) It has been advocated by Büttiker and Meißner [80] that a much better determination can be obtained working in an unphysical region of the Mandelstam plane, namely in the inside of the Mandelstam triangle defined by $s < (m + M_\pi)^2$, $u < (m + M_\pi)^2$ and $t < 4M_\pi^2$. Indeed in this region the scattering amplitude is purely real and furthermore the kinematical variables t and $(s - u)/4m$ take their smallest values. However in this region which is by definition unphysical there is no direct access by experimental data. Use of dispersion relations allows to circumvent this problem. In this framework each LEC appears in one particular invariant amplitude only but for c_4 and \bar{d}_{18} present in two different ones. Thus most of the dimension three LECs cannot be pinned down accurately since they appear in the amplitude with small prefactors. The problem of this framework is that it is unfortunately hard to determine the theoretical uncertainties.

A summary of the by now admitted values of the LECs of order two [81] are given in Table 2. They have been determined combining results from [35, 50, 80, 82] and using a value of the sigma term of 45 MeV consistent with [83] ([82] is a determination of c_3 and c_4 from pp and np scattering). We have discarded here the values obtained at tree level. Note that attention has to be paid to the definition used for the finite parts of the counterterms b_i^r (see Eq. (15)) when doing a calculation, their values depending on the regularization scheme used [84]. This of course does not hold for the c 's.

Two order three counterterms enter many of the studied quantities. These are d_{16} and d_{18} . The first one has been studied in $\pi N \rightarrow \pi\pi N$ [85] but not very precisely determined. d_{18} is calculated via the so-called Goldberger-Treiman discrepancy i.e the deviation from the Goldberger-Treiman relation which states that the πNN coupling constant deviates from the ratio of the axial vector coupling and

Table 2: 4 LECs of $\mathcal{L}_{\pi N}^{(2)}$ and 2 LECs of $\mathcal{L}_{\pi N}^{(3)}$. Values determined as explained in the text.

order 2 [GeV ⁻¹]				order 3 [GeV ⁻²]	
c_1	c_2	c_3	c_4	d_{16}	d_{18}
				$\kappa_{16} = g_A(4 - g_A^2)/8$	$\kappa_{18} = 0$
$\sigma_{\pi N}$	$\pi N \rightarrow \pi N$	$\pi N \rightarrow \pi N$	$\pi N \rightarrow \pi N$	$\pi N \rightarrow \pi\pi N$	GT rel.
$-0.9_{-0.5}^{+0.2}$	3.3 ± 0.2	$-4.7_{-1.0}^{+1.2}$	$3.5_{-0.2}^{+0.5}$	$-3.4 \cdots - 0.92$	-0.72 ± 0.27

the pion decay constant by terms of order M_π^2 . It has been found [41, 77, 78] that the non-analytic terms in the ratio $g_A m/F_\pi$ and in $g_{\pi NN}$ are the same up to M_π^3 so that one has:

$$g_{\pi N} = \frac{g_A m}{F_\pi} \left(1 - \frac{2M_\pi^2 \bar{d}_{18}}{g_A} \right) + \mathcal{O}(M_\pi^4) \quad (17)$$

(the Golderger Treiman discrepancy has also been studied within SU(3), see [86]). The values of these two counterterms are given in Table 2, the one for \bar{d}_{18} uses $g_{\pi NN} = 13.18$. Note that this number is subject to some uncertainty, having decreased from the 1983 Höhler's value of $f^2 = g_{\pi NN}^2 M_\pi^2 / 16\pi m^2 = 0.079$ to nowadays somewhat smaller values in the range from 0.075 to 0.076, see for example [87]. A very recent determination of f from the Goldberger-Miyazawa-Oehme sum rule can be found in [88].

The discussion of the LECs related to the inclusion of photons is given in Section 4.1.2.

2.3.3 HBCHPT

Let us come back briefly to the power counting, for more details see for example [7]. We have seen that in the meson sector loops and chiral order are intimately connected. In the nucleon case however, an extra scale appears, the nucleon mass which is of the order of the symmetry breaking scale and which does not vanish in the chiral limit. It was first pointed out by [41] that this new scale destroys the power counting, namely an arbitrary number of loops contributes to a certain chiral order (apart for the first order).

The first to bring a solution to this problem were Jenkins and Manohar [89] following methods from heavy quark physics. The idea in this framework called heavy baryon chiral perturbation theory (HBCHPT) is to consider the nucleon as extremely heavy, thus only the baryon momenta relative to the rest mass will be relevant and can be small. One has

$$p_\mu = mv_\mu + k_\mu \quad (18)$$

with $k_\mu \ll v \cdot p$. The baryon field is split into velocity-dependent “heavy” and “light” components

$$N_v(x) = e^{imv \cdot x} P_v^+ \psi(x), \quad H_v(x) = e^{imv \cdot x} P_v^- \psi(x), \quad P_v^\pm = \frac{1}{2}(1 \pm \not{v}) \quad (19)$$

and the heavy component $H_v(x)$ is integrated out from the Lagrangian. One finally gets [90]

$$\begin{aligned} \mathcal{L}_{\pi N} = & \bar{N}_v \{ \mathcal{A}^{(1)} + \mathcal{A}^{(2)} + \mathcal{A}^{(3)} + (\gamma_0 \mathcal{B}^{(1)\dagger} \gamma_0) \frac{1}{2m} \mathcal{B}^{(1)} + \frac{(\gamma_0 \mathcal{B}^{(1)\dagger} \gamma_0) \mathcal{B}^{(2)} + (\gamma_0 \mathcal{B}^{(2)\dagger} \gamma_0) \mathcal{B}^{(1)}}{2m} \\ & - (\gamma_0 \mathcal{B}^{(1)\dagger} \gamma_0) \frac{i(v \cdot D) + g_A(u \cdot S)}{(2m)^2} \mathcal{B}^{(1)} \} N_v + \mathcal{O}(p^4). \end{aligned} \quad (20)$$

In this equation $\mathcal{A}^{(1)}$ is given by

$$\mathcal{A}^{(1)} = i(v \cdot D + g_A u \cdot S) \quad (21)$$

and the spin operator $2S_\mu = i\gamma_5 \sigma_{\mu\nu} v^\nu$ obeys the following relations (in d space-time dimensions)

$$S \cdot v = 0, S^2 = \frac{1-d}{4}, S_\mu, S_\nu = \frac{1}{2}(v_\mu v_\nu - g_{\mu\nu}), [S_\mu, S_\nu] = i\epsilon_{\mu\nu\alpha\beta} v^\alpha S^\beta. \quad (22)$$

Expressions for the other operators can be found in [90]. As can be seen from Eqs. (20), (21) the heavy nucleon mass is, in this way, shuffled from the propagators to the vertices. HBCHPT is thus a double expansion in q/Λ and q/m . At a given order any observable is given as a sum of a finite amount of terms. We will see that this is not the case for the other regularizations discussed. Note that an advantage of this method is its extreme computational simplicity.

As discussed in detail by Becher and Leutwyler [91], let us look at the convergence of this $1/m$ expansion in the case of one specific scalar loop function corresponding to the triangle graph shown in Fig. 1. This graph enters into a whole series of processes as for example, the nucleon electroweak and scalar form factors. The external sources depicted by the wiggly line are in these cases the photon and the weak bosons or a scalar source, respectively. It is given in the relativistic formulation by:

$$\gamma(t) = \frac{1}{i} \int \frac{d^4 k}{(2\pi)^4} \frac{1}{(M^2 - k^2 - i\epsilon)(M^2 - (k - q)^2 - i\epsilon)(m^2 - (P - k)^2 - i\epsilon)}. \quad (23)$$

This function is analytic in $t = q^2$ except for a cut along the positive real axis starting at $t = 4M^2$. Its

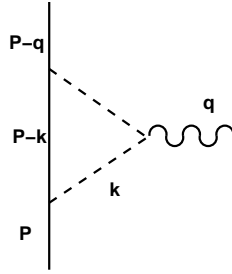


Figure 1: Triangle graph. The solid, dashed and wiggly lines represent the nucleons, pions and an external source, respectively.

imaginary part is expressed in terms of elementary functions:

$$\text{Im}\gamma(t) = \frac{\theta(t - 4m^2)}{16\pi m\sqrt{t}} \left\{ \arctan \frac{\sqrt{(t - 4M^2)(4m^2 - t)}}{t - 2M^2} \right\}. \quad (24)$$

The analytic continuation of $\gamma(t)$ to the second sheet contains a branch point $t_c = 4M^2 - M^4/m^2$ just below threshold coming from the arctan. This turns out to be very important in the calculation of the isovector charge and magnetic radii for example, for a quantification of the effect see [92]. In fact Frazer and Fulco [93] long time ago pointed out that extended unitarity leads to a drastic enhancement of the isovector electromagnetic spectral function on the left wing of the ρ resonance, exactly due to this singularity at the anomalous threshold t_c . Note, however, that even though a similar branch point appears in the isoscalar spectral function [94], the three-body phase factors suppress its influence in the physical region. In that case, the spectral function rises smoothly up to the ω pole.

What happens within HBCHPT? As was shown in [90] the heavy baryon perturbation series corresponds to the $1/m$ expansion of the relativistic result. Due to the power counting the coefficient of the arctan is a quantity of order $\mathcal{O}(1/p)$ so that to $\mathcal{O}(p^3)$

$$\text{Im}\gamma(t) = \frac{\theta(t - 4m^2)}{32\pi m\sqrt{t}} \left\{ \pi - \frac{(t - 2M^2)}{m\sqrt{(t - 4M^2)}} + \mathcal{O}(p^2) \right\}. \quad (25)$$

Clearly at this order the normal and the anomalous threshold have coalesced. There is a breakdown of the expansion Eq. (25) close to threshold. The series indeed converges if the quantity $(t - 2M^2)/m\sqrt{(t - 4M^2)}$ is small which is obviously not the case in that region. Thus the loop function Eq. (25) is a decent representation only away from threshold. In HBCHPT an infinite series of internal insertions must be summed up to properly describe the loop function near threshold. As a consequence the isovector electromagnetic spectral functions for example show an abnormal threshold behaviour in this framework. The origin of the problem is that for some of the graphs the loop integration cannot be interchanged with the nonrelativistic expansion.

Similar problems appear with Born terms [95] where in HBCHPT the positions of the poles are moved due to the expansion of the nucleon propagator leading again to a breakdown of the series close to the singularity. An example of such a problem will be given in Section 5.3 when the Furlan-Fubini-Rosetti sum rule will be discussed.

Kaiser proposed in his calculation of the electromagnetic form factors [96] to expand all but the arctan function in order to incorporate in a proper way the anomalous singularity, this being taken as a compromise between the correct analytical structure and the strict chiral power counting. This, however, is a minimal prescription. We will now see how to deal with the problem in a consistent way.

2.3.4 Infrared regularization

The idea is then to formulate a theory which has the proper power counting and at the same time the proper analytic structures. The first attempt in that direction is due to Tang and Ellis [97,98]. While in HBCHPT the anti-nucleon field is integrated out in order to recover the proper power counting, Tang [97] noted that their contributions are hard-momentum effects, and that EFT's permit useful low-energy expansion only if all hard momentum effects are absorbed into the parameters of the Lagrangian. He thus proposed to deviate from [41] at the loop integral level in the following way:

- i) take the loop momenta to be of order p ,
- ii) make a covariant p/m expansion of the integrand,
- iii) exchange the order of the integration and summation of the resulting power series.

He showed that this prescription indeed extracts the soft part of a Feynman diagram and that it fulfils the power counting. The hard momentum part which is a local polynomial in the small chiral parameters is then absorbed into the parameters of the most general effective Lagrangian.

This method however relies on the chiral expansion of the loop integrals which is not always convergent. Thus Becher and Leutwyler [91] took up this idea of extracting the soft momentum parts or so called infrared singular parts and proposed a more formal scheme which is known as Infrared Regularization of baryon CHPT. It relies on the fact that these infrared singular parts of the loop graphs can unambiguously be separated from the remainder for non integer-values of the space-time dimension, leading to a unique, i.e process independent result in accordance with the chiral Ward identities of QCD. In order to illustrate the method let us look at the simplest case, namely the self-energy, Fig. 2.

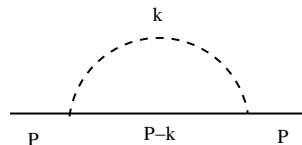


Figure 2: Self-energy graph

The corresponding scalar loop integral is given by

$$H(P^2) = \frac{1}{i} \int \frac{d^4 k}{(2\pi)^4} \frac{1}{(M^2 - k^2 - i\epsilon)(m^2 - (P - k)^2 - i\epsilon)} . \quad (26)$$

This integral develops an infrared singularity as M goes to zero coming from the low momentum region of integration. The high momentum one is free of infrared singularities and thus leads to a contribution which can be expanded in an ordinary power series. These corresponds to the soft and hard momentum parts of Tang, respectively. In order to isolate the infrared parts one introduces the standard Feynman parametrization

$$\frac{1}{ab} = \int_0^1 dz \frac{1}{\{(1-z)a + zb\}^2} \quad (27)$$

where in our case a corresponds to the pion propagator and performs a change of variable $z = \alpha u$ with $\alpha = M/m$. The upper limit of integration becomes large as M goes to zero so that one can extend the integration to infinity. One thus extracts the infrared singular part:

$$I = \kappa \alpha^{d-3} \int_0^\infty du D^{\frac{d}{2}-2}, \quad D = 1 - 2\Omega u + u^2 + 2\alpha u(\Omega u - 1) + \alpha^2 u^2 - i\epsilon, \quad \kappa = (4\pi)^{-\frac{d}{2}} m^{d-4} \Gamma\left(2 - \frac{d}{2}\right), \quad (28)$$

where $\Omega = (P^2 - m^2 - M^2)/2mM$ is a dimensionless quantity of order one. Clearly the chiral expansion of I exclusively contains fractional powers of M for non integer-value of the dimension. One thus gets the following decomposition of the scalar loop integral, Eq. (26):

$$H = \kappa \int_0^1 dz C^{\frac{d}{2}-2} = \kappa \left(\int_0^\infty dz - \int_1^\infty dz \right) C^{\frac{d}{2}-2} = I + R, \quad (29)$$

where the explicit expression for C can be found in [91]. The infrared singularity coming from the small values of z is clearly excluded in the expression for R . This quantity contains the fractional powers of m and its expansion is an ordinary Taylor series. Both parts I and R are chirally symmetric by themselves so that R can be absorbed in the low-energy constants of the effective Lagrangian. In the Feynman parametrization, the only difference between H , I , and R is that the integrations extend over different intervals. The one relevant for R is $1 < z < \infty$ which is mapped onto $-\infty < s < 0$. Accordingly R has a cut along the negative real axis. The infrared singular part contains a whole string of $1/m$ suppressed terms which corresponds to the resummation of the kinetic energy corrections to the nucleon propagator. To leading order it reproduces the HBCHPT result. Different possibilities were explored in the treatment of these $1/m$ terms. Becher and Leutwyler who were mostly concerned with the correct treatment of the relativistic properties kept in their applications the full denominators of loop integrals while expanding the numerator to the desired chiral order only. However they tried to choose the kinematic variables to be kept fixed when performing the chiral expansion so as to lead to the best possible convergence. Others more concerned with expanding the range of validity of the chiral series to somewhat higher energies kept all terms. Differences between the two approaches are of higher order in the expansion.

What has happened to the regularization scale λ ?

- Due to the presence of the extra scale m the quantity κ in Eq. (28) which in dimensional regularization is defined in terms of the regularization scale λ , is proportional to m so that one naturally gets here $\lambda = m$. In fact it was already stressed in [90] that such a condition led to a proper matching of the relativistic approach to the heavy baryon one which, as was argued in that paper, is not quite unexpected since the heavy field of mass $2m$ were integrated out of the latter theory. It has one advantage. As we have just seen the infrared singular parts contain a whole string of $1/m$ suppressed terms which may contain infinite pieces. These divergences are accompanied by the appearance of a logarithmic dependence on the scale λ . Both these infinite parts and the logarithms cannot be taken care of as long as one introduces running coupling constants to a finite order. Thus using the natural scale m as the regularization scale removes the otherwise

unphysical scale dependence in the physical results. For the higher order divergences they have to be removed by hand.

- Another alternative is to keep λ free and study the λ dependence of the results as was done for example in [99].
- Another philosophy has been proposed in [100]. The idea is to promote to the order one is working counterterms of effectively higher order when getting $1/m$ suppressed divergences compared to this order, thus getting rid of the λ dependence. In the calculation of the nucleon mass to $\mathcal{O}(p^3)$ for example, only one divergence proportional to M_π^4 is found and absorbed by adding a counterterm of $\mathcal{O}(p^4)$.

The analysis of the self-energy can be generalized to arbitrary one-loop graphs which carry factors of the loop momentum in the numerator. They can always be reduced to combinations of the scalar ones:

$$H_{mn} = \frac{1}{i} \int \frac{d^d k}{(2\pi)^d} \frac{1}{a_1 \cdots a_m b_1 \cdots b_n} . \quad (30)$$

The representation of the corresponding infrared parts in terms of Feynman parameters coincides with the one obtained for H_{mn} except that the integration over the parameter which combines the meson propagators with the nucleon ones runs from 0 to ∞ instead of 0 to 1. One has the special cases:

$$I_{m0} = H_{m0} , \quad R_{m0} = 0 , \quad I_{0m} = 0 , \quad R_{0m} = H_{0m} . \quad (31)$$

For more details on the calculations see [91].

It was shown in [91] that the procedure just discussed can be viewed as a manifestly Lorentz-invariant alternative regularization thus the name infrared regularization given to it.

This IR method has been extended to the case of two heavy particles [101] and referred to as EFT dimensional regularization. Recently the case where spin 1 fields are accounted for explicitly in the theory [102] has been considered in the same framework. Indeed the appearance of the large mass scale, the mass of the vector fields, lead to the same problem as in the nucleon case when calculating loop diagrams. This new scale destroys the one to one correspondence between the chiral expansion and the loop expansion as discussed before. There is an additional complication here, namely that the vector particles can decay into Goldstone bosons and thus appear in loops without appearing in external lines.

2.3.5 Other regularizations

The most important step made by Ellis and Tang was to realize that the power violating terms were just polynomials. This makes it possible to come back to the relativistic theory and within this framework to get rid of these unwanted terms. We have just seen one possible systematic way to do so namely IR which directly calculates the infrared terms obeying the power counting. Soon after some other approaches have been derived which, contrary to IR, evaluate the power counting violating regular part R which is then subtracted to the relativistic contribution. One of these is the extended on-mass-shell (EOMS) scheme [103, 104]. The central idea consists in performing additional subtractions beyond the $\overline{\text{MS}}$ scheme. It was shown in [105] that R can be obtained by first expanding the integrand in small quantities and then performing the integration for each term in much the same way as the expansion of the infrared part in Ellis and Tang. One has in the massless pion case

$$R = \int \frac{d^n k}{(2\pi)^n} \sum_{l=0}^{\infty} \frac{(p^2 - m^2)^l}{l!} \left[\left(\frac{1}{2p^2} p^\mu \frac{\partial}{\partial p_\mu} \right)^l \frac{1}{(k^2 + i0^+)[k^2 - 2k \cdot p + (p^2 - m^2) + i0^+]} \right]_{p^2=m^2}$$

$$\begin{aligned}
&= \int \frac{d^n k}{(2\pi)^n} \left[\frac{1}{(k^2 + i0^+)(k^2 - 2k \cdot p + i0^+)} \right]_{p^2=m^2} \\
&\quad + (p^2 - m^2) \left[\frac{1}{2m^2} \frac{1}{(k^2 - 2k \cdot p + i0^+)^2} - \frac{1}{2m^2} \frac{1}{(k^2 + i0^+)(k^2 - 2k \cdot p + i0^+)} \right. \\
&\quad \left. - \frac{1}{(k^2 + i0^+)(k^2 - 2k \cdot p + i0^+)^2} \right]_{p^2=m^2} + \dots \Big]. \quad (32)
\end{aligned}$$

The use of the subtraction point $p^2 = m^2$ in Eq. (32) gave rise to the name EOMS for the renormalization condition in analogy with the on-mass-shell renormalization scheme in renormalizable theories. In this example only the first term of the series violates the power counting and is thus a priori the only term which one needs to subtract to H in order to get a renormalized expression H^R which fulfils the proper power counting. Thus in the EOMS one has $H^R = H - H^{subtr}$ with :

$$H^{subtr} = -i \int \frac{d^n k}{(2\pi)^n} \frac{1}{(k^2 + i0^+)(k^2 - 2k \cdot p + i0^+)} \Big|_{p^2=m^2} \quad (33)$$

the first term in the expansion of R . In IR, the full series is subtracted, I will comment on that in the summary. Note that the infrared regularization has been formulated in [106] in a form analogous to the EOMS renormalization. Also it has been explicitly demonstrated within a toy model [107] that theses two schemes can be applied to the calculation of multiloop diagrams. Extending the EOMS a consistent power counting in manifestly Lorentz invariant baryon CHPT including vector mesons as internal fields [108] or the Δ resonance [109] has been obtained.

Based on these same ideas, namely to extract from a loop integral H_G

$$H_G = \mu^{L(4-d)} \int \prod_{l=1}^L \frac{d^d k_l}{(2\pi)^d} \prod_{i=1}^I \frac{i}{q_i^2 - m_i^2 + i\epsilon}, \quad (34)$$

the regular part R_G proportional to fractional power of the heavy mass m and thus responsible for the violation of power counting, a Lorentz covariant regularization scheme for effective field theories with an arbitrary number of propagating heavy and light particles is derived in [110]. In Eq. (34) I is the number of internal lines, L the number of loops, μ the renormalization scale of dimensional regularization and q_i^μ the momentum of each internal line i . Based on the Landau equations [111] which gives a necessary but not sufficient condition for the occurrence of singularities in H_G , the separation $H_G = I_G + R_G$ is achieved by systematically separating out subgraphs of the original graphs G representing singularities that lie outside of the low energy region. These subgraphs are called regular subgraphs. Let us consider here the case of one loop graphs and let us, following [110], define a minimally contracted regular subgraph (MCR) as a regular graph g which is not a subgraph of any other regular graph with more lines than g . The regular part is given as a sum on these MCR as follows:

$$\begin{aligned}
R_G &= -\kappa_I \sum_g \int_1^\infty d\lambda \lambda^{|g|-1} (1-\lambda)^{I-|g|-1} \int_0^1 \left(\prod_{i \in g} dz_i \right) \delta(1 - \sum_{k \in g} z_k) \int_0^1 \left(\prod_{j \notin g} dz_j \right) \delta(1 - \sum_{k \notin g} z_k) \\
&\quad \times \left[(1-\lambda)^2 \sum_{i,j \notin g} z_i \Omega_{ij} z_j + \lambda^2 \sum_{i,j \in g} z_i \Omega_{ij} z_j + 2\lambda(1-\lambda) \sum_{i \in g, j \notin g} z_i \Omega_{ij} z_j - i\epsilon \right]^{\frac{d}{2}-I} \quad (35)
\end{aligned}$$

where

$$\kappa_I = (-)^I \frac{i^{I+1}}{16\pi^2} \frac{\Gamma(I-d/2)}{(4\pi\mu^2)^{d/2-2}}, \quad \Omega_{ij} = \frac{1}{2} \left(m_i^2 + m_j^2 - (q_i - q_j)^2 \right). \quad (36)$$

As an example let us look one more time at the triangle graph Fig. 2. It has two subgraphs Fig. 3 obtained by contracting $n = 1$ internal lines of the original graphs. They correspond to a $(\text{sub})^n$ -leading



Figure 3: Subgraphs of the triangle graph

singularity with $n = 1$. Studying the Landau equations one finds that the tadpole Fig. 3a yields a singularity $m^2 = 0$ which lies outside the low energy region defined by $p^2 - m^2 \ll \Lambda$, $M_\pi \ll \Lambda$ and $m \sim \Lambda$ while the other one has a singularity $M_\pi^2 = 0$ well inside the low energy region. Thus graph 3a is the regular graph and the expression for R_G reads:

$$R_G = -\kappa \int_1^\infty d\lambda \left[(1-\lambda)^2 M_\pi^2 + \lambda^2 m^2 + 2\lambda(1-\lambda) \frac{(m^2 + M_\pi^2 - P^2)}{2} \right]^{\frac{d}{2}-2} \quad (37)$$

which is nothing but the result obtained by Becher and Leutwyler Eq. (28).

In Ref. [110] the Taylor series expansion of R_G in powers of p is truncated at the order of the EFT Lagrangian. For a more detailed discussion we refer the reader to that paper.

Up to now we have discussed schemes which used dimensional regularization. In fact any other scheme can be used as long as it respects the Ward identities. For example cut-off methods have a long history in CHPT [112]. However it has been demonstrated in [113] that the Ward identities severely constrain the choice of regulators. Also, doubts have been issued in the literature [114–117] whether an effective field theory when utilized in connection with dimensional regularization is “effective” enough to be applied to extended objects with complicated internal structure like baryons. These are of course not acceptable since from the viewpoint of field theory one scheme cannot provide superior results over the other. I will come back to this issue when discussing recent analysis of the nucleon mass as well as calculations within SU(3). We will see that in some of these analysis Ward identities are not respected. A way of implementing a cut-off regularization which do not break chiral symmetry or gauge invariance has been discussed in [118]. Also Djukanovic et al. [119] have introduced a method of improving the ultraviolet behavior of the propagators which is a smooth cutoff regularization scheme and which preserves all symmetries.

2.3.6 Summary

A summary of the differences between the relativistic, heavy m and infrared approaches is given in Table 3. As seen there, while in HBCHPT the series is finite – it sums terms up to the order one is working – it is infinite in the other approaches, higher order terms compared to the order one is calculating being included. However if one expands a physical quantity obtained in these different approaches up to a certain order the result will of course be the same. What can be different in these different regularizations are the numerical values of the counterterms since the treatment of the analytic terms differs. Let us come back to the higher order terms. In the infrared regularization one knows exactly what they are. They come from a resummation of the $1/m$ kinetic energy terms. However the prize to pay is the appearance of additional unphysical cuts (see discussion after Eq. (29)). These can give rise to rapidly growing quantities when one goes toward larger momentum or larger pion masses that is when one goes beyond the validity of the theory. This is thus not a problem in itself. It only becomes one if *one wants to push the theory too far*. The problem comes merely from the fact that whereas functions like $\arccos(M/m)$ appear in the relativistic calculation they are transformed into $\arccos(-M/m)$ in IR. We will show this in one application in section 3.3.

Table 3: Properties of diverse approaches to CHPT with nucleons.

	Relativistic	Heavy m	IR
Power counting	no	yes	yes
\rightarrow series contributions at q^N	infinite: all orders	finite the order N	infinite: $1/m$ kinetic energy included. orders $\geq N$
analyticity	yes	not always	yes (modulo unphys. cuts at large energies)
regularization	dim. reg.: fractional powers of m	dim. reg.	infrared reg.: eliminates fractional powers of m
order by order renormalization	exact	exact	higher order divergences removed by hand, $\lambda = m$
convergence	property not applicable	not good in certain cases	improved with resp. to HBCHPT, larger energy range in certain cases
leading non-anal. terms	yes	yes	yes

2.4 *Effective theory with Δ 's*

Up to now we have considered the nucleon as the only degree of freedom in the baryon sector. Any QCD state of higher mass appeared only implicitly in the values of certain LECs. A reason for that is the existence of the decoupling theorem [120] which states that in the chiral limit all S-matrix elements and transition currents are given in terms of the Goldstone bosons and the ground-state baryon octet. However it is well-known that the $\Delta(1232)$ resonance plays an important role in many phenomenological descriptions of low- and medium-energy processes as we will see examples in the next sections. One can understand this very well at least for three reasons: first, there is a very small mass gap between this particle and the nucleon, second it is rather strongly coupled to the πN channel and finally it has relatively large photon decay amplitudes. It thus seems quite legitimate to ask oneself whether one should not include this particle as an explicit dynamical degree of freedom of an effective field theory, as was first stressed by Jenkins and Manohar [121], for describing processes which are not restricted to the threshold domain but which cover energies up to the resonance region. The idea is that the convergence of the chiral expansion could be improved by shuffling to lower order some terms which would appear later in the series in conventional BCHPT. The problem is again to define a scheme with a proper power counting.

- *Small scale expansion*

It turns out that it is possible to do so if one counts the nucleon-delta mass splitting Δ as an additional small parameter, as was first shown by Hemmert, Holstein and Kambor [122]. Indeed

$$\Delta \equiv m_\Delta - m = 294 \text{ MeV} \sim 3F_\pi \quad (38)$$

where F_π was taken as scale since Δ is not vanishing in the chiral limit. Thus, one can formulate an extended EFT in which any matrix element or transition current has a low energy expansion in power

of ϵ where

$$\epsilon \in \left\{ \frac{p}{\Lambda_\chi}, \frac{M_\pi}{\Lambda_\chi}, \frac{\Delta}{\Lambda_\chi} \right\}, \quad (39)$$

with $\Lambda_\chi \simeq 1 \text{ GeV}$ the scale of chiral symmetry breaking. This power counting scheme is often called ϵ - or small scale expansion (SSE). Such an EFT however does not have the same chiral limit as QCD as it is well known [120] since in the chiral limit of vanishing quark masses, neither Δ nor F_π vanish. Strictly speaking it is a phenomenological extension of HBCHPT.

The Δ is described within the Rarita-Schwinger (R-S) formalism. A few points in that respect have to be remembered. The R-S spinor ψ_μ has more degrees of freedom than required which has a certain number of consequences. Indeed the need of subsidiary conditions that the spinor must fulfil leads to the non-uniqueness of the classical Δ Lagrangian. The family of one parameter Lagrangians $\mathcal{L}(A)$ which can be constructed is invariant under the following point transformation: $\psi_\mu \rightarrow \psi'_\mu = R_{\mu\alpha}(a)\psi_\alpha$ where $A \rightarrow A' = (A - 2a)/(1 + 4a)$ and $R_{\mu\nu}(a) = g_{\mu\nu} + a\gamma_\mu\gamma_\nu$, $a \neq -\frac{1}{4}$, the operator $R_{\mu\nu}$ acting only on the spin 1/2 content of ψ_μ . The physical quantities should of course be A -independent which is assured by the Kamefuchi- O’Raifeartaigh-Salam theorem. This last property as well as the fact that only the correct number of degrees of freedom have to be left constrain the construction of any interaction terms. This leads to the appearance of the so-called “off-shell parameters” in these interaction terms.

As in heavy baryon CHPT one has to identify the “light” and “heavy” degrees of freedom, the problem being somewhat more challenging due to these off-shell spin-1/2 degrees of freedom associated with the R-S field. In order to separate the spin-3/2 from the spin-1/2 components it is convenient to introduce a complete set of orthonormal spin projection operators for fields with *fixed velocity* v_μ . For example the projector on the 3/2 component reads:

$$P_{(33)\mu\nu}^{3/2} = g_{\mu\nu} - \frac{1}{3}\gamma_\mu\gamma_\nu - \frac{1}{3}(\not{v}\gamma_\mu v_\nu + v_\mu\gamma_\nu \not{v}). \quad (40)$$

The “light” spin-3/2 degrees of freedom are then defined by

$$T_\mu^i(x) \equiv P_v^+ P_{(33)\mu\nu}^{3/2} \psi_i^\nu(x) \exp(im_B v \cdot x) \quad (41)$$

where m_B is a baryon mass scale and P_v^+ is the projection operator of the heavy mass formalism, see Eq. (19). T_μ^i satisfy the constraints

$$v_\mu T_\mu^i = \gamma_\mu T_\mu^i = 0 \quad (42)$$

and correspond to the SU(2) version of the decuplet field introduced in Ref. [121]. The remaining degrees of freedom -the heavy 3/2 components and the four off-shell spin-1/2 contributions - form the heavy baryon fields. They are combined in a five component vector denoted by $G_\mu^i(x)$ and are integrated out.

Let us now consider the most general Lagrangian involving relativistic spin-1/2 (ψ_N) and spin-3/2 (ψ_μ) fields:

$$\mathcal{L} = \mathcal{L}_N + \mathcal{L}_\Delta + (\mathcal{L}_{\Delta N} + h.c.) . \quad (43)$$

The part describing the nucleon will not be discussed here since it is the same as in heavy baryon CHPT. Rewriting \mathcal{L} in terms of the “light” and “heavy” components one finds [122]

$$\begin{aligned} \mathcal{L}_{\Delta N} &= \bar{T}\mathcal{A}_{\Delta N}N + \bar{G}\mathcal{B}_{\Delta N}N + \bar{H}\mathcal{D}_{N\Delta}T + \bar{H}\mathcal{C}_{N\Delta}G + h.c. , \\ \mathcal{L}_\Delta &= \bar{T}\mathcal{A}_\Delta T + (\bar{G}\mathcal{B}_\Delta T + h.c.) - \bar{G}\mathcal{C}_\Delta G , \end{aligned} \quad (44)$$

where the \mathcal{B} are five components vectors and the \mathcal{C} 5×5 matrices. \mathcal{A} , \mathcal{B} , \mathcal{D} and \mathcal{C} have a low energy expansion which starts at $\mathcal{O}(p)$ for the first three quantities and at $\mathcal{O}(p^0)$ for the last one. Explicit expressions for these quantities can be found in [123]. Note that the definition of the heavy nucleon

field must involve the same mass m_B as in the heavy Δ one in order that all exponential factors drop out in Eq. (44). Choosing the heavy baryon mass parameter $m_B = m$ the leading order matrices are given by

$$\begin{aligned}\mathcal{A}_{\Delta N}^{(1)} &= g_{\pi N \Delta} w_\mu^i, \\ \mathcal{A}_\Delta^{(1)} &= -[i v \cdot D^{ij} - \Delta \delta^{ij} + g_1 S \cdot u^{ij}] g_{\mu\nu},\end{aligned}\quad (45)$$

where the chiral invariant couplings are defined as:

$$D_\mu^{ij} \psi_j^\nu = (\partial_\mu \delta^{ij} + \Gamma_\mu^{ij}) \psi_j^\nu, u_\mu^{ij} = u_\mu \delta^{ij} - i \epsilon^{ijk} w_\mu^k, w_\mu^i = \frac{1}{2} \text{Tr} [\tau^i u_\mu]. \quad (46)$$

Shifting variables and completing the square in analogy to the heavy mass formalism one gets:

$$S_{\text{eff}} = \int d^4x \left\{ \bar{T} \tilde{\mathcal{A}}_\Delta T + \bar{N} \tilde{\mathcal{A}}_N N + \left[\bar{T} \tilde{\mathcal{A}}_{\Delta N} N + h.c. \right] \right\} \quad (47)$$

with

$$\begin{aligned}\tilde{\mathcal{A}}_\Delta &= \mathcal{A}_\Delta + \gamma_0 \tilde{\mathcal{D}}_{N\Delta}^\dagger \gamma_0 \tilde{\mathcal{C}}_N^{-1} \tilde{\mathcal{D}}_{N\Delta} + \gamma_0 \mathcal{B}_\Delta^\dagger \gamma_0 \mathcal{C}_\Delta^{-1} \mathcal{B}_\Delta, \\ \tilde{\mathcal{A}}_N &= \mathcal{A}_N + \gamma_0 \tilde{\mathcal{B}}_N^\dagger \gamma_0 \tilde{\mathcal{C}}_N^{-1} \tilde{\mathcal{B}}_N + \gamma_0 \mathcal{B}_{\Delta N}^\dagger \gamma_0 \mathcal{C}_\Delta^{-1} \mathcal{B}_{\Delta N}, \\ \tilde{\mathcal{A}}_{\Delta N} &= \mathcal{A}_{\Delta N} + \gamma_0 \tilde{\mathcal{D}}_{N\Delta}^\dagger \gamma_0 \tilde{\mathcal{C}}_N^{-1} \tilde{\mathcal{B}}_N + \gamma_0 \mathcal{B}_\Delta^\dagger \gamma_0 \mathcal{C}_\Delta^{-1} \mathcal{B}_{\Delta N},\end{aligned}\quad (48)$$

which represents the master formula of the treatment of a coupled spin-1/2 - spin-3/2 system in HBCHPT. It enables one to construct the $1/m_B$ corrections to the leading order contributions Eq. (45). One of course has to add at each order the most general counterterm Lagrangian consistent with the symmetries of the system. It has been given to $\mathcal{O}(\epsilon^2)$ in [123,124].

- *Infrared and other regularization*

As in the case without Δ other regularizations than the one discussed here can be used. I will not report here on the attempts to develop new regularizations in the line of what has been done in the pure nucleon sector but just refer the reader to the papers by [125] and [109,126,127].

2.5 Lattice QCD and CHPT

We have just seen that CHPT is the low energy effective theory of the Standard Model and that it allows for analytical calculations of low-energy QCD processes in terms of the light pseudoscalar mesons masses. Another model-independent way to try and solve QCD is lattice QCD. Since Wilson first introduced this method [128] enormous progress in that field has been made due to advances in computer power as well as improvements in algorithms and actions. First of all the question of how to deal with chiral symmetry on the lattice has been solved with the Ginsparg-Wilson relation [129]. There exists thus today essentially two categories of fermions depending on whether they obey (type II) or not (type I) this relation. Contrary to the latter the former preserves chiral symmetry for zero lattice spacing. Also an important feature is that chiral fermions are automatically $\mathcal{O}(a)$ improved. For a review on chiral fermions see for example [130]. Second from the quenched era where the fermion determinant was taken as a constant one has now come to the dynamical era where full unquenched calculations are slowly becoming available. Different sea and valence quark masses are also taken leading to partially quenched theories. There are, however, still problems to be solved essentially linked to the cost of the simulations. Let me summarize the different realizations of fermions which are actually used each of them having their own advantages and disadvantages. The Wilson fermions, historically the first, $\mathcal{O}(a)$ improved ones [131] and the staggered fermions [132], see also [133,134]) are of type

Table 4: Collaborations cited in the text and corresponding action. References are given in the text.

action	Collaboration			
Wilson	JLQCD	CP-PACS	QCDSF & UKQCD	LPHC/SESAM
Kogut-Susskind	MILC			
Domain wall	RBC	CP-PACS		
Hybrid	LPHC/MILC			

I. They have the advantage of being simple to deal with. However they have some drawbacks. The staggered fermions for example naturally appear with four copies (tastes). For the sea quarks a fourth root trick has thus to be used to reduce the determinant to one flavour which may lead to errors arising from non-localities. Lattice QCD with Wilson quarks and a chirally twisted term represents a promising alternative regularization which does not suffer from unphysical fermion zero modes, it is referred as twisted mass QCD (tmQCD) [135]. However some technical complications arise due to the fact that some of the physical symmetries such as flavour symmetry and parity are only restored in the continuum limit. Domain wall fermions (II) [136, 137] have the great advantage that chiral symmetry can be preserved to a very high accuracy depending on the size of the fifth dimension L_5 , the problem being that the computational cost grows with L_5 . Calculations with overlap fermions (II) which have exact $\mathcal{O}(a)$ improvement and exact chiral symmetry [138] turn out to be expensive and thus involve dynamical simulations on small volumes. In order to try to optimize all these problems the use of mixed-action calculational schemes have been recently developed [139]. An example of the latter is the use of Domain-Wall or Overlap fermions as valence quarks and staggered or Wilson-like as cheaper sea quarks [140]. However the fact that valence quarks do not match with the sea quarks leads to scaling violations. A summary of some collaborations cited in the following and the type of fermions they use is given in Table 4.

Every lattice calculation is done in finite volume, finite lattice spacing and finite quark mass. The state of the art calculation involves $L > 2.5$ fm, $a < 0.1$ fm and $M_\pi > 250$ MeV which is still far from the real situation. Actually the Kogut-Susskind (staggered) formulation enables to go to the smallest quark masses. To improve on these numbers demands much more computational efforts which turns out to be quite expensive and are not foreseen for the near future. It thus seems very appreciable to have an analytical method which would help understanding the dependence on these three extrapolation parameters as well as on the diverse approximations which have to be done when one works on the lattice.

In fact CHPT is such a method. For a recent review on the applications of CHPT to lattice QCD see [141]. Here I will just briefly sketch the diverse extensions of this method which have been performed to estimate the size of systematic effects in lattice calculations:

- It was for example proposed [142, 143] to include non-zero lattice spacing in CHPT. In that case the two-step matching procedure to effective field theories (Lattice \rightarrow Symanzik \rightarrow CHPT) has proven to be an appropriate tool [144]. Presently the chiral Lagrangian including the $\mathcal{O}(a^2)$ lattice artifacts has been derived [145]. It is indeed important to go up to that order since lattice spacings in current unquenched simulations are not very small. Also it will allow to learn how the continuum limit is approached in the case of the improved Wilson fermions since for these fermions the leading corrections are precisely of that order.

- Finite volume effects have also been examined within CHPT [146, 147]. Gasser and Leutwyler [148, 149] were the first to extend the CHPT framework to a finite volume: it becomes a systematic

expansion in both the quark masses and the inverse box size. In order for CHPT to be valid L has to fulfil the following condition: $L \gg 1/2F_\pi \sim 1\text{ fm}$, where $4\pi F_\pi$ has been taken as the chiral symmetry breaking scale. There is another important relation which has to be considered namely the one between the pion mass M_π and L . Indeed it determines the importance of the Goldstone boson zero modes in the evaluation of the path integral in CHPT. $M_\pi L \ll 1$ defines the so called ϵ -regime, there the contribution from the zero-modes are non-perturbative and one has to modify the usual power counting. Approaching the chiral limit on the lattice implies working in this regime. In the other extreme, $M_\pi L \gg 1$, one is in the p -regime, standard CHPT can be applied. In that case, finite-volume effects are typically small, deviations are exponentially suppressed by factors of $M_\pi L$ and relevant for very precise lattice calculations. Calculations done within the ϵ and p regime can be found for example in [38, 150, 151] in the meson case and in [152, 153] in the nucleon one. Note that finite volume effects start only at the one loop level requiring two-loop calculations to check the convergence of the series. As has been pointed out in [154] another regime could be of interest for heavy objects as the nucleon, the so-called ϵ' regime. There, the behavior of observables are explored in highly asymmetric volumes, long in the time-dimension allowing these heavy objects to be near their mass-shell, and short in the spatial dimensions.

- Staggered CHPT has been developed in order to control the extrapolation and the taste breaking. The chiral Lagrangian for one single staggered fermion was first derived by Lee and Sharpe [155] considering the quark mass and a^2 to be of the same order. Aubin and Bernard have generalized it to n staggered flavors and shown how to accommodate the root square trick in loop calculations [156]. A discussion of the validity of the procedure can be found in [157]. Fitting their lattice data to NNLO calculations [158] the MILC collaboration has provided a sensitive test of the lattice simulations and especially of the chiral behavior, including the effects of chiral logarithms. Most of the studies so far involve the mesons, however staggered lattice artefacts have also recently been incorporated into heavy baryon CHPT [159]. Extension of CHPT to mixed actions have also been performed [160].

- All these extensions are done using dimensional regularization or some other continuum regularization method. An interesting development is the definition of lattice CHPT as an effective theory that exists directly in the same discrete space-time where lattice QCD resides [161–163].

We have demonstrated that CHPT is a useful tool to understand some of the limitations linked with calculations done on the lattice. However the inverse is also true: lattice calculations are a useful tool for determining hadron properties within CHPT. Indeed we have seen in Section 2 that in this last framework low-energy constants appear which are not fixed by symmetry considerations but are in principle calculable in QCD, the underlying fundamental theory. This is where lattice QCD enters. Already a lot of effort has been made to pin down some of the $\mathcal{O}(p^4)$ low-energy constants in the meson sector [158] especially the combination $2L_8 - L_5$ whose knowledge is required to test whether the up quark mass is massless [164–166], see also section 2.3.2. It was suggested in [152] that the low-energy constant c_3 of the nucleon chiral Lagrangian could be determined by fitting to the nucleon mass at a magic ratio $\beta = 1.22262L$ where β is the temporal extend of the box and L the size in the spatial direction, however, there exists at present no lattice determination of any LECs in the baryon sector.

3 Chiral extrapolations

Numerous works on chiral extrapolation have been done in the last years in the meson sector as well as in the baryon one. In this section I will essentially report on the quark mass extrapolation of some physical nucleon properties in continuum CHPT. One will have of course to keep in mind that the lattice artifacts might not be small. I will also touch upon the question of how to treat unstable particles in a finite volume. In the next subsections I will concentrate on SU(2) and leave the discussion of the SU(3) case for the last section.

3.1 Nucleon mass

The nucleon mass is particularly interesting from the lattice point of view since, once chiral extrapolation will be under control, it will be one of the best ways to estimate the lattice spacings. The general expression for the nucleon mass to fifth order [167] is given in terms of the leading term in the chiral expansion of the pion mass M by (the fourth order calculation can be found in [168, 169]):

$$m = m_0 - 4c_1 M^2 - \frac{3g_0^2 M^3}{32\pi F^2} + k_1 M^4 \ln \frac{M}{m} + k_2 M^4 + k_3 M^5 \ln \frac{M}{m} + k_4 M^5 + \mathcal{O}(M^6) \quad (49)$$

where m_0 and g_0 are respectively the nucleon mass and the axial coupling in the chiral SU(2) limit. For a recent full two-loop expression involving terms up to M^6 see [170]. Replacing in Eq. (49) M^2 by its one loop result brings an extra M_π^4 contribution proportional to the LEC l_3 from the $\mathcal{L}_{\pi\pi}^{(4)}$ Lagrangian. The coefficients k_1 and k_2 are combinations of second (c_1, c_2, c_3) and fourth order LECs while k_3 and k_4 involves the third order (d_{16}, d_{18}, d_{28}) as well as the fourth order LECs from the meson sector l_3 and l_4 :

$$\begin{aligned} k_1 &= -(3/32\pi^2 F^2)(-8c_1 + c_2 + 4c_3 + g_A^2/m_0) \quad , k_2 = -4e_1 + (3/128\pi^2 F^2)(c_2 - 2g_A^2/m_0) \quad , \\ k_3 &= (3/1024\pi^3 F^4)(16g_0^2 - 3) \quad , \\ k_4 &= (3/32\pi F^2)((2l_4^r - 3l_3^r)/F^2 - 4(2d_{16}^r - d_{18})/g + 16d_{28}^r + g_0^2/(8\pi^2 F^2) + 1/8M^2) \quad . \end{aligned} \quad (50)$$

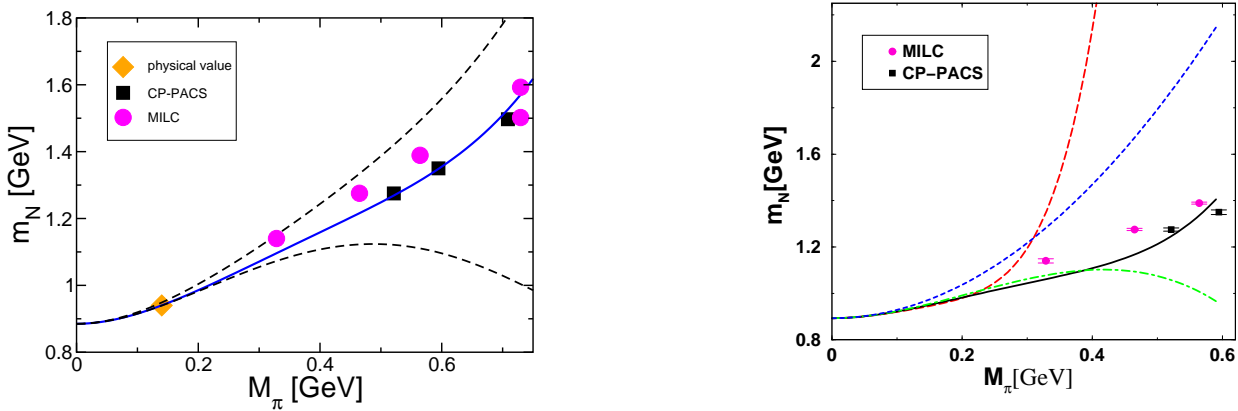


Figure 4: Nucleon mass. Left panel: the solid line refers to the best fit and the dashed line to the theoretical uncertainty. Results are from Ref. [118]. Right panel: convergence of the chiral series. The long-dashed, solid, dot-dashed and dashed lines correspond to $n = 5, 4, 3, 2$, respectively, where n is the order of the series (without theoretical errors).

Apart from a combination of three different fourth order LECs denoted by e_1 , the values of all these low-energy constants are known within some error bars as has been discussed in Section 2.3.2. Thus the coefficient of the M^5 term is rather well determined. The $\mathcal{O}(p^4)$ result for the nucleon mass [118] is shown on the l.h.s. of Fig. 4 in comparison to the lattice data from MILC [171] and CP-PACS [172]. There are also published results concerning the hadron masses from the JLQCD [173] and UKQCD and QCDSF [174, 175] collaborations not shown here, which remarkably fall (with a rather good accuracy) onto the same curve as the CP-PACS one even though they correspond to different lattice actions and algorithms (see for example [176]). An extremely good fit of the lattice data up to amazingly large values of the pion mass is obtained with $c_1 = -0.9$, $c_2 = 3.2$, $c_3 = -3.5$ (all in GeV^{-1}) and $e_1(m) = -1 \text{ GeV}^{-3}$ where g_0 and F have been taken at their physical values. With these parameters the chiral limit value of the nucleon mass is 0.89 GeV. In this fit the constraint that m gets its physical value at the physical value of M_π was imposed. The fact that the c_i 's are consistent with their expected values and that e_1 is of natural size has led in some literature (see for example [100]) to the claim that the chiral expansion is valid up to rather high pion masses. This is of course not correct. First of all as shown on Fig. 4 there

is a rather large theoretical uncertainty as M_π becomes large due to our rather bad knowledge of e_1 . Secondly as naively expected the convergence of the series worsens as M_π increases as is clearly seen on the r.h.s. of Fig 4. There c_3 is taken at its somewhat bigger central value and F and g as obtained from chiral extrapolation (see Eq. (12) and Section 3.2), $F = 86.5$ MeV, $g = 1.2$, $\bar{d}_{16} = -1.76$ GeV $^{-2}$ and $e_1 = 5$ GeV $^{-3}$. One gets the following result (with coefficients in appropriate units of powers of GeV):

$$m = 0.893 + 3.6M^2 - 5.74M^3 - 20.01M^4 \ln \frac{M}{m} + 8.62M^4 + 55.99M^5 \ln \frac{M}{m} + 213.38M^5 + \mathcal{O}(M^6) , \quad (51)$$

where the large contribution to the M^5 terms comes essentially from the d_i . In this expression all but the M^4 and the M^5 terms (the one independent of the \ln terms) are known to a very good approximation. At the physical value of the pion mass this leads to $m = 0.893(1+0.078-0.017-0.015+0.006)$ MeV which is a rather well converging series. Note that one should compare the $O(p^2)$ with the full one loop $O(p^4)$ and full two-loop $O(p^6)$ (not yet analysed) results. An early attempt to quantify the errors associated with terms of order higher than M_π^4 can be found in [153]. In view of Fig. 4 the chiral extrapolation can be trusted for pion masses below ~ 350 MeV. Calculations of the nucleon mass including the Δ as an explicit degree of freedom have also been performed [177, 178] leading to similar fits.

Here we have studied the nucleon mass as an expanded series in M_π discussing the range of validity of the calculation keeping in mind that CHPT is by construction a “**low energy effective field theory**”. In the literature another philosophy has also been pursued based on the observation that the lattice data show a slow variation as the pion mass becomes moderately large presenting a clear signal that the higher order terms must cancel as M_π increases toward big values. The idea is thus to try and fit the data in the mass range covered by the simulation by not expanding the series but keeping all possible higher order terms within one regularization (this automatically excludes HBCHPT and the IR regularization). The first to have done so in a series of paper is the Adelaide group [179], introducing some model-dependence by the use of some regularized functions. More recently Pascalutsa and Vanderhaeghen [180] have obtained a good fit of the nucleon mass within the EOMS framework where the regularized one-loop functions indeed tend to zero for large masses. Let me point out a few problems in these works. First, there is no systematic studies of baryon properties within these frameworks so that the values of the LECs are unknown in these cases. As already discussed they can be in principle somewhat different from the one discussed in Section 2.3.2 if the higher order terms turned out to be important. As we have seen in that section LECs are *not* independent but relate many observables so that it is mandatory to check whether the values obtained via a fit to the lattice data are relevant for other processes. Furthermore these calculations are done at one loop-order only. Even though the function obtained

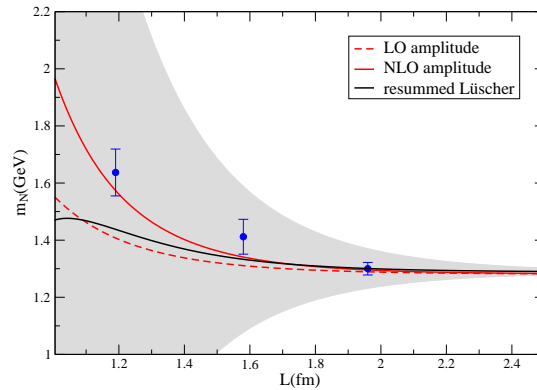


Figure 5: Finite volume effect for the nucleon mass as a function of L for $M_\pi = 0.545$ GeV. The lattice data are from Ref. [182]. The shaded band represents the uncertainty of the calculation. Figure taken from [183].

has the requested proper smoothness property it is not clear how the result would be modified would a two-loop calculation be done. For example let us expand the nucleon mass as given in [181]. One finds with a monopole regulator: $m = 0.898 + 3.09M^2 - 5.74M^3 + 5.77M^4 \ln(M/m) + 23.6M^4 - 45.0M^5$. The non-analytic $M^5 \ln(M)$ term coming from a two-loop calculation is totally absent in this framework. This has, however, a fixed coefficient independent of the regularization as long as this one does not violate chiral symmetry as can be seen from Eqs.(49) and (50). Its contribution at moderate M_π is, however, non-negligible. Note also that the $M^4 \ln(M)$ term is far from its expected value, cf. Eq. (51).

An important quantity related to the nucleon mass is the so-called sigma term defined as: $\sigma_{\pi N} = \langle N(p) | \hat{m}(\bar{u}u + \bar{d}d) | N(p) \rangle$. Best fits of the nucleon mass to the lattice data give $\sigma_{\pi N} \sim 40 - 50$ MeV whatever the regularization used or whether one works with Δ degrees of freedom or not [100, 177]. This value is consistent with [80, 83], see the discussion in Section 4.1.1.

The question is: what is the validity of the comparison between the CHPT calculation in the infinite volume limit and the lattice calculation? In the case of a stable particle of mass m the finite-size corrections to the lowest energy level given by the poles of the propagator vanish exponentially, $E_1(L) - m = \exp(-\text{const} \cdot L)$ and in the large L limit this level yields the value of the stable particle (see e.g. [149, 184]). In Fig. 5 where the nucleon mass is drawn as a function of L for $M_\pi = 0.545$ GeV a comparison of a lattice versus a CHPT calculation is made. As can be seen, for rather large values of L , $L > 2$ fm, good agreement is obtained between the two calculations. It has been shown [185] using a resummed Lüscher formula [146, 186] that the finite volume effects for nucleon mass inside a $L = 2$ fm box are below 4% within the error bars for a pion mass of the order of $M_\pi = 0.5$ GeV. What happens for lower values of L ? NLO results have been obtained in [175] which show a very good agreement with the lattice data. The significance of this agreement has been questioned in [183] since no estimate of the uncertainties had been made. Using a resummed Lüscher formula it was found that the inclusion of higher orders spoiled the good agreement as is illustrated on Fig. 5. Even worse, the uncertainties turned out to be extremely large which can be seen from the shaded area in the figure, so that at present it appears difficult to make reliable predictions for the size of the finite volume effects in the nucleon sector in contrast with the meson sector. This is due to the fact that chiral symmetry restricts πN interactions less severely than pionic ones. However, it is necessary to pursue the effort since such studies give further constraints on the LECs, different combinations entering the finite volume corrections [178].

3.2 axial-vector coupling

The axial-vector coupling constant g_A is a fundamental property of the nucleon that can, e.g. be determined in neutron β -decay. It is directly related to the fundamental pion-nucleon coupling constant by the Goldberger-Treiman relation, Eq. (17) and thus of great importance for the problem of nuclear binding. Its formal expression up to two-loop is given by:

$$\begin{aligned} g_A &= g_0 \left\{ 1 + \left(\frac{\alpha_2}{(4\pi F)^2} \ln \frac{M_\pi}{\lambda} + \beta_2 \right) M_\pi^2 + \alpha_3 M_\pi^3 \right. \\ &\quad \left. + \left(\frac{\alpha_4}{(4\pi F)^4} \ln^2 \frac{M_\pi}{\lambda} + \frac{\gamma_4}{(4\pi F)^2} \ln \frac{M_\pi}{\lambda} + \beta_4 \right) M_\pi^4 + \alpha_5 M_\pi^5 \right\} + \mathcal{O}(M_\pi^6), \\ &= g_0 \left\{ 1 + \Delta^{(2)} + \Delta^{(3)} + \Delta^{(4)} + \Delta^{(5)} \right\} + \mathcal{O}(M_\pi^6). \end{aligned} \quad (52)$$

The coefficients up to one loop have been first worked out by [169]:

$$\begin{aligned} \alpha_2 &= -2 - 4g_0^2, \quad \beta_2 = \frac{4}{g_0} \left(d_{16}^r(\lambda) - 2d_{28}^r(\lambda) \right) - \frac{g_0^2}{(4\pi F)^2}, \\ \alpha_3 &= \frac{1}{24\pi F^2 m_0} (3 + 3g_0^2 - 4m_0 c_3 + 8m_0 c_4). \end{aligned} \quad (53)$$

At the physical pion mass and for the central values of the LECs one has $g_A = g_0(1 - 0.15 + 0.26 + \dots)$. The corrections $\sim M_\pi^2$ are of natural size, however the corrections $\sim M_\pi^3$ are unnaturally large. This comes from the rather large values of each of the c_i combined with the fact that they are of opposite sign so that their effects get reinforced from their relative minus sign. Clearly if the pion mass increases the effect will be strengthened. One indeed observes a sharp rise of the function beyond $M_\pi \sim 300$ MeV (see Fig.4 in [81]). However lattice data show a rather flat dependence in the pion mass as is illustrated in Fig. 6 where a compilation of these data are presented. Note again the consistency of the lattice results for which different lattice actions have been used. Only the preliminary QCDSF values are somewhat below the others but this could come from a different treatment of the renormalization. A first try to understand these lattice data was made in [193]. The idea was that the Δ degree of freedom should be important in understanding the axial-vector coupling. This is corroborated for example by the Adler-Weisberger relation which relates the deviation of g_A from 1 to the excess of π^+p cross section over the π^-p one where the Δ dominates. Also as we have seen previously the convergence of the chiral expansion could be improved in that way. In this framework some additional terms appear which to $O(\epsilon^3)$ are of the form M_π^3/Δ_0 , $M_\pi^2 \ln R$ and $\Delta_0^2 \ln R$ with $R = \Delta_0/M_\pi + \sqrt{\Delta_0^2/M_\pi^2 - 1}$ and Δ_0 is the small scale parameter defined in Eq. (38) in the chiral limit. In this framework one combination of LECs, $C(\lambda)$, appear which is unknown. In order to determine it, a matching with HBCHPT has been made at a scale $\lambda = 2\Delta_0$, the results being insensitive to the exact choice of this scale between 0.4 and 0.8 MeV. This leads to $C(1 \text{ GeV}) = (-3.4 \pm 1.2) \text{ GeV}$. A flat dependence of g_A was found as is shown on Fig. 7 for the set of parameter $g_0 = 1.21$, $g_1 = 5.6$, and $C(1 \text{ GeV}) = -3.4 \text{ GeV}$, where g_1 is the axial $\Delta\Delta$ coupling constant. However this nice fitting up to rather large pion mass results from a fine tuning of the LECs. First g_1 turns out to be much larger than its $SU(6)$ value in contradiction to what is suggested in the study of the Δ mass (see next section). Furthermore if one lets the LECs vary within their error bars one finds rather large uncertainties in the result as can be seen on Fig. 7. Thus the result of [193] cannot support the claim of a controlled and precise determination of g_A .

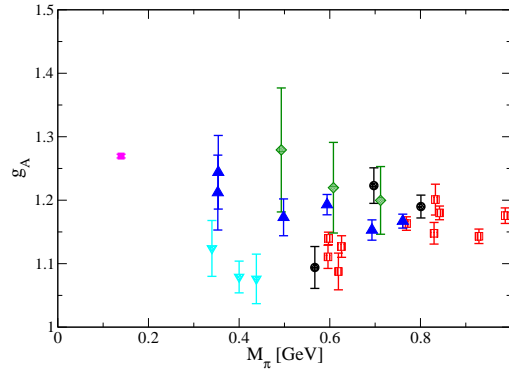


Figure 6: Lattice data: up triangle are from the LPHC/MILC collaboration, Ref. [188], the square from QCDSF/UKQCD [189], the lozenge from RBC [190], the circle from LPHC/SESAM [191] and the down triangle from QCDSF [192].

In view of all this it became clear that a two-loop calculation of g_A was needed. The coefficients $\alpha_{4,5}$, β_4 , γ_4 were determined in [194]. The double logarithm can easily be obtained using renormalization group techniques as was shown in the meson sector by [18]. Indeed the non-local pieces which appear in a two-loop calculation

$$k(d) \frac{\lambda^{2\epsilon}}{(4\pi)^4} \left[\frac{1}{\epsilon^2} + \frac{2}{\epsilon} \ln \frac{M_\pi}{\lambda} + \ln^2 \frac{M_\pi}{\lambda} + \dots \right], \quad (54)$$

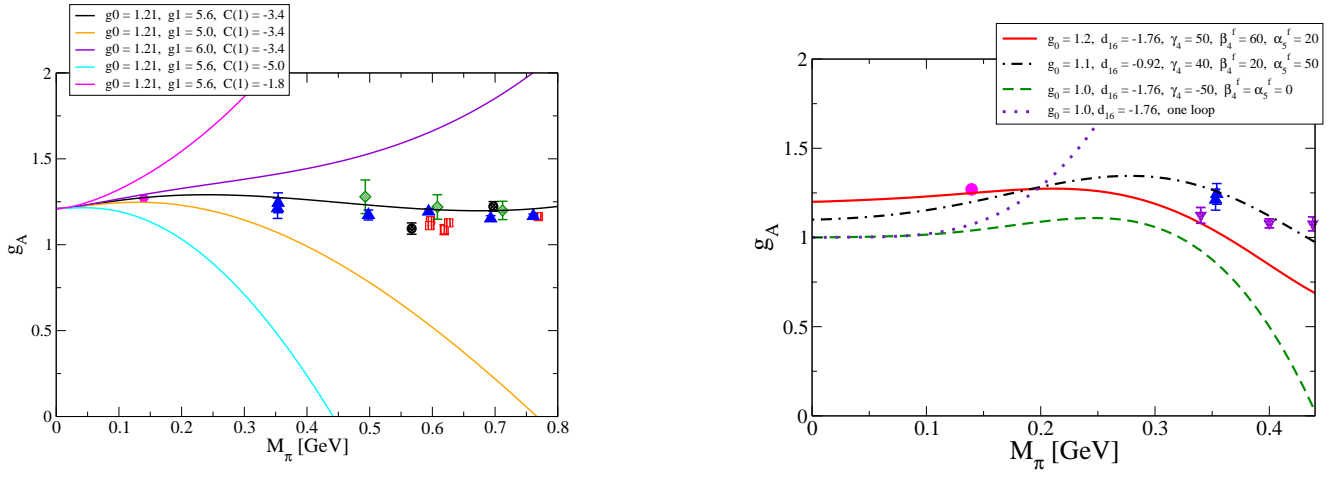


Figure 7: The axial vector coupling as a function of the pion mass. Left panel: SSE result to $\mathcal{O}(\epsilon^3)$. Right Panel: two-loop results as described in the text. The triangle are the lowest mass data from [188] and the inverted triangles are recent results from QCDSF [192].

have necessarily to be cancelled by terms coming from one loop graphs with vertices involving LECs, in the case at hand coming from the πN Lagrangian of dimension 3

$$-\frac{h_i(d)}{2} \frac{\lambda^{2\epsilon}}{(4\pi)^4} \left[\frac{\kappa_i}{\epsilon^2} + \frac{\kappa_i}{\epsilon} \ln \frac{M_\pi}{\lambda} + \frac{(4\pi)^2 d_i^r(\lambda)}{\epsilon} + (4\pi)^2 d_i^r(\lambda) \ln \frac{M_\pi}{\lambda} + \dots \right]. \quad (55)$$

In fact the renormalization group condition $k_0 = h_i^0 k_i$ ensures that this indeed happens. The topologies of the one loop graphs that generate the coefficient of the double log are shown in Fig. 8.

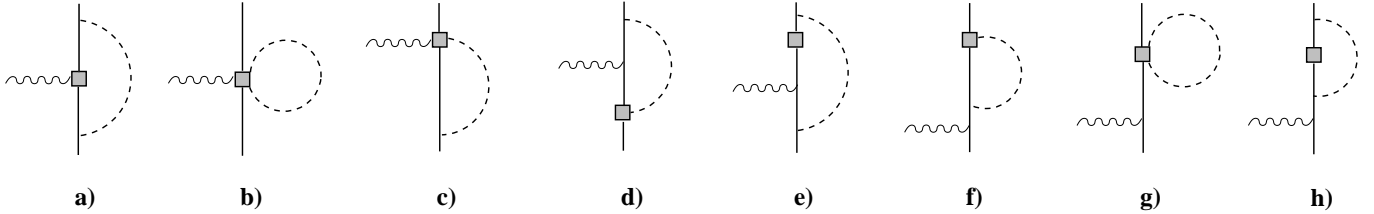


Figure 8: Topologies of the one-loop graphs that generate the coefficient of the double log at two-loop order. The hatched square denotes a dimension three insertion proportional to some of the LECs d_i .

Altogether 8 LECs from the non-equation-of-motion terms contribute, from which d_{16} . From the knowledge of the β functions κ_i [35, 40] one deduces:

$$\alpha_4 = \alpha_4^{\text{irr}} + \alpha_4^{\text{red}} + \tilde{\alpha}_4 = -\frac{16}{3} - \frac{11}{3} g_0^2 + 16 g_0^4. \quad (56)$$

Taking into account the contribution from the LEC d_{16} to γ_4 , the $1/m_0$ and $1/m_0^2$ corrections to the large contribution α_3 and induced terms from the quark mass expansion of the pion decay constant, the numerical values of the two-loop coefficients for the central values of the LECs are:

$$\alpha_4 = 7, \quad \gamma_4 = 115.3 \text{ GeV}^{-2} + \gamma_4^f, \quad \beta_4 = 14.2 \text{ GeV}^{-4} + \beta_4^f, \quad \alpha_5 = -20.3 \text{ GeV}^{-5} + \alpha_5^f, \quad (57)$$

where γ_4^f , β_4^f and α_5^f denote the additional contributions from unknown LECs which have to be determined, e.g. from an analysis of lattice data and assuming naturalness. Some typical examples of

such a fit are shown on the l.h.s. of Fig. 7. One finds that the pion mass dependence of g_A stays flat for $M_\pi \leq 350$ MeV. One obtains at the physical pion mass a good convergent representation, typically $g_A = 1.21(1 - 0.15 + 0.26 - 0.06 - 0.001)$. The finite volume dependence of g_A which I will not discuss here can be found in [195].

3.3 magnetic moment

The magnetic moments provide a nice illustration of the difference between different regularizations. They have been calculated in [196] using a sum rule, for more details see that paper. The proton magnetic moment is given by:

$$\kappa_p = \kappa_0 + \frac{g_A^2 m^2}{(4\pi F_\pi)^2} \left\{ 1 - \frac{\mu (4 - 11\mu^2 + 3\mu^4)}{\sqrt{1 - \mu^2/4}} \arccos \frac{\mu}{2} - 6\mu^2 + 2\mu^2 (-5 + 3\mu^2) \ln \mu \right\}. \quad (58)$$

where $\mu = M_\pi/m$ and κ_0 , the chiral limit value of κ_p , is given by a combination of two LECs of order two: $\kappa_0 = c_6 + c_7$ [90]. Now let us look at the IR result [197]. One has

$$\kappa_p = \kappa_0 + \frac{g_A^2 m^2}{(4\pi F_\pi)^2} \left\{ -\frac{\mu (4 - 11\mu^2 + 3\mu^4)}{\sqrt{1 - \mu^2/4}} \arccos(-\frac{\mu}{2}) - \frac{3}{2}\mu^4 + 2\mu^2 (-5 + 3\mu^2) \ln \mu \right\}, \quad (59)$$

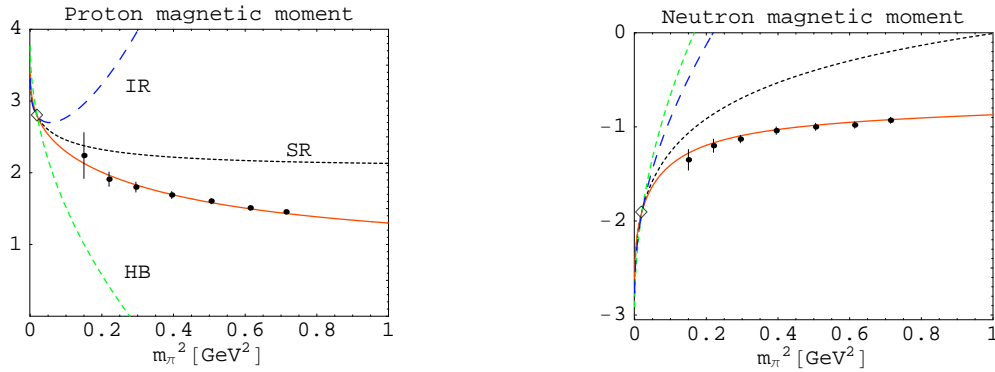


Figure 9: Proton and neutron magnetic moments to one loop compared with lattice data. The open diamonds represent the experimental values at the physical pion mass. For a discussion of the solid line see [196] from which the figures are taken.

The difference in the two expressions only appear – as it should – in the terms that are analytic in the quark mass. In the sum rule approach which is equivalent to the relativistic framework terms violating power counting appear. The term ~ 1 in Eq.(58) is such a term. As explained before it can be absorbed in the LECs, illustrating the fact that the counterterms can have different values in different regularizations. Once this is done, expanding Eqs.(58) and (59) around $\mu = 0$, one recovers the HBCHPT result namely,

$$\kappa_p = \kappa_0 + \frac{g^2 m^2}{(4\pi F_\pi)^2} \left\{ -2\pi\mu - 2(1 + 5 \ln \mu) \mu^2 + \frac{21\pi}{4} \mu^3 + O(\mu^4) \right\}. \quad (60)$$

As pointed out before the argument of the arccos term is positive within the sum rule approach while it is negative in IR. This difference of course affects the high energy behaviour of the magnetic moments. While $\delta\kappa_p = \kappa_p - \kappa_0$ vanishes in the large M_π limit in the first calculation behaving like $1/M_\pi$, it diverges for $M_\pi = 2m$ in the IR case due to these unphysical cuts discussed previously. Let me stress again

that this is not a problem since the region where it becomes large is outside the range of validity of the theory. The M_π dependence of the three calculations, Eqs. (58), (59) and 60) is shown on Fig.9. It coincides up to roughly 350 MeV and starts to depart then. In [81] an investigation of the convergence of the series was made with the same conclusion, namely the theoretical uncertainty is modest up to 350 MeV and starts to increase then. Thus, as for the two other observables discussed above, the chiral extrapolation can be believed up to roughly 350 MeV.

3.4 Δ and Roper masses

3.4.1 infinite volume limit

Other baryon properties have been determined on the lattice. Let me review briefly results on the Δ and the Roper mass.

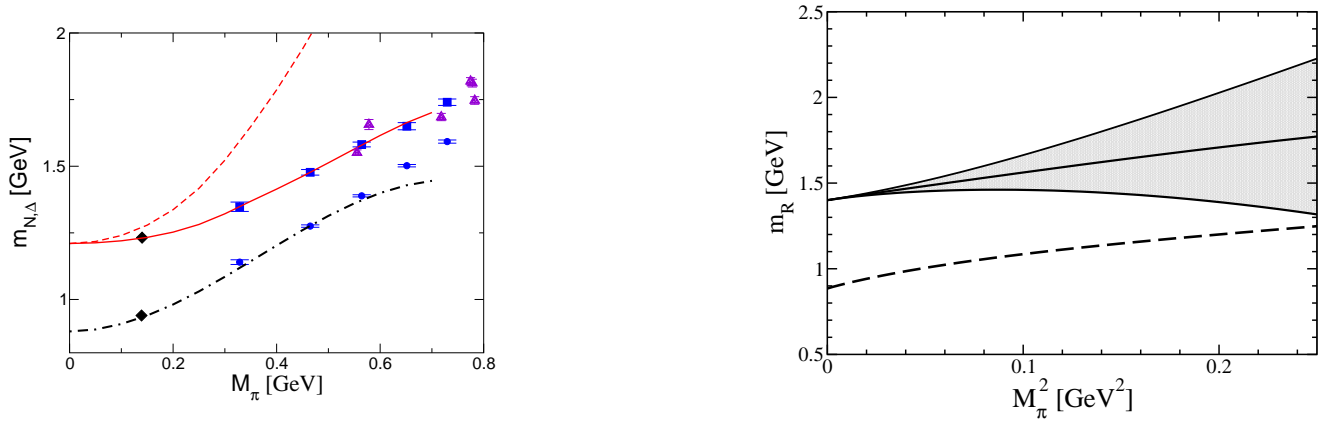


Figure 10: Left panel: The nucleon (dot-dashed line) and the (real part) of the Δ mass (solid line) as a function of the pion mass. The filled diamonds denote their physical values at the physical pion mass. The dashed line is the chiral extrapolation with a_1 fixed at its SU(6) based value. The filled squares and circles are the MILC data [171] and the filled triangles the recent data from QCDSF. Figure from [177]. Right panel: The Roper mass as a function of the square of the pion mass. The grey band indicates the theoretical uncertainties. The nucleon mass, dotted line, is shown for comparison. For more details see [198]. Figure courtesy of Ulf-G. Meißner.

The dependence of the Δ mass on the pion mass can easily be obtained within the SSE framework [177]. To fourth order in the ϵ expansion one obtains:

$$m_\Delta = m_0^\Delta - 4a_1 M_\pi^2 - 4e_1^\Delta M_\pi^4 + m_\Delta^{N\text{-loop}} + m_\Delta^{\Delta\text{-loop}} \quad (61)$$

where $m_\Delta^{N\text{-loop}}$ and $m_\Delta^{\Delta\text{-loop}}$ are the nucleon/ Δ loop contributions respectively. a_1 is the symmetry breaker term analog to c_1 for the nucleon. The vertices involve the axial $N\Delta$ coupling c_A and the $\Delta\Delta$ coupling g_1 as well as 4 unknown LECs, 2 from the $N\Delta$ Lagrangian and two combinations from the $\Delta\Delta$ one. In [177] a combined study of the nucleon and Δ mass was performed. Thus 6 combinations of LECs have to be fitted to the lattice data imposing again the constraint from their physical values at the physical π mass. The dependence of these masses on the pion mass is shown on the l.h.s. of Fig. 10. A good fit is obtained for $g_1 = 2$ not far from its SU(6) value $9g_A/5 = 2.28$ and $a_1 = -0.3 \text{ GeV}^{-1}$ markedly smaller than c_1 although both couplings should be equal in the SU(6) limit. As can be seen from the dashed line in Fig. 10 the assumption of strict SU(6) symmetry is clearly at odds with the lattice data. The smallness of a_1 compared to c_1 leads to a $\pi\Delta$ sigma term much smaller than the nucleon one, $\sigma_{\pi\Delta} = 20.6 \text{ MeV}$. Before drawing any conclusion, constraints from other physical processes

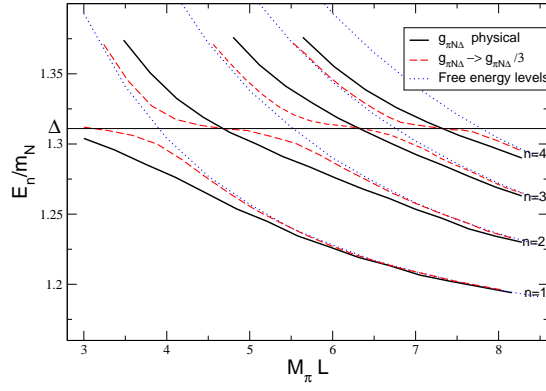


Figure 11: The dependence of the energy levels in a finite box size L for a small value of the coupling constant $g_{\pi N \Delta}$ (dashed line) and its physical value (solid line). For comparison, the free energy levels are also displayed (dotted lines). Figure taken from [201].

would be needed to confirm the values of the LECs obtained. Also more detailed precise fits to the lattice data including error and correlation analysis should be done.

A formalism has been developed in [198] which is suited to study systems with two heavy mass scales in addition to a light mass scale. It has been applied to the case of the Roper resonance $N^*(1440)$, a very intriguing excited state of the nucleon. This first even-parity state is lighter than the first odd-parity one, the $S_{11}(1535)$ and has a significant branching ratio into two pions. The relevant effective Lagrangian needed to study this particle has been given in [198] as well as the modification of the regularization scheme due to the appearance of an extra large mass scale m_R in addition to the already present one, m . The case $m^2/m_R^2 \ll 1$ (in nature this ratio is $\sim 1/2.4$) has been described. Results of the one loop calculation of the quark mass dependence of the Roper mass are shown on the r.h.s. of Fig. 10, using naturalness arguments as well as some bounds from the nucleon to determine the new LECs which appear in the Roper Lagrangian. As can be seen the dependence is similar to the one of the nucleon. It should be emphasized again that the one loop formula cannot be trusted for pion masses beyond 350 MeV. On the lattice side there is not yet a clear picture on the nucleon resonance spectrum. In [199] a rapid cross over of the first positive and negative excited nucleon states is found close to the chiral limit, whether this does not seem to be the case in [200] for example. Simulations closer to the chiral regime are certainly needed.

3.4.2 finite volume

Again arises the question of the comparison between the CHPT calculation discussed here and the lattice data. As we have seen lattice calculations are not only done in a finite volume but also at rather high pion masses so that the “lattice Δ particle” contrary to the physical one does not decay. The calculation thus proceeds in exactly the same way as for the nucleon discussed above. At some point, however, lattice calculations will reach values of pion masses for which the Δ will be unstable. Clearly unstable particles are more complex to treat than the stable ones. The question of identification of the resonances on the lattice has been addressed in a series of papers [202–206]. It has been demonstrated that, in the presence of a narrow resonance, the dependence of the energy spectrum of the system on the box size L exhibits a very peculiar behavior near the resonance energy, where the so-called “avoided level crossing” takes place, for more details see the references above. In this case the dependence of the energy levels on L is governed by a power rather than by an exponential law. In [201] the specific question of how to determine the mass of the Δ in an effective field theory approach has been discussed. Several questions arise:

- Lattice data being always real, does one get only the real part of the resonance pole mass as a result of a chiral extrapolation?

- Is there a way to determine the decay width of a resonance?

Typical energy levels obtained in the $\mathcal{O}(\epsilon^3)$ SSE calculation [201] are shown on Fig. 11. It is seen that the energy levels in the presence of an interaction interpolate between different free energy levels. An abrupt change emerges in the vicinity of the resonance when $g_{\pi N\Delta}$ is taken at 1/3 of its physical value, nicely illustrating the phenomena of avoided level crossing. In the case of the physical value, the width of the Δ is too large and the phenomenon is washed out. In that case the mass cannot be determined so easily. However the lowest energy level E_1 and the difference between the first two lowest energy levels $E_2 - E_1$ show some significant dependence in the Δ mass and in the $\pi N\Delta$ coupling respectively. It was thus suggested in [201] to use these properties to determine the mass and $g_{\pi N\Delta}$: having fixed a value for the coupling constant the Δ mass is obtained from the $M_\pi L$ dependence of E_1 . Then a fit of $E_2 - E_1$ to the data gives a new value for the coupling constant, the finite volume results for m_Δ and $g_{\pi N\Delta}$ being obtained once convergence is achieved.

CONCLUSION: From the analyses done above it is fair to say that *chiral extrapolations of nucleon properties can be trusted for pion masses below ~ 350 MeV.*

4 Pion-nucleon and Pion-deuteron scattering

Let us come back to the real world and look at some applications of the CHPT machinery. A systematic investigation of processes involving pions will allow to understand in a precise manner how the chiral symmetry violation takes place. In this section I will concentrate on elastic πN and πd scattering.

4.1 πN scattering

Elastic pion-nucleon scattering has been one of the most intensively studied process in hadron physics with a long history in theory and experiment (e.g. [207]). In chiral perturbation theory it has been studied within different regularization approaches [77, 78, 208–211] and isospin symmetry breaking effects have been evaluated. As we will see the experimental situation is unfortunately not yet totally satisfactory. There has been two generations of πN measurements. The first two decades (1957 through 1979) of experiments focused on the πN system and nonstrange baryon resonances and produced a large amount of data below 2.6 GeV. These were analysed for example in [212]. A second generation of πN measurements (both unpolarized and polarized) were carried out at high-intensity facilities such as LAMPF, TRIUMF, and PSI. These more recent measurements generally have small statistical and systematic uncertainties. Some of them are included in the analysis discussed here [213, 214]. Other very recent ones [215–217] are still being analysed [218]. Particular interest in these recent experiments comes from the fact that they were done at very low energy where information is still missing and there are regions where existing experimental data are contradictory. Clearly more precise data at energies below 100 MeV are still needed to get a precise knowledge of πN scattering amplitude and to finally settle the problem of the σ term, the πNN coupling as well as the isospin breaking effects which will be discussed here. However as we have seen in Section 2.3.2 some LECs could still be obtained with rather good precision. Note that in the most recent analysis of these data [218] where an overall fit up to 2.6 GeV is done no important changes were found in the low energy region which we are concerned here, so that results reported in this review based on older data should not be altered.

The scattering amplitude for the process $\pi(p, a)N(q) \rightarrow \pi(p', a')N(q')$ is given by (with a, a' isospin indices)

$$T_{a'a} = \delta_{a'a} T^+ + \frac{1}{2} [\tau_{a'}, \tau_a] T^- , \quad (62)$$

$$T^\pm = \bar{u}' \left(A^\pm + \frac{1}{2} (\not{q}' + \not{q}) B^\pm \right) u = \bar{u}' \left(D^\pm - \frac{1}{4m} [\not{q}', \not{q}] B^\pm \right) u ,$$

where $D = A + \nu B$ with $\nu = (s - u)/4m$, s and u being the usual Mandelstam variables. Note that the usual decomposition in terms of the A and B amplitudes is best suited for a dispersive analysis while it is not useful when performing a low energy expansion since the leading contributions from these amplitudes cancel [41].

4.1.1 isospin symmetric case

Calculations of πN scattering in the isospin symmetric case have been performed in CHPT up to fourth order. The amplitudes decompose into three pieces, the tree and counterterm parts of polynomial type and pion loop corrections which start at order q^3 . The number of counterterms are 4, 9 and 14 to orders q^2 , q^3 and q^4 , respectively. As already noted this is much less than the total number of terms in the Lagrangian allowed at the various orders. In fact these numbers can be determined by looking at the most general polynomial for A^\pm and B^\pm . The values of these counterterms have already been discussed in Section 2.3.2. Explicit expressions for the amplitudes can be found in [77] for HBCHPT. An analysis of these amplitudes using dispersion relations has been performed by [78] as an alternative regularization procedure. It has indeed been shown in this paper that the result of the dispersive representation agrees with the representation in terms of infrared regularized loop integrals up to terms that are beyond the accuracy of a one loop calculation. It has the advantage that it exhibits the structure of the amplitude in a more transparent way and involves only the expressions for the imaginary parts which are determined from the tree level amplitude due to unitarity. For a very recent review on the relation between CHPT and dispersive analysis, see [14].

- phase shift analysis

The strategy in [77] is to fit to the phase shifts provided by three different partial wave analysis [212–214] for pion momentum in the laboratory frame typically in the range from 40 to 100 MeV. This allows a determination of the LECs as well as a prediction of the threshold parameters and of the phase shifts at higher energies. On the upper panel of Fig 12 we show the result of such a fit for two partial waves, namely S_{11} and P_{33} in the case of the KA85 analysis. The two other analysis give comparable results. As can be seen the fits are rather good with a χ^2/dof of 0.5. In these plots the dot-dashed, dotted, dashed and solid lines show the contributions from the amplitude up to first, second, third and fourth order, respectively. The convergence is rather good, the fourth order contribution is mostly rather small. Other partial waves can be found in [77] with the same conclusion for the quality of the fit and the convergence of the series.

The representation of the scattering amplitude to $O(q^4)$ incorporates the pole and cuts generated by the exchange of one or two stable particles (nucleons or pions) but account for all other singularities only through their contributions to the effective coupling constants. However, resonances generate poles on unphysical sheets of the scattering amplitude, the first resonance in the s - and u - channels being the $\Delta(1232)$ and the ρ in the t -channel. Whereas in the region $|t| \leq 10M_\pi^2$ the ρ meson pole which occurs at $t \sim 30M_\pi^2$ is well represented by a polynomial the situation is different for the Δ . A description of the πN amplitude has thus been considered within an effective theory with explicit Δ degrees of freedom [219]. On the lower panel of Fig 12 is shown a fit comparable to the upper one just discussed but now with the Δ included in a third order calculation in the small scale expansion as described in Section 2.3.2. As expected a clear improvement on the description of the resonant P_{33} phase-shift is obtained, an extremely good fit being extended up to pion momentum in the laboratory of 300 MeV. For the other partial waves the fits are comparable to the fourth order one although the overall description is still better here. Note that to this order the number of counterterms is the same as in the effective theory without Δ up to fourth order. Also in all these fits with and without Δ the counterterms are all

of natural sizes.

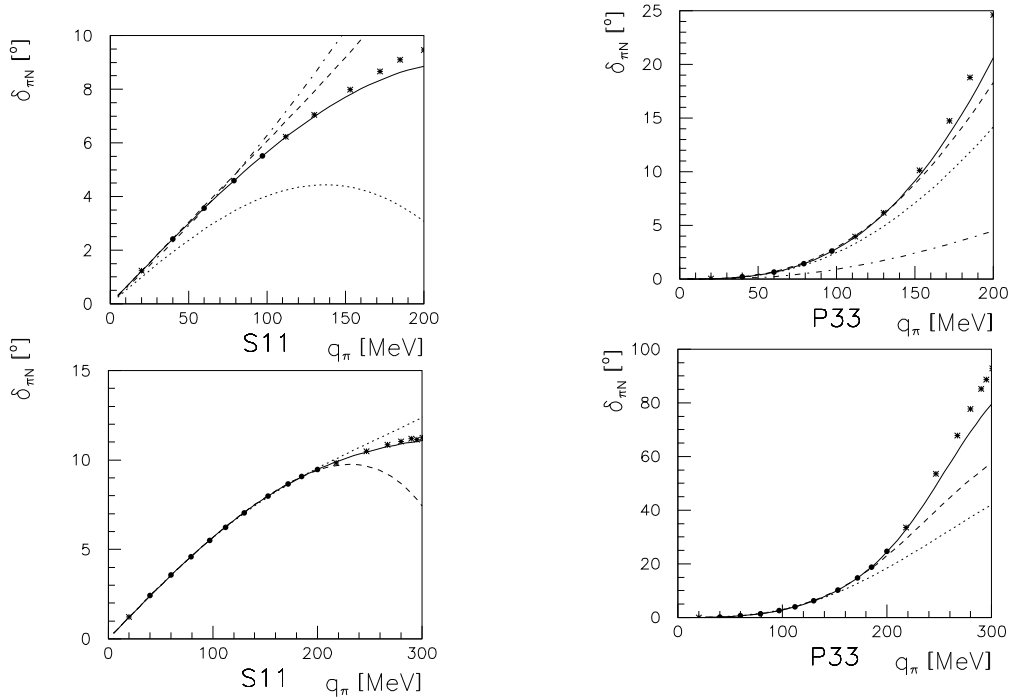


Figure 12: Fit to the KA85 phases (solid dots) between 40 and 97 MeV and predictions for higher and lower energies for two phase shifts as a function of the pion laboratory momentum q_π . The various lines refer to the contributions from the various order as explained in the text. Note the different scales on the different panels. Figure from [77, 219]

A different strategy has been used in [78]. There the four LECs are determined from four equations relating them either to threshold or subthreshold parameters, but, as noted in Section 2.3.2, at tree level. Differences are in principle of higher orders. However, this leads to values for the c 's about 1.5 times smaller. For example

$$c_3 = -a_{01}^+ F_\pi^2 - \frac{g_A^2 M_\pi}{16\pi F_\pi^2} \left(g_A^2 + \frac{77}{48} \right), \quad (63)$$

which leads to a correction of 40% compared to the tree result. In this equation a_{01}^+ is the standard notation for one coefficient in a subthreshold expansion around $\nu = t = 0$ of the πN amplitude. Hence, using the Karlsruhe analysis the one-loop result [78] for the total cross section starts deviating from the experimental values already at rather low energies. It has thus been stressed in this reference that the work of [220] would not describe well the subthreshold amplitudes. This would of course be true if one would do a tree level calculation. However taking into account higher order corrections as given in [50] one obtains an overall good description of the subthreshold quantities. Discrepancies for some quantities clearly survive especially in the isoscalar case. As discussed in [78] the one loop result for the contribution of the dispersion integrals to D^+ at $\nu = M_\pi$, $t = 0$ is a factor of two smaller than the experimental result. Even though these are small effects they do indeed matter at the level of accuracy needed in the discussion of some low-energy theorems of chiral symmetry (see below).

- low energy theorems and scattering lengths

Chiral symmetry imposes two constraints on πN scattering. There are different ways of implementing them. Either one writes two relations for the subthreshold coefficients or two low-energy theorems. The first variant of these theorems concerns the scattering amplitudes D^+ and D^- both evaluated at

the Cheng-Dashen point $\nu = 0$, $t = 2M_\pi^2$ [221, 222]. The first low-energy theorem

$$\Sigma = \sigma(2M_\pi^2) + \mathcal{O}(M_\pi^2) \quad (64)$$

relates the quantity $\Sigma = F_\pi^2 \bar{D}^+(0, 2M_\pi^2)$, where D is defined in Eq. (62) and the bar means that the pseudoscalar Born term is subtracted, to the scalar form factor of the nucleon

$$\langle N(p') | m_u \bar{u}u + m_d \bar{d}d | N(p) \rangle = \sigma(t) \bar{u}'u, \quad t = (p' - p)^2. \quad (65)$$

The difference between Σ and $\sigma(2M_\pi^2)$ has been evaluated in [223] and found to be of order $\mathcal{O}(M_\pi^4)$ and free of infrared singularities up-to-and-including that order. This result was later confirmed [78]. It is expected to be a small correction since one is comparing the properties of the amplitude at the Cheng-Dashen point with those at $s = u = m^2 + M_\pi^2$, $t = 0$. In this region, the amplitude does not contain branch points and the relevant distance is small, of order M_π^2 . In fact it was estimated to be of the order of 1 MeV so that the deviation to the low-energy theorem is rather small.

The second of the two low-energy theorem reads

$$C = F_\pi^2 \frac{\bar{D}^-(\nu, t)}{\nu} \Big|_{\nu=0, t=2M_\pi^2} = 1 + \mathcal{O}(M_\pi^2). \quad (66)$$

The difference to one contains in that case infrared singularities and starts already at order M_π^2 . It was evaluated in [78] and found to be equal to 0.02 ± 0.01 .

Another variant of these low-energy theorems are the Weinberg's current algebra prediction [224] for the scattering lengths:

$$a^+ = \mathcal{O}(M_\pi^2), \quad a^- = \frac{M_\pi}{8\pi(1 + M_\pi/m)F_\pi^2} + \mathcal{O}(M_\pi^3), \quad (67)$$

where $a^\pm = 1/4\pi(1 + M_\pi/m)^{-1}T^\pm(M_\pi)$. In this case the corrections are expected to be large (for a first calculation see [49]). Indeed the amplitude is analyzed at a singular point, the threshold sitting on top of the branch point required by unitarity. The πN scattering analyses of the scattering lengths [78, 220] lead to a range of values,

$$a^+ = -0.83 \cdots 0.5, \quad a^- = 7.7 \cdots 9.2, \quad (68)$$

in units of inverse powers of the pion mass times 10^{-2} compared to the Weinberg's results $a^+ = 0$, $a^- = 8.76$, Eq.(67) in the same units. In [220] good fits of these quantities have been obtained and it was shown that the series converges well.

However the most direct way to get a handle on these threshold quantities experimentally is the measurement of the strong interaction shift and the decay width in pionic atoms. A whole effort is being pursued in PSI in order to get to these quantities as well as on the πNN coupling constant to better than a percent. I will come back to the discussion of the scattering lengths in more detail when discussing pionic deuterium and isospin breaking.

• σ - term

One quantity of great interest is the σ -term, $\sigma(t=0)$, see Eq. (65) since it is related to the strange quark content in the nucleon, y :

$$\sigma(t=0) = \frac{\hat{\sigma}}{1-y}, \quad y = \frac{2\langle N | \bar{s}s | N \rangle}{\langle N | \bar{u}u + \bar{d}d | N \rangle} \quad (69)$$

where the canonical result $\hat{\sigma} = 35 \pm 5$ MeV which measures the nucleon mass shift away from the chiral limit ($m_u = m_d = 0$) is due to Gasser [112] based on SU(2) CHPT. A more recent determination [225]

gives $\hat{\sigma} = 36 \pm 7$ MeV. The determination of the σ -term and thus of y has spawned a whole generation of πN scattering experiments. Indeed the canonical value obtained by Koch in the 80's [226] yielded $y = 0.11 \pm 0.07$ a value considered large in light of results from e.g. neutrino scattering.

Up to $O(q^3)$ the σ -term can be directly calculated. However at next order appears a combination of LECs denoted e_1 in Section 3.1 which has no pion matrix-element and therefore cannot appear in the scattering amplitude. One can then evaluate the σ -term indirectly using the low energy theorem, Eq. (64) and the fact that the difference $\sigma(2M_\pi^2) - \sigma(0)$ is well understood – the evaluation within CHPT confirms the result of the dispersive analysis [227], $\sigma(2M_\pi^2) - \sigma(0) = 15.2 \pm 0.4$ MeV:

$$\sigma = \Sigma - \sigma(2M_\pi^2) + \sigma(0) + \Delta = \Sigma - (15.2 \pm 0.4 \pm 1) \text{ MeV} . \quad (70)$$

In this equation use has been made of $\Delta \sim 1$ MeV as discussed previously. A rather large range of values for Σ at $O(q^4)$ has been obtained depending on the way of evaluating it. In [83] it is divided into two subthreshold parameters plus a curvature term Δ_d which is determined using $\pi\pi N\bar{N}$ phase shifts extrapolated from the KH80 πN phases. A variant which contains some fourth order pieces has been given in [228]. One gets $\Sigma \sim 61 \dots 104$ MeV which can be translated into $\sigma \sim 46 \dots 89$ MeV. There is still controversy concerning the empirical value of Σ . The latest analysis of the VPI/GW group advocates a rather large value $\Sigma = 79 \pm 7$ MeV while the older Karlsruhe one gives a smaller value 64 ± 8 MeV. Such a large value of Σ and thus of σ leads to an astonishingly large value of y . It would certainly be of great interest to have a lattice determination of the σ -term, the question being how long one will have to wait for having the desired precision to settle the problem. For an attempt, see e.g. [100].

Even though a lot of work has been done, the analysis of πN scattering has not yet reached the high precision of the $\pi\pi$ scattering case where the amplitude is now known in the threshold region to an amazing degree of accuracy solving Roy equations below 800 MeV [32]. Such an analysis remains to be done for πN using the Roy type equations which have been derived in [78], allowing to link the physical and the subthreshold region.

4.1.2 isospin violating case

Having obtained a rather accurate representation of the isospin symmetric amplitude one can attack the more subtle problem of isospin violation. Indeed it has been pointed out by Weinberg already in the seventies in his seminal paper [229] that reactions involving nucleons and neutral pions might lead to gross violations of isospin symmetry. This was reformulated in more modern terminology in [230]. However in order to really pin down isospin breaking due to the light quark mass difference one needs a machinery that allows to *simultaneously* treat the electromagnetic and the strong contributions. CHPT is such a machinery, it is in fact the only known framework at present which allows to do so.

i) formalism

Efforts to include virtual photons were first done in the meson sector. An extended power counting [52, 231–234] is introduced since one has to deal now with an expansion in the small momenta/masses (the chiral expansion) and a second one in the electromagnetic coupling. A priori, these two expansions can be treated separately. It was proposed in [231] based on the observation that $e^2/4\pi \sim M_\pi^2/(4\pi F_\pi)^2 \sim 1/100$ to count the electric charge as a small momentum

$$e = \mathcal{O}(p) , \quad (71)$$

which is the most economic way of organizing the double expansions in terms of one. Along the same line, the construction of the generating functional of two flavor HBCHPT in the presence of virtual photons with all finite terms up-to-and-including third order in the chiral dimension was then done

in [235, 236] and extended to fourth order in [237] where the relativistic case was also considered. It turns out that contrary to the pions where G parity forbids a term of the type $(\bar{u}u - \bar{d}d)$ at leading order giving a pion mass difference dominated by electromagnetic effects, such terms are allowed in the pion-nucleon sector allowing for large isospin breaking effects.

The inclusion of virtual photons proceeds as follows. One works with the nucleon charge matrix

$$Q = e \begin{pmatrix} 1 & 0 \\ 0 & 0 \end{pmatrix} = \frac{e}{2}(\tau^3 + 1) \quad (72)$$

and introduces spurions

$$Q_{\pm} = \frac{1}{2}(uQu^{\dagger} \pm u^{\dagger}Qu) \quad (73)$$

which under chiral $SU(2)_L \times SU(2)_R$ symmetry transform as any matrix-valued matter field,

$$Q_{\pm} \rightarrow KQ_{\pm}K^{\dagger} \quad (74)$$

where K is the compensator field representing an element of the conserved subgroup $SU(2)_V$. This leads for example to the generalized pion covariant derivative, see Eq. (9)

$$d_{\mu}U = \partial_{\mu}U - i(v_{\mu} + a_{\mu} + QA_{\mu})U + iU(v_{\mu} - a_{\mu} + QA_{\mu}) \quad (75)$$

and to additional local contact terms. At second order for example one has

$$\mathcal{L}_{\pi N, em}^{(2)} = \sum_{i=1}^3 F_{\pi}^2 f_i \bar{N} \mathcal{O}_i^{(2)} N \quad (76)$$

with the operators $\mathcal{O}_i^{(2)}$,

$$\mathcal{O}_1^{(2)} = \langle \tilde{Q}_+^2 - \tilde{Q}_-^2 \rangle, \quad \mathcal{O}_2^{(2)} = \langle Q_+ \rangle \tilde{Q}_+, \quad \mathcal{O}_3^{(2)} = \langle \tilde{Q}_-^2 - \tilde{Q}_+^2 \rangle \quad (77)$$

where $\tilde{Q}_{\pm} = Q_{\pm} - \langle Q_{\pm} \rangle / 2$. Apart from f_2 which can be deduced from the neutron-proton mass difference, $-e^2 F_{\pi}^2 f_2 = (m_p - m_n)^{\text{em}}$ [236] not much is known about the new LECs. f_1 has been recently determined from a combined analysis of pionic hydrogen and pionic deuterium [238]. The values for these two LECs are:

$f_2 = -(0.97 \pm 0.38), \quad f_1 = -2.1_{-2.2}^{+3.2} \quad \text{in units of } \text{GeV}^{-1}.$

Note that the central value of f_1 agrees with a model-based estimate [239]. Also its errors do not include the uncertainty coming from the higher orders in ChPT and should thus be considered as preliminary. An estimate of the size of the other LECs has been done in [237] by dimensional analysis. It was argued there that, measured in appropriate powers of the inverse scale of chiral symmetry breaking, these should be of order $1/4\pi$ or $1/(4\pi)^2$. The detailed expressions of the Lagrangian up to $\mathcal{O}(p^4, e^2 p^2)$ as well as the divergent parts of the low energy couplings is given in [43]. As already stressed care has to be taken on the definition of the $\pi\pi$ Lagrangian. For more details see [43]. Subtleties on the separation between QCD and QED can be found in [240].

ii) Studies of the isospin violation of $\pi - N$ scattering can be summarized as follows:

- Isospin-violating contributions to the σ -term can be as large as 10% but are negligible for the shift to the Cheng-Dashen point [236].
- The corrections to Weinberg's time-honored prediction for the difference of the S -wave scattering for the neutral pions off nucleons are small, their numerical value lies in the range from 4 to 18% [237].

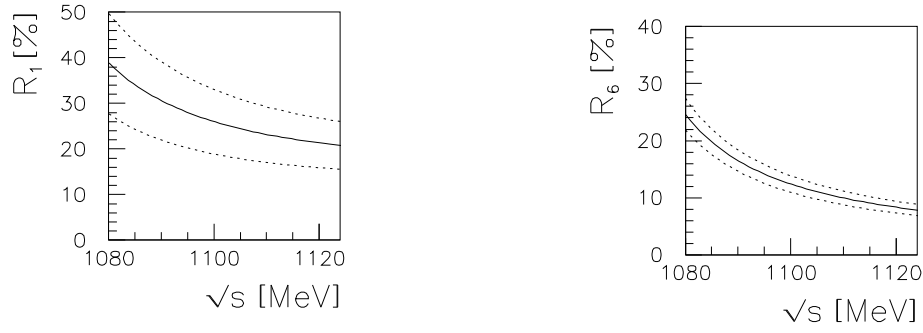


Figure 13: Isospin violation in the S wave projection of the ratios R_1 and R_6 . The dashed line indicate the range for isospin violation. Figure taken from [243].

- A variety of triangle relations between measurable channels that vanish if isospin were an exact symmetry can be established, two of them being of purely isoscalar type:

$$\begin{aligned}
 R_1 &= 2 \frac{T_{\pi^+ p \rightarrow \pi^+ p} + T_{\pi^- p \rightarrow \pi^- p} - 2T_{\pi^0 p \rightarrow \pi^0 p}}{T_{\pi^+ p \rightarrow \pi^+ p} + T_{\pi^- p \rightarrow \pi^- p} + 2T_{\pi^0 p \rightarrow \pi^0 p}} \\
 R_6 &= 2 \frac{T_{\pi^0 p \rightarrow \pi^0 p} - T_{\pi^0 n \rightarrow \pi^0 n}}{T_{\pi^0 p \rightarrow \pi^0 p} + T_{\pi^0 n \rightarrow \pi^0 n}}.
 \end{aligned} \tag{78}$$

In the analysis [236, 241] the strong violation of the triangle relation R_6 predicted by Weinberg was confirmed,

$$R_6 \sim 25\%. \tag{79}$$

However an even more important isospin violating effects was found in the isoscalar triangle relation R_1 connecting the charged and neutral pion scattering off protons [241]:

$$R_1 = 36.7\%. \tag{80}$$

Interestingly this ratio could be accessible experimentally extracting the $\pi^0 p$ scattering by a precise pion photoproduction experiment as proposed by Bernstein [242]. Note that these results are sensitive to the exact value of the isoscalar scattering length and thus efforts should be made to measure it more precisely. The analysis of these triangle relations was extended in [243] to the energy range above threshold. In Fig. 13 are depicted the two previous relations as a function of the total center-of-mass energies \sqrt{s} . The isospin breaking effect drops by a factor of two over the first 50 MeV. This was to be expected since the lower the energy, the more important the quark mass difference is compared to the kinetic energies of the particles and the larger the isospin breaking should be.

- A *complete* analysis of πN scattering including the yet missing part in the previously described analysis [236, 237, 241] – loops with virtual photons as well as electromagnetic counterterms – was performed in [220]. A fit to all data (with the exception of the ones generally considered inconsistent) below pion lab momenta of 100 MeV was done. A very pronounced difference in the hadronic amplitude for elastic scattering $\pi^- p \rightarrow \pi^- p$ compared to the standard PWA's was observed. This difference could be traced back to the inclusion of non-linear $\pi\pi\bar{N}N\gamma^*$ couplings as demanded by chiral symmetry. These effects should be included in any calculations of em corrections. In the S-wave triangle relation between elastic scattering, $\pi^\pm p \rightarrow \pi^\pm$, and charge exchange, $\pi^- p \rightarrow \pi^0 n$ a strong isospin violation of 0.75% was found in the low-energy region, an order of magnitude smaller than reported in the literature [244] but consistent with the expected size of isospin violation.

- Use of pionic atoms to measure scattering lengths have developed throughout the years. Let me stress here again the importance of a precise determination of these scattering lengths. In the case

of the πN system for example they are correlated with the pion-nucleon sigma-term, the pion-nucleon coupling constant and the Goldberger-Treiman relation. Moreover constraining the πN interactions at low energies also affects our understanding of more complicated systems where πN interaction serves as input, e.g. NN interaction, π -nucleus scattering, three-nucleon forces, etc. There are actually three types of on-going experiments on hadronic atoms (see for example [245]): the DIRAC experiment which aims at the measurement of the $\pi^+\pi^-$ atom lifetime within a 10% accuracy, allowing to determine the difference of the $\pi\pi$ scattering lengths $a_0 - a_2$ with a 5% accuracy, the DEAR collaboration at the DAΦNE facility which measures the energy levels shift and lifetime of the $1s$ state in K^-p and K^-d atoms aiming at a precise determination of the $I = 0, 1$ S -wave scattering lengths and finally the PSI experiments [246] which we are interested in here, which aims at a determination of the πN scattering lengths by measuring at the percent level the strong energy level shift ϵ_{1s} , and the decay width into $\pi^0 n$ state, Γ_{1s} , in π^-p atom. Therefore the knowledge of the relation between the scattering lengths and the threshold amplitude should match the accuracy of the experiment.

The energy shift in pionic hydrogen is given at leading order in isospin breaking by the well known formula of Deser et al. [247]. At next to leading order, that is at $\mathcal{O}(\alpha^4, \alpha^3(m_d - m_u))$ it reads [248]

$$\epsilon_{1s} = -2\alpha^3 \mu_c^2 (a^+ + a^-)(1 + \delta_\epsilon) \quad (81)$$

with $\mu_c = m_p M_\pi (m_p + M_\pi)^{-1}$ the reduced mass of the π^-p system, $\alpha \sim 1/137.036$ and δ_ϵ describes the isospin breaking effects. This is the quantity to be determined very precisely in order to be able to determine the scattering lengths. Its expression is given by:

$$\delta_\epsilon = \frac{\alpha T^\gamma + (m_d - m_u) T^m}{4\pi(1 + M_\pi/m_p)(a^+ + a^-)} + K + \delta_\epsilon^{vac}, \quad K = -2\alpha(\ln \alpha - 1)\mu_c(a^+ + a^-), \quad (82)$$

where T^γ , T^m are the electromagnetic and strong isospin breaking parts of the πN amplitude and δ_ϵ^{vac} is a correction due to the interference of vacuum polarization and strong interactions which is in principle of order α^5 but is amplified by the large factor $(M_\pi^+/m_e)^2$. A study of this quantity has been first done in [248] where the leading order result was obtained. It was then refined in [43] with next-to-leading order calculation. In the expression of δ_ϵ some LECs appear. At next-to-leading order one has two LECs from the isospin symmetric part and five from the isospin breaking part of the Lagrangian. These are f_1 (see Eq. (76)) and two combinations of two LECS from $\mathcal{L}_{\pi N}(e^2 p^2)$ and $\mathcal{L}_{\pi N}(e^2 p)$. It turns out that in the calculation of δ_ϵ [43] the most important contribution comes from the LEC f_1 . In this reference these LECs have been put to zero and their contribution have been taken into account in the error bars. They find:

$$\delta_\epsilon = (-7.2 \pm 2.9) \cdot 10^{-2} \quad (83)$$

where an important contribution comes from the triangle graph discussed in Section 2.3.3. Such a triangle graph has also shown to be important in the photoproduction process which will be discussed in Section 5.3. The leading order result gives $\delta_\epsilon = (-2.1 \pm 0.5) \cdot 10^{-2}$. As we have seen previously a recent determination of f_1 has been obtained. With it the central value, Eq. (83) increases since the contribution of f_1 is positive and the error bars are bigger due to the large error on its value:

$$\delta_\epsilon = (-3.0_{-4.5}^{+6.4}) \cdot 10^{-2}. \quad (84)$$

This has to be compared with the potential model result [257] which predicts $\delta_\epsilon = (-2.1 \pm 0.5) \cdot 10^{-2}$. Note that there no unknown LECs appear and thus the result is much more precise. However it is well known that potential models do not, in general, include all effects of QCD+QED. In view of the error bars a precise determination of the scattering lengths has clearly at present to await a more precise determination of f_1 .

4.2 πd scattering

As we have just seen the pionic hydrogen energy shift allows to determine the combination $(a^+ + a^-)$. From the width which has not yet been discussed $\Gamma = 8\alpha^3\mu_c^2 p_0(1 + 1/P)(a^-(1 + \delta_\Gamma))^2$ where $P = 1.546 \pm 0.009$ is the Panofsky ratio, p_0 the center-of-mass momentum of the $\pi^0 n$ pair and δ_Γ , the isospin breaking correction, one can access a^- . However, a^+ being much smaller than a^- , a very high accuracy is needed in order to determine this quantity from the combination $(a^+ + a^-)$. A complementary piece of information comes from a measurement of the ground-state energy shift of pionic deuterium. The determination of a^+ and a^- from such a measurement is a two-step process. First one has to relate the energy shift to πd scattering and then this scattering to a^+ , a^- . As was stressed in [250] this requires different effective theories, scales being different in the two steps. In the first one the hard momentum scale is given by the average value of the three-momentum of the nucleons bound within the deuteron, $\gamma = \sqrt{\epsilon m} \simeq 45$ MeV (with $\epsilon = 2.22$ MeV the deuteron binding energy) and one can perform an expansion in the ratio of the scales $\alpha\mu_d/\gamma \simeq \mathcal{O}(\alpha)$ where $\alpha\mu_d$ is the momentum scale at which the charged pion and the deuteron form an atom whose observables are measured by the experiment.

Let us look at the second step. There are different ways of dealing with the study of very low-energy pion-deuteron scattering within the framework of effective field theories.

- the oldest approach is the so called hybrid approach. It follows the seminal paper by Weinberg [251] where chiral Lagrangians were systematically applied for the description of interactions of pions with nuclei. πd scattering is calculated by sandwiching the irreducible transition kernel for pion scattering on two nucleons obtained by use of the chiral Lagrangian between “realistic” deuteron wave function [252, 253]. However, this hybrid approach is only justified for processes dominated by the long-range mechanism.

- Weinberg’s proposal could be improved with the development of chiral effective theories for the NN system, for a review see [2]. Both the kernel and the deuteron wave function could then be calculated within ChPT. This was applied to πd in [249]. It was demonstrated there that the usual chiral counting was not suitable for the description of low-energy πd scattering due to infrared enhancements resulting from the anomalously small deuteron binding energy. Indeed it was shown that diagrams describing processes with a virtual pion emission/absorption were two orders of magnitude smaller than other diagrams appearing at the same order. A modified power-counting was thus introduced, for more details see this reference.

- Other approaches were developed, like the framework with perturbative pions which has been used for example in [254]. A so called Heavy Pion EFT with the dibaryon field has also been introduced [255]. In these two approaches the magnitude of the LECs can be estimated to be large leading to rather large theoretical uncertainties in the relation between the πd and πN scattering lengths.

- Recently another approach [250] was developed based on the finding of Ref. [249]. There the absorption and emission of hadrons do not appear explicitly at the level of Feynman diagrams but is included in the couplings of the effective Lagrangian much in the spirit of the Heavy Pion approach. A detailed comparison of these different approaches is discussed in [250].

In this second step the hard momentum scale is M_π and the expansion is done in terms of $\gamma/M_\pi \sim 1/3$. This is indeed the most efficient expansion of the effective theory following the remarks above. The matching between the theory in the first and in the second step is then performed for the πd scattering amplitude at threshold: this quantity must be the same in both theories.

Here I will follow Ref. [249]. In the isospin symmetric case the relation between the pion-deuteron scattering length $a_{\pi d}$ and the πN ones is given by:

$$\begin{aligned} \text{Re } a_{\pi d} = & 2 \frac{1 + \mu}{1 + \mu/2} a^+ + 2 \frac{(1 + \mu)^2}{1 + \mu/2} ((a^+)^2 - 2(a^-)^2) \frac{1}{2\pi^2} \left\langle \frac{1}{\mathbf{q}^2} \right\rangle_{\text{wf}} \\ & + 2 \frac{(1 + \mu)^3}{1 + \mu/2} ((a^+)^3 - 2(a^-)^2(a^+ - a^-)) \frac{1}{4\pi} \left\langle \frac{1}{|\mathbf{q}|} \right\rangle_{\text{wf}} + a_{\text{boost}} + \dots \end{aligned} \quad (85)$$

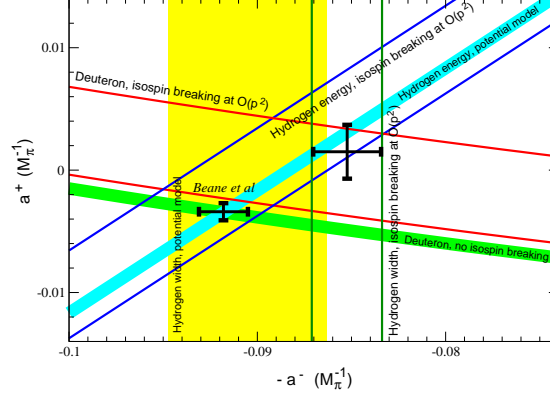


Figure 14: Determination of the πN S -wave scattering lengths a^+ and a^- from the combined analysis of the experimental data on the pionic hydrogen energy shift and width, as well as the pionic deuterium energy shift. The cross denoted *Beane et al* is taken from Ref. [249]. The second cross corresponds to the scattering lengths obtained in [238] from which the figure is taken.

In the above equation, $a_{\text{boost}} = (0.00369 \cdots 0.00511)M_\pi^{-1}$, $\langle 1/\mathbf{q}^2 \rangle_{\text{wf}} = (12.3 \pm 0.3)M_\pi$ and $\langle 1/|\mathbf{q}| \rangle_{\text{wf}} = (7.2 \pm 1.0)M_\pi^2$, where NLO wave functions with cutoff mass in the interval $\Lambda = (500 \cdots 600)$ MeV [256] have been used in order to evaluate the above wave-function averages. Result for a^+ and a^- , cross denoted Beane et al, using Eq. (85) and the experimental value:

$$a_{\pi d}^{\text{exp}} = (-26.1 \pm 0.5 + i(6.3 \pm 0.7) \cdots 10^{-3}M_\pi^{-1} \quad (86)$$

is displayed on Fig.14 which gives the state of the art determination of the πN scattering lengths. Also shown are the experimental bands [258, 259] which uses a potential model approach [257] to calculate a set of correction like δ_ϵ as discussed before and the new experimental values (denoted isospin breaking on the Fig.) on the width and shift in hydrogen atoms with an improved accuracy [260]. In these new shifted bands isospin symmetric corrections at leading order have been applied [43, 248]. Treating the deuteron in the isospin symmetric case there is a discrepancy between the new pionic hydrogen and the deuterium experimental bands. It was a serious problem for some time and it was first argued that the discrepancy was due to the incomplete treatment of the deuteron structure. However investigations in this direction [249, 250, 254, 255, 261] showed that the uncertainty in the three-body calculations cannot be solely responsible for the large discrepancy observed. Isospin breaking effects for the deuterium have then been calculated at leading order [238]. As can be seen they are in fact important. They shift the isospin symmetric result [249] in a non negligible way. For example corrections to $a_{\pi d}$ are found to be [238]

$$\Delta a_{\pi d}^{\text{LO}} = -(0.0110_{-0.0058}^{+0.0081})M_\pi^{-1} . \quad (87)$$

These corrections in the deuterium can thus reconcile, as shown in [238] the experimental bands coming from pionic hydrogen and deuterium. All these bands once the isospin breaking is included in the deuterium case have now a common intersection area in the a^+ , a^- -plane. This leads to [238]

$$\begin{aligned} a^+ &= (0.0015 \pm 0.0022)M_\pi^{-1} , \\ a^- &= (0.0852 \pm 0.0018)M_\pi^{-1} . \end{aligned} \quad (88)$$

Estimation of higher orders have been made in [238] but clearly the isospin-breaking corrections in pionic deuterium should be evaluated at least at $\mathcal{O}(p^3)$ in CHPT.

Interestingly, the πd scattering length is a complex-valued quantity already at threshold, see Eq. (86). Diagrams contributing to the imaginary parts are of higher order and thus have not been included in the calculations I have discussed up to now. These are called dispersive contributions. However a first estimate by Brückner [262] already speculated that the real part and the imaginary part of these contributions should be of the same order, an expectation which was confirmed later [263, 264]. Given the high accuracy of the measurement and the size of the imaginary part these dispersive contributions were very recently looked up within CHPT [265]. What is needed is a controlled power counting for $NN \rightarrow NN\pi$ consistent with the one used for πd . This was developed in recent years [266, 267] – for a review see [268]. Once all diagrams contributing to leading order to the hadronic part of the dispersive and absorptive corrections as well as to the transition $\pi d \rightarrow \gamma NN \rightarrow \pi d$ are included, their net effect provides a small correction to the real part of $a_{\pi d}$ of the order of 6.5% of the experimental value. The absorptive part is found to be

$$\text{Im}(a_{\pi d}) = ((4.25 \pm 1.2) + (1.4 \pm 0.4)) \cdot 10^{-3} M_{\pi}^{-1} , \quad (89)$$

in very good agreement with the experimental value:

$$\text{Im}(a_{\pi d}^{\text{exp}}) = ((4.7 \pm 0.5) + (1.6 \pm 0.2)) \cdot 10^{-3} M_{\pi}^{-1} . \quad (90)$$

In both these equations the hadronic and electromagnetic contributions are given separately.

In view of all these developments an improved measurement of the energy shift in pionic deuterium would certainly be welcome. In fact in the near future a new measurement with a projected total uncertainty of 0.5% for the real part and 4% for the imaginary part of the scattering length will be performed at PSI [269]. For the reader interested on older works there is a review in [270].

5 Electromagnetic properties

Processes involving nucleons interacting with one or several photons are also of particular interest. They contain fundamental observables describing the internal structure of the nucleon.

5.1 Form Factors

The structure of the nucleon as probed by virtual photons is parametrized in terms of four form factors,

$$\langle N(p') | \bar{q} \mathcal{Q} \gamma_{\mu} q | N(p) \rangle = e \bar{u}(p') \left\{ \gamma_{\mu} F_1^N(t) + \frac{i \sigma_{\mu\nu} q^{\nu}}{2m} F_2^N(t) \right\} u(p) , \quad N = p, n , \quad (91)$$

with \mathcal{Q} the quark charge matrix and $t = q^2 = (p' - p)^2$ the invariant momentum transfer squared. F_1 and F_2 are called the Dirac and the Pauli form factor, respectively, with the normalizations $F_1^p(0) = 1$, $F_1^n(0) = 0$, $F_2^p(0) = \kappa_p$ and $F_2^n(0) = \kappa_n$. Here, κ denotes the anomalous magnetic moment. One also uses the electric and magnetic Sachs form factors,

$$G_E(t) = F_1(t) + \frac{t}{4m^2} F_2(t) , \quad G_M(t) = F_1(t) + F_2(t) . \quad (92)$$

In the Breit-frame, G_E and G_M are nothing but the Fourier-transforms of the charge and the magnetization distribution, respectively. The understanding of these form factors is of utmost importance in any theory or model of strong interactions. They have thus been extensively studied experimentally as well as theoretically, for a recent review see [272] and references therein. Experiments have been performed or are underway at NIKHEF, MAMI, ELSA, MIT-Bates, JLAB \dots . On the theory side it was already established a long time ago that the isovector charge radii are diverging in the chiral limit

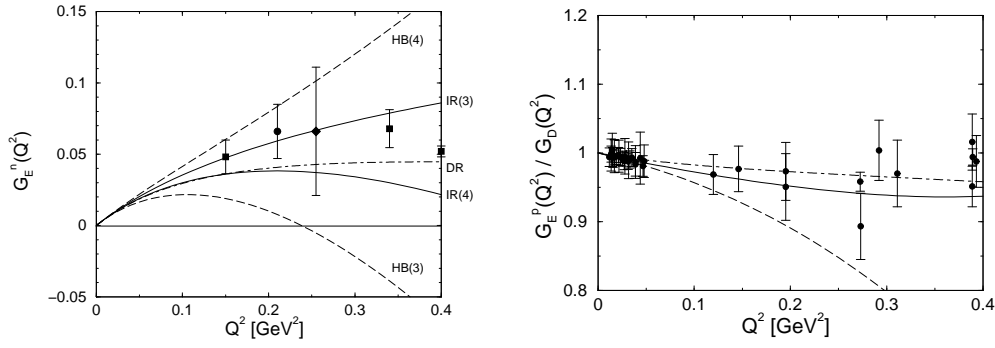


Figure 15: Left panel: The neutron electric form factor in IR regularization. All LECs are determined by a fit to the neutron charge radius measured in neutron-atom scattering. The data are from [271]. Right panel: The proton electric form factor including vector mesons to third (dashed curve) and fourth (solid curve) order, divided by the dipole form factor. The data are world average. In both panel the dot-dashed curve is the dispersion theoretical result. Figures taken from [197].

of vanishing pion mass [273]. Since then there has been several calculations within CHPT with different regularization scheme [41, 90, 197, 274–276] as well as in the SSE approach [277]. As has been pointed out in Section 2.3.3, HBCHPT suffers in this case from a distortion of the analytical structure of the isovector spectral function [94, 96]. I will thus report here on the calculation done within IR [197]. As can be seen on the l.h.s. of Fig.15 a good description of the neutron charge form factor is obtained for momentum transfer up to about $Q^2 = 0.4 \text{ GeV}^2$. Also shown is, as expected, the much better convergence of the series compared to HBCHPT. For the other three form-factors not shown here the agreement with the data is not very good. This however can be easily understood. It has indeed long been established that vector mesons play an important role in these form factors. In [197] the low-lying vector mesons ρ , ω and ϕ have been included in a chirally symmetric manner based on an antisymmetric tensor field representation. Refitting the LECs by subtracting the vector meson contribution a good agreement for all four form factors is obtained. As an example the right panel of Fig.15 shows the electric proton form factor with the vector mesons included. Similar findings have been obtained in [276].

5.2 Compton Scattering

Let me now come to processes involving two photons. We will consider here real, virtual and double virtual Compton scattering (V²CS) off nucleons (neutrons or protons) in forward direction, that is the reaction

$$\gamma^{(*)}(q, \epsilon) + N(p, s) \rightarrow \gamma^{(*)}(q, \epsilon') + N(p, s') , \quad (93)$$

with q (p) the real/virtual photon (nucleon) four-momentum, s (s') the nucleon spin (polarization) and ϵ (ϵ') the polarization four-vector of the incoming (outgoing) photon.

5.2.1 Real and Virtual Compton Scattering

Real Compton scattering has been considered since the early 1950s with the determination of the electric α and magnetic β polarizabilities. Note that their determination within CHPT was one of the successes of this framework which showed the importance of pion loop effects. The $\mathcal{O}(p^3)$ result [278] which is completely given by the pion loops is in remarkable agreement with the experimental results. Also interesting is that these quantities diverge in the chiral limit which is a challenge for lattice QCD

calculations. Since these first results extensions to $\mathcal{O}(p^4)$ have been performed [279,280] and the role of the resonances has been examined [281]. Note that in this SSE calculation a discrepancy between theory and experiment for the proton magnetic polarizability was obtained due to a large contribution from the Δ driven to lowest order and the absence of the large negative non-analytic pion loop contribution due to the order the calculation was done, see [279]. For the precision aimed at, a calculation at the next order $\mathcal{O}(\epsilon^4)$ within this framework has certainly to be performed. For real photons two spin-dependent polarizabilities have been measured. Let me mention here the backward spin polarizability, I will come back to the forward spin one in the next section. A first experiment by the LEGS group [282] has challenged the theoretical predictions with a value much smaller in absolute value. However there is now contradicting evidence from recent MAMI data [283,284], their new results being well in the range from both dispersion theory [285] and CHPT [286,287]. Extension of these polarizabilities to non-zero energies have been defined in [288]. These are the so-called dynamical polarizabilities which test the global low energy excitation spectrum of the nucleon at non-zero energy. A first analysis of the sensitivity of proton Compton cross section data to these quantities has been done in [289].

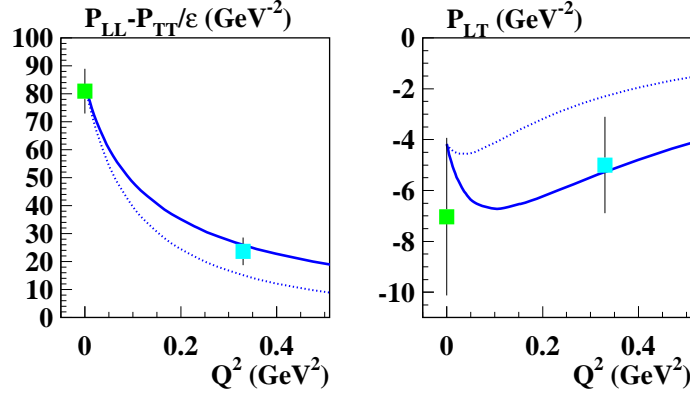


Figure 16: Comparison of a HBCHPT (solid line) calculation of two generalized polarizabilities with the MAMI measurement at $Q^2 = 0.33 \text{ GeV}^2$. The dashed line shows the structure functions obtained by switching off the spin-dependent polarizabilities. Figure courtesy of N. D'Hose.

It is only by the seventies that it was recognized that VCS would enable one to measure generalized polarizabilities (GPs) [290]. The theoretical framework for this reaction can be found in [291,292]. There are altogether 6 GPs that are independent due to crossing symmetry and charge conjugation invariance. From these 6 two are spin independent and are extensions of α and β at finite Q^2 . They provide information about the spatial distribution of charge and magnetism inside the nucleon. There have been during the last 10 years a lot of experimental (at MAMI, Jlab and MIT-Bates) and theoretical activities to determine these quantities, a summary can be found in [293]. As illustration Fig.16 compares the result of a HBCHPT calculation at $\mathcal{O}(p^3)$ of two particular combinations of spin-independent and spin-dependent GPs with the MAMI data. A very nice agreement is obtained. Clearly it would be interesting to perform an $\mathcal{O}(p^4)$ calculation to check the convergence of the series. HBCHPT $\mathcal{O}(p^4)$ calculations have been performed [294] but only for the spin dependent polarizabilities. The first HBCHPT calculation of the GPs can be found in [295]. In the existing unpolarized as well as polarized experiments it is not possible to resolve the 6 GPs. However the double polarization experiment A1/1-00 which is being realized at MAMI will allow to disentangle them and its result is thus eagerly awaited. A new program at HIGS will also allow to measure these GPs. These experiments will shed new light on our understanding of the internal structure of the proton and serve as a check on the theoretical explanations of the polarizabilities. In the next section I will concentrate on spin-dependent observables obtained in $V^2\text{CS}$ and discuss two specific combinations of the spin GPs.

5.2.2 V²CS: spin structure functions and sum rules

There are many on-going activities concerning the spin of the nucleon, as for example understanding how it is built from quarks and gluons. Apart from the GPs, other interesting quantities to test CHPT are the spin structure functions and their moments. Experiments with polarized beams and polarized p , d , ^3He targets are performed over a very wide range of Q^2 , with Q^2 the negative of the photon virtuality (momentum transfer squared). Nowadays rather low values for this momentum transfer are reached at JLAB in the range of applicability of CHPT. Indeed preliminary results for Q^2 values as low as 0.05 GeV^2 have been reported while data taking have started for very low Q^2 down to 0.015 GeV^2 [296]. At high energy systematic and controlled theoretical calculations can also be performed. The region of intermediate momentum transfer is accessible using quark/resonance models or can be investigated using dispersion relations [297]. Thus ultimately these investigations will lead to an understanding of how in QCD the transition from the non-perturbative to the perturbative regime takes place, guided by the precise experimental mapping of spin-dependent observables from low momentum transfer to the multi-GeV region.

It is common to express the spin-dependent amplitude of V²CS in terms of two structure functions, called $S_1(\nu, Q^2)$ and $S_2(\nu, Q^2)$. In the rest frame and in the Coulomb gauge $\epsilon_0 = \epsilon'_0$ the V²CS forward matrix element is given by:

$$\begin{aligned} \epsilon' \cdot T \cdot \epsilon|_{\text{rest}} = & \frac{1}{2m} \chi^\dagger \{ i \vec{\sigma} \cdot (\vec{\epsilon}' \times \vec{\epsilon}) [m\nu S_1(\nu, Q^2) - Q^2 S_2(\nu, Q^2)] \\ & + i [\vec{\sigma} \cdot (\vec{\epsilon}' \times \hat{q}) \vec{\epsilon} \cdot \hat{q} - \vec{\sigma} \cdot (\vec{\epsilon} \times \hat{q}) \vec{\epsilon}' \cdot \hat{q}] (\nu^2 + Q^2) S_2(\nu, Q^2) \} \chi, \end{aligned} \quad (94)$$

where $\nu = p \cdot q/m$ the energy transfer and $Q^2 = -q^2 \geq 0$ the (negative of the) photon virtuality. Note that while $S_1(\nu, Q^2)$ is even under crossing $\nu \leftrightarrow -\nu$, the structure function $S_2(\nu, Q^2)$ is odd. Because of unitarity, there is a basic connection between spin structure functions in V²CS and the ones $G_{1,2}$ probed in inelastic electroproduction experiments. One has

$$\text{Im } S_i(\nu, Q^2) = 2\pi G_i(\nu, Q^2), \quad (i = 1, 2). \quad (95)$$

This is simply related to the fact that the imaginary part of the Compton tensor is given in terms of nucleon plus meson states, the lowest one being the pion-nucleon state. This gives rise to sum rules as the well-known Drell-Hearn-Gerasimov sum rule [298] for real photons which relates the anomalous magnetic moment to the total photoabsorption cross sections $\sigma_{1/2}$ and $\sigma_{3/2}$ corresponding to the excitation of intermediate states with spin projection $3/2$ and $1/2$, respectively:

$$-\frac{2\pi^2 \alpha \kappa^2}{m^2} = \int \frac{d\nu}{\nu} [\sigma_{3/2} - \sigma_{1/2}]. \quad (96)$$

The value of the l.h.s. of the sum rule is $-204 \mu\text{b}$ for the proton and $-232 \mu\text{b}$ for the neutron. This sum rule is presently under active experimental investigation at MAMI, ELSA, GRAAL, CEBAF and Spring-8. First measurements on the proton agree with this sum rule within some assumptions from contributions coming from un-measured regions. For the neutron only estimates can be given. For an experimental review see [299].

The DHG sum rule has been generalized to finite Q^2 [297, 300]. There are different possibilities, an interesting definition being:

$$I_1(Q^2) = \frac{2m^2}{Q^2} \int_0^{x_0} m\nu G_1(x, Q^2) dx. \quad (97)$$

Indeed while at low Q^2 one recovers the DHG sum rule this definition leads to the Ellis-Jaffe sum-rule at very large momentum transfer [301]. In this equation $x = Q^2/2m\nu$ is the standard scaling variable

and x_0 corresponds to the pion production threshold. Other sum rules can be defined involving also the structure function G_2 as the so-called Burkhardt-Cottingham sum rule [302]. Expanding the V^2CS structure functions at low energies ν , that is around $\nu = 0$, one has for example

$$\bar{S}_1^{(0)}(0, Q^2) = \frac{4e^2}{m^2} I_1(Q^2) , \quad (98)$$

where $\bar{S}_1^{(0)}(0, Q^2)$ is the first constant term in the expansion of S_1 and the bar means that the elastic contribution (nucleon pole term) has been subtracted. For the relations of the other structure functions see [303]. Two other interesting quantities as mentioned above are the following combinations of GPs, the forward spin polarizability γ_0 and the longitudinal-transverse polarizability δ_0 . They are defined and given by:

$$\begin{aligned} \gamma_0(Q^2) &\equiv \frac{1}{4\pi^2} \int \frac{d\nu}{\nu^3} (1-x) (\sigma_{1/2}(\nu, 0) - \sigma_{3/2}(\nu, 0)) = \frac{1}{8\pi} \left(\bar{S}_1^{(2)}(0, Q^2) - \frac{Q^2}{m} \bar{S}_2^{(3)}(0, Q^2) \right) , \\ \delta_0(Q^2) &\equiv \frac{1}{2\pi^2} \int \frac{d\nu}{\nu^3} (1-x) \lim_{Q^2 \rightarrow 0} \left(\frac{\nu}{Q} (\sigma_{1/2}(\nu, 0)) \right) = \frac{1}{8\pi} \left(\bar{S}_1^{(2)}(0, Q^2) + \bar{S}_2^{(1)}(0, Q^2) \right) . \end{aligned} \quad (99)$$

They involve an extra $1/\nu^2$ weighting compared to the first moments so that they have the experimental advantage that the uncertainty due to the unmeasured region at large ν is minimized.

The two spin structure functions $S^{(1,2)}$ have been calculated within HBCHPT [304–306] and to fourth order (one loop) in the IR regularization [303, 307]. At this order no unknown low-energy constants appear and thus parameter-free predictions are obtained. It is, however, well-known that the excitation of the $\Delta(1232)$ plays a significant role in the spin sector of the nucleon. A first attempt to include the Δ explicitly has thus been done in [303]. There the relativistic Born graphs were calculated in order to get an estimate of the contribution of this resonance. In order to take into account the fact that the $\Delta \rightarrow N\gamma$ transition occurs at finite Q^2 the possibility of introducing a transition form factor $G_{\Delta N\gamma}(Q^2)$ as extracted from pion electroproduction in the $\Delta(1232)$ -resonance region [308] was also studied in that reference. A less pronounced though important resonance contribution is related to the vector mesons. These were thus also included in [303].

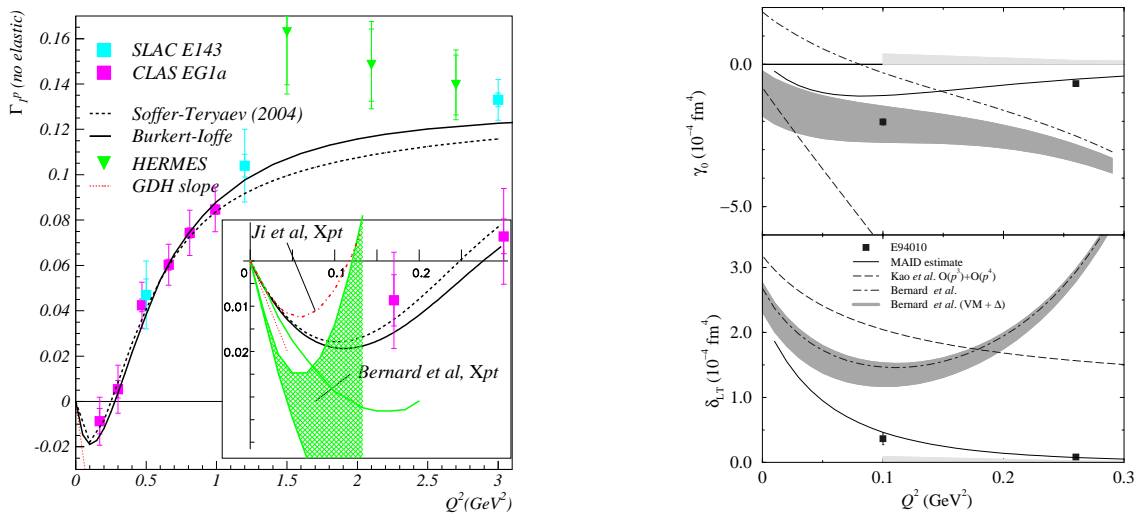


Figure 17: Left panel: Experimental results for $\Gamma_1^p(Q^2)$ compared to model predictions and CHPT calculations. The full lines (bands) at low Q^2 are the next to leading order CHPT predictions by Ji et al. [304] and Bernard et al. [303]. Right panel: neutron generalized spin polarizabilities γ_0 and δ_{LT} . The dashed lines are the HBCHPT calculation by [306]. Figure courtesy of A. Deur.

On the l.h.s. of Fig.17 is shown the first moment $\Gamma_1^p(Q^2)$ for the proton: $\Gamma_1(Q^2) = Q^2/2m^2 I_1(Q^2)$ over a wide range of Q^2 . We are interested in the region $Q^2 < 0.1$ GeV as detailed on the insert of the figure. There are shown the JLAB CLAS EG1a data [309] together with the HBCHPT results from Ji et al [304] and the IR ones from Bernard et al [303]. The difference between these two CHPT results comes from higher order terms which improves the convergence of the series of the latter at higher values of Q^2 as already explained. The data are at somewhat too high Q^2 to compare with these results. However preliminary data at lower Q^2 have been reported at Chiral Dynamics 2006. As can be inferred from Fig.2 of Chen's proceedings [296] there is a nice agreement between the IR calculation, black curve in the shaded area denoted Bernard et al. in the Figure, up to values of $Q^2 \sim 0.07$ GeV² which is roughly the range of validity of the calculation. It turns out that the inclusion of the Δ and vector mesons as just described above makes the agreement somewhat worse. However, a full $\mathcal{O}(\epsilon^3)$ calculation has to be performed, the shown results giving just a first estimate of the contribution of these degrees of freedom. For results on other moments and the neutron, see Chen's proceedings.

On the right panel of Fig. 17 are shown the neutron generalized polarizabilities, see Eq. (99). γ_0 is one of the quantities known to be rather sensitive to the Δ degrees of freedom as illustrated in the figure by comparing the two CHPT calculations with and without Δ . The data point at $Q^2 = 0.1$ GeV² nicely lies in the band of the calculation of ref. [303] with Δ degrees of freedom. The proton case not shown here is more problematic due to a very bad convergence of the chiral series [307]. δ_{LT} is an interesting quantity, it can indeed serve as a testing ground of the chiral dynamics of QCD since contrary to γ_0 the Δ contributes only marginally and its chiral expansion at the photon point is very well behaved, for a discussion see [307]. There is, however, a problem here with the IR result linked to the unphysical cuts appearing in the regular function R as discussed in Section 2.3.4. In principle these cuts lie far away from the region where CHPT is valid and are of no relevance. In the particular case of concern here they lead to a change of curvature already at $Q^2 \sim 0.1$ GeV² and thus to a disagreement with the lower data point. Clearly for that particular quantity data points at rather low Q^2 are needed to be able to compare the experimental result with the IR one. Alternatively one could use another regularization which does not have this problem like EOMS for example. Let me point out again that the same happens in the case of the nucleon mass or, as we have seen, in the anomalous magnetic moment, both quantities go to infinity as M_π goes to infinity due to these unphysical cuts. In the relativistic framework they would go to zero. This has, however, in those cases no impact on the result in the low energy region.

As we have seen there are in fact four independent spin independent GPs. γ_0 for example is a particular combination of three of them. HBCHPT predictions to $\mathcal{O}(q^4)$ for all spin-flip GPs have been obtained in [294].

5.3 Photo-and Electroproduction

I will concentrate here on Pion and Electroproduction in the threshold region. For a discussion of the Δ region, see the very recent review [310] and references therein. I will also concentrate on neutral pions. For charged pions and its relation to the nucleon axial radius and pion charge (vector) radius, see [187]. For a discussion of pion electroproduction and chiral Ward identities see [311].

5.3.1 off the nucleon

The electric dipole amplitude E_{0+} is a very interesting quantity since it vanishes in the chiral limit. It admits an expansion in terms of the quark (pion) mass, $E_{0+} = aM_\pi + bM_\pi^2 + \dots$, where a, b, \dots are calculable coefficients. This defines a venerable low-energy theorem (LET) which has been the source of a lot of activities, related to what is now known as the LEG (low energy guess) of the 70's [312, 313], for details see [314, 315]. See also [316] for a definition of a LET. In case of the neutron, i.e. for $E_{0+}^{\pi^0 n}$, the coefficient a is zero because of gauge invariance. There have been many experimental

and theoretical developments concerning the electric dipole amplitude for neutral pion production off protons [314,315,317]. Let me summarize what is the status today. Even though the convergence for the electric dipole amplitude is slow due to some strong final-state interactions, a CHPT calculation to order p^4 does allow to understand its energy dependence in the threshold region once three LECs are fitted to the total and differential cross section data [318], see the left panel of Fig.18. The threshold value $E_{0+}^{\text{thr}}(\pi^0 p) = -1.16$ (in units $10^{-3}/M_\pi$) thus obtained agrees with the data, $E_{0+}^{\text{thr}}(\pi^0 p) = -1.31 \pm 0.08$ [319], -1.32 ± 0.05 [320], $-1.33 \pm 0.08 \pm 0.03$ [321]. Even more interesting is the case of the neutron. Here, CHPT predicts a sizeably larger E_{0+} than for the proton (in magnitude). The CHPT predictions for $E_{0+}(\pi^0 p, \pi^0 n)$ in the threshold region clearly exhibit the unitary cusp due to the opening of the secondary threshold, $\gamma p \rightarrow \pi^+ n \rightarrow \pi^0 p$ and $\gamma n \rightarrow \pi^- p \rightarrow \pi^0 n$, respectively. Its strength is directly proportional to the isovector (charge exchange) πN scattering length. An average value of 3.3 ± 0.5 was given by the MAMI A2 collaboration in [322]. However, more work with polarized targets is required to have a more precise determination of this strength allowing to get additional informations [323] on zero-energy pion-nucleon scattering as well as on isospin breaking effects in the πN system [242]. Note that while $E_{0+}(\pi^0 p)$ is almost vanishing after the secondary threshold, the neutron electric dipole amplitude is sizeable.

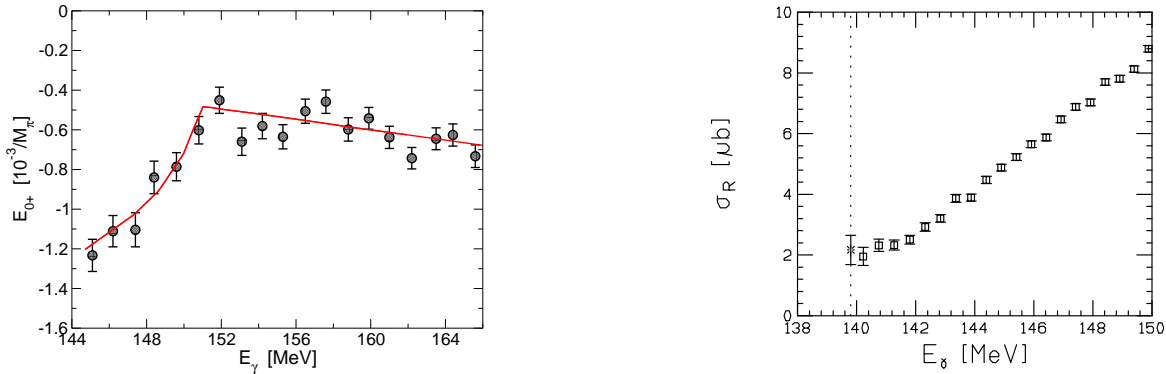


Figure 18: Left panel: CHPT prediction (solid line) for the electric dipole amplitude in $\gamma p \rightarrow \pi^0 p$ in comparison to the data from MAMI. Right panel: Reduced total cross section for $\gamma d \rightarrow \pi^0 d$. The data from SAL are depicted by the boxes, the CHPT threshold prediction is the star on the dotted line (indicating the threshold photon energy).

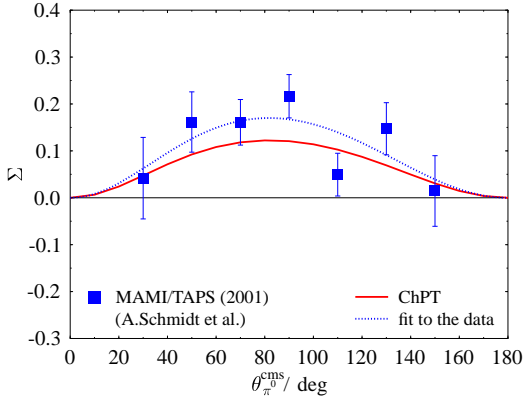
Quite in contrast to what was believed for a long time, there exists a set of LETs for the slopes of the P-waves $P_{1,2} = 3E_{1+} \pm M_{1+} \mp M_{1-}$ at threshold, for example

$$\frac{1}{|\vec{q}|} P_{1,\text{thr}}^{\pi^0 p} = \frac{eg_{\pi N}}{8\pi m^2} \left\{ 1 + \kappa_p + \mu \left[-1 - \frac{\kappa_p}{2} + \frac{g_{\pi N}^2}{48\pi} (10 - 3\pi) \right] + \mathcal{O}(\mu^2) \right\}, \quad (100)$$

and similarly for the slope of P_2 at threshold. Here, $g_{\pi N}$, m and κ_p are the pion-nucleon coupling constant, the proton mass and the proton anomalous magnetic moment, in order.

To disentangle the P-wave multipoles P_2 and P_3 , one has to perform an experiment involving polarization. This has been achieved at MAMI, where the photon asymmetry $\Sigma(\theta)$ in $\vec{\gamma} p \rightarrow \pi^0 p$ has been measured at $E_\gamma = 159.5$ MeV, see Fig.19 [321]. The analysis of these data together with the unpolarized ones leads to the values for the slopes of P_1 and P_2 at threshold given on the r.h.s. of this figure (in units of $q \cdot 10^{-3}/M_{\pi+}^2$). As can be seen the third order theoretical predictions compare well with the MAMI data. The fourth order corrections to these predictions have been analyzed in detail in [324]. One obtains for the sum of renormalized Born, third and fourth order loop and counterterm contributions

$$\frac{1}{|\vec{q}|} P_{1,\text{thr}}^{\pi^0 p} = (0.460 + 0.017 - 0.133 + 0.0048 \xi_1) \text{ GeV}^{-2}, \quad (101)$$



	CHPT $\mathcal{O}(p^3)$	MAMI/TAPS [321]	SAL [320]
$P_{1,\text{thr}}$	9.14 ± 0.50	$9.47 \pm 0.08 \pm 0.29$	9.08 ± 0.14
$P_{2,\text{thr}}$	-9.70 ± 0.50	$-9.46 \pm 0.10 \pm 0.29$	—

Figure 19: The photon asymmetry at $E_\gamma = 159.5$ MeV. Solid line: CHPT prediction. The data are from [321]. Dashed line: Fit to the data. Figure courtesy of Reinhard Beck.

$$\frac{1}{|\vec{q}|} P_{2,\text{thr}}^{\pi^0 p} = -(0.449 + 0.058 - 0.109 + 0.0048 \xi_2) \text{ GeV}^{-2}, \quad (102)$$

where the $\xi_{1,2}$ are LECs contributing to P_1 and P_2 at fourth order, respectively. In a resonance saturation picture, these LECs only depend on the $N\Delta$ transition magnetic moment κ^* (for details see [324]). We note the rather sizeable (25%) correction from the fourth order loops which at first sight seems to destroy the agreement between the LETs and the data. However, it is known that $\kappa^* \simeq 4 \dots 6$. For $\kappa^* = 4$, the delta contribution almost completely cancels the large fourth order loop effect and thus the predictions for the P-wave slopes are within 7% of the empirical values, see Table 3 in ref. [324]. Note, however, that the empirical finding $P_1^{\text{exp}}/|\vec{q}| = -P_2^{\text{exp}}/|\vec{q}|$ is difficult to reconcile with any theory.

Producing the pion with virtual photons offers further insight since one can extract the longitudinal S-wave multipole L_{0+} and also novel P-wave multipoles. Data have been taken at NIKHEF [325] [326] and MAMI [327] for photon virtuality of $k^2 = -0.1 \text{ GeV}^2$. CHPT calculations have been performed in the relativistic framework [328] and then redone in the heavy fermion formalism [329]. The above-mentioned data for the differential cross sections, the only one available at the time the calculations were done, were used to determine the three novel S-wave LECs. Note, however, that the photon four-momenta are already somewhat too large for CHPT tests since the loop corrections are large [329]. Also an operator of dimension five, i.e. one order higher than the calculation done had to be taken into account since it was shown that the two S-waves are over-constrained by a LET valid up to order p^4 . In [329], many predictions for $k^2 \simeq -0.05 \text{ GeV}^2$ were given. At MAMI, data have then been taken for this value of k^2 [330], see also [331]. The measured cross section is significantly lower than predicted by chiral perturbation theory [329] or by the most sophisticated phenomenological model of the Mainz group [332]. As an example, the total cross section is shown in Fig.20 as a function of $Q^2 = -k^2 \geq 0$ from the photoproduction point at $Q^2 = 0$ up to the older measurement at $Q^2 = 0.1 \text{ GeV}^2$. In all energy bins above threshold (with ΔW the pion energy with respect to the threshold value) one observes a “kinky structure”, a non-smooth momentum dependence at odds with expectations based on resonance excitation. This is even more strikingly observed in the fitted value for the P-wave combination $|P_2|^2 + |P_3|^2$ given in Table II of ref. [330]. It comes out significantly smaller than what CHPT or models predict. This is rather surprising since P_3 is believed to be saturated by the Δ and P_2 , as we have seen, is further constrained by a LET, this combination should thus be understood to some precision. To resolve the problem of the Q^2 dependence of the total cross-section MAMI performed an experiment where three different Q^2 values were measured. Preliminary data seem to indicate that the data points of the previous measurement at $Q^2 = 0.1 \text{ GeV}^2$ are somewhat high [333]. Furthermore, the

BigBite Collaboration at Jefferson Lab plans to measure neutral pion electroproduction from low to intermediate Q^2 in small steps of ΔQ^2 , see [334]. On the theoretical side a refit will have to be done once data at lower Q^2 will be available. Also up to now the P-waves have only been calculated to third order beyond the photon point. A fourth order calculation is clearly needed.

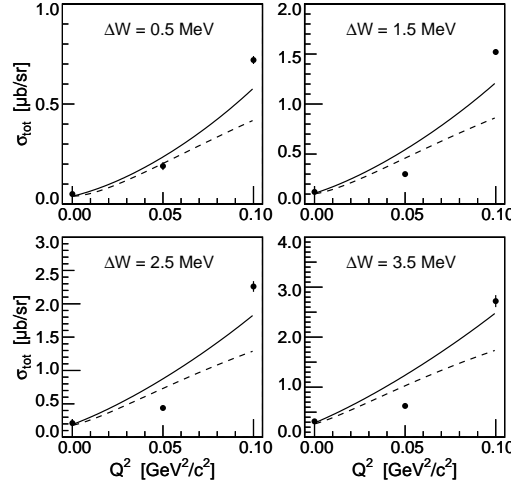


Figure 20: Total cross section of pion electroproduction off protons for a polarization of the photon $\epsilon = 0.8$. The solid (dashed) line is the prediction of CHPT (MAID). The data points at $Q^2 = 0, 0.05$ and 0.1 GeV^2 are from [321], [330] and [327].

There exists an interesting sum rule, the Fubini-Furlan-Rosetti (FFR) derived in the sixties [335] which relates the nucleon anomalous magnetic moment to an integral over the invariant amplitude A_1 of pion photoproduction:

$$\kappa^{V,S} = \frac{8m^2}{e\pi g_{\pi N}} \int \frac{d\nu'}{\nu'} \text{Im} A_1^{(+,0)}(\nu', t=0) , \quad (103)$$

with κ_V and κ_S the isovector and isoscalar anomalous magnetic moments and $A_1^{(+,0)}$ the respective combinations of A_1 . It is exact in the chiral limit of QCD and thus all quantities in Eq. (103) are to be understood in the limit of vanishing quark masses. It allows to analyze the relation between dispersion relations [336] and the chiral representation for neutral pion photoproduction. As pointed out in [336] this sum rule is a nice example where use of HBCHPT is not appropriate since in this framework the nucleon pole positions are slightly moved leading e.g. to an incorrect curvature of the discrepancy function (which measures the corrections to the sum-rule due to the finite pion mass) for energies below threshold. It has thus been considered in the framework of covariant chiral perturbation theory [337]. It was shown in that reference that one can achieve a good description of the energy dependence of the discrepancy function for the proton together with the one of the electric dipole amplitude at threshold and the P-wave slopes at threshold. Relations between the LECs and the subtraction constants of the dispersive analysis could thus be established with an unprecedented accuracy [337, 338].

5.3.2 off deuterium

The question arises how to measure the neutron amplitude? This is of particular interest in order to understand isospin breaking violation. The natural neutron target is the deuteron. The electric dipole E_d amplitude has been calculated to order p^4 in Ref. [339]. It was shown that the next-to-leading order three-body corrections and the possible four-fermion contact terms do not induce any new unknown LEC and one therefore can calculate E_d in a parameter-free manner. Furthermore, the leading order three-body terms (the well known charge exchange contribution) are dominant, but one finds a good

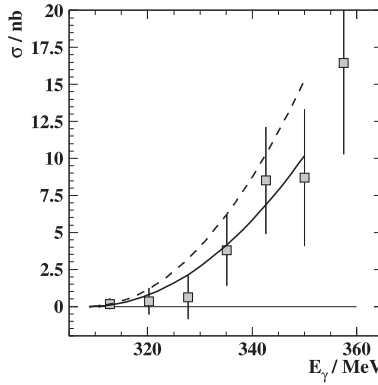


Figure 21: Total cross section for the process $\gamma p \rightarrow \pi^0 \pi^0 p$ as measured by the TAPS collaboration at MAMI [345]. The solid line is the fourth order central HBCHPT prediction, 0.6nb in Eq. (104) and the dashed line the upper limit (0.9nb). Figure taken from [346].

convergence for these corrections and also a sizeable sensitivity to the elementary neutron amplitude. The CHPT prediction in comparison to the SAL data [340] for the reduced cross section of coherent neutral pion production off deuterium is shown in the right panel of Fig.18. The predicted value for the deuteron electric dipole amplitude $E_d = E_{0+}^{\pi^0 d}$ at threshold [339] is $E_d^{\text{thr}} = -1.8 \pm 0.2$ compared to the experimental result -1.5 ± 0.1 [340]. It shows a rather strong dependence in the values of the elementary amplitude $\pi^0 n$. Neutral pion electroproduction has been investigated in [341]. As can be seen from the figures in this paper the predicted differential cross sections are satisfactorily described although some systematic discrepancies for the higher values of the excess energy ΔW remain. The threshold multipoles $|E_d|$ and $|L_d|$ are consistent with the data.

5.4 Two-pion production

One of the nice successes of baryon CHPT is the prediction of the electromagnetic two-pion production off the proton. I will briefly discuss it here. Due to space limitation I will not review here the reaction $\pi N \rightarrow \pi \pi N$. The interested reader can consult [342] and references therein.

Electromagnetic production of two pions off a nucleon can be used to study the excitation of certain nucleon resonances, in particular the $\Delta(1232)$, the Roper $N^*(1440)$ or the $D_{15}(1520)$. However, close to threshold one observes an interesting effect due to the chiral pion loops of QCD. To be specific, consider the reaction $\gamma p \rightarrow \pi \pi N$, where the two pions in the final state can both be charged, both neutral or one charged and one neutral. To leading order in the chiral expansion, the production of two neutral pions is strictly suppressed. However, at next-to-leading order, due to finite chiral loops the production cross section for final states with two neutral pions is considerably enhanced [343]. Also, in a small window above threshold, the potentially large contribution from double-delta excitation is strongly suppressed, leaving a window in which one can detect much more neutrals than expected. This prediction was further sharpened in [344], where all fourth order corrections including the excitation of the Roper and its successive decay into two neutral pions were considered. The predicted near threshold cross section is

$$\sigma_{\text{tot}}(E_\gamma) \leq 0.91 \text{ nb} \left(\frac{E_\gamma - E_\gamma^{\text{thr}}}{10 \text{ MeV}} \right)^2, \quad (104)$$

with $E_\gamma^{\text{thr}} = 308.8 \text{ MeV}$ the threshold energy for $\gamma p \rightarrow \pi^0 \pi^0 p$ (in the lab system). This prediction can only be applied for the first 30 MeV above threshold. A measurement by the TAPS collaboration [346] has shown that such an enhancement of the $2\pi^0$ production indeed happens, see Fig.21, proving once again the importance of pion loop effects, which can lead to rather unexpected predictions and

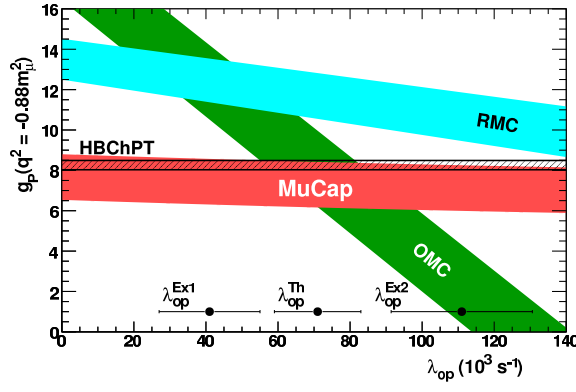


Figure 22: Comparison of a HBChPT (hatched line) calculation of g_P with experimental measurements as a function of the ortho-para transition rate λ_{op} in the $p\mu p$ molecule. Figure courtesy of C. Petitjean for the MuCap collaboration.

results. New data with much higher precision measured with the Crystal Ball and TAPS at MAMI will soon be published [347].

6 Axial properties

I will be very brief here and only report on very recent determinations of the induced pseudoscalar coupling constant g_P . For more details on axial properties see [187]. A very precise prediction of the induced pseudoscalar form factor based on chiral Ward identities has been given in [348]:

$$G_P(t) = \frac{4m g_{\pi N} F_\pi}{M_\pi^2 - t} - \frac{2}{3} g_A m^2 r_A^2 \quad (105)$$

leading to

$$g_P = (M_\mu/2m) G_P(t = -0.88 M_\mu^2) = 8.26 \pm 0.23. \quad (106)$$

In Eq. (105) M_μ is the muon mass and r_A the axial radius which can be determined from charged pion electroproduction or neutrino-proton scattering. Note that the difference between the two extracted experimental values of r_A can be understood by a computable and unique loop correction within CHPT [349]. The effect on Eq. (106) of the three-pion continuum determined in a two-loop HBChPT calculation is negligibly small [350]. The value, Eq. (106) where the error is almost entirely due to the uncertainty on the value of the pion-nucleon coupling constant, agreed with the much less precise experimental determination extracted from ordinary muon capture (OMC) [351]. This was however challenged by the TRIUMF result from radiative muon capture: $g_P = 12.35 \pm 0.88 \pm 0.38$ [352]. This has lead to some sizeable theoretical activity [274, 353–356] and it was conjectured that in fact a sum of various small effects could make up for the discrepancy. However, both the RMC and OMC experimental determination of g_P depend on the ortho-para transition rate λ_{op} in the $p\mu p$ molecule as shown on Fig.22. Its value is poorly known due to mutually inconsistent experimental and theoretical results. Very recently, a new experimental result on g_P has been reported by the MuCap collaboration [357]. It is also shown on the figure. It is nearly independent of molecular effects and is nicely consistent with the CHPT prediction. The experimental MuCap result $g_P = 7.3 \pm 1.1$, takes into account recently calculated radiative corrections [358].

7 Three flavors

7.1 Chiral dynamics with strange quarks: General remarks

I will now turn to the case of 3 flavors. As we have briefly seen in the introduction matters are more delicate in SU(3) since the strange quark plays a special role. Indeed its mass is of the order of 100 MeV. The question is whether one can consider it as light compared to the QCD scale $\Lambda_{QCD} \sim 200$ MeV or should it be treated as heavy. Related to that is the question whether standard CHPT is a well converging series, the relevant expansion parameter being in that case $m_K/\Lambda_\chi \sim 0.4$ and whether $\bar{s}s$ sea quark pairs may play a significant role in chiral dynamics leading to different patterns of chiral symmetry breaking in the $N_f = 2$ and $N_f = 3$ chiral limits. These are all very interesting questions which have been mostly touched upon in the meson sector and which are still rather open questions.

Let me briefly summarize what is known on the dependence of the chiral order parameters on N_f . The order parameters F^2 , the decay constant, and Σ , the quark condensate, can be obtained in terms of eigenvalues of the Euclidean Dirac operator $\gamma_\mu D_\mu$ defined in a box $L \times L \times L \times L$ with periodic boundary conditions via the well-known Banks-Casher formula [23]. Being dominated by the IR end of the Dirac spectrum one expects a paramagnetic effect such that

$$\Sigma(N_f) < \Sigma(N_f - 1) \sim 1/L^4, \quad F^2(N_f) < F^2(N_f - 1) \sim 1/L^2. \quad (107)$$

Let us concentrate on $N_f = 2, 3$ and define what is exactly meant by $\Sigma(3)$ and $\Sigma(2)$. One considers N_f quarks as massless, keeping the remaining masses at their physical mass so that:

$$\Sigma(3) = \lim_{m_s \rightarrow 0} \Sigma(2, m_s), \quad (108)$$

where, in the limit $N_f = 2$, Σ depends on the physical mass m_s (I don't consider here the heavier quarks). It can be shown that $\Sigma(3)$ and $\Sigma(2)$ are related via:

$$\Sigma(3) = \Sigma(2) + m_s Z^s + \mathcal{O}(m_s^2 \log m_s^2), \quad (109)$$

with Z^s related to the correlator $\Pi(0)$

$$mm_s \partial \Sigma(2) / \partial m_s = M_\pi^2 M_K^2 \Pi(0), \quad \Pi(0) = i \frac{mm_s}{M_\pi^2 M_K^2} \lim_{m \rightarrow 0} \int dx \langle T \{ \bar{u}u(x) \bar{s}s(0) \} \rangle_{\text{conn}}. \quad (110)$$

$\Pi(0)$ measures the violation of the OZI rule in the isoscalar-scalar (vacuum) channel. In the limit of large N_c the OZI rule is exact thus the correlator Z^s vanishes and the difference between $\Sigma(3)$ and $\Sigma(2)$ cancels. This is the standard scenario. The real world seems, however, to be different from the large N_c scenario in the scalar sector. For example the scalar meson $f_0(980)$ is found to be rather light and narrow and it couples strongly to both $K\bar{K}$ and $\pi\pi$ channels in violation to the large N_c expectation. At present one does not really know the size of the violation. Investigating a superconvergent sum rule for the OZI violating correlator Π with the strong constraint that its imaginary part satisfies a Weinberg type sum rule, Moussallam [27] gave an estimate $2 \lesssim 16\pi^2 \Pi \lesssim 6$. The $f_0(980)$ contributes in an important way to these numbers. Within CHPT this OZI violation is encoded in certain LECs whose values will thus depend on its strength. These are the SU(3) $\mathcal{O}(p^4)$ meson LECs L_6, L_8 which enter the meson masses and L_4 which merely shows up in the decay constants. For example the previous estimate for Π leads to $0.4 \lesssim 10^3 L_6(M_\eta) \lesssim 0.8$ to be compared with the standard scenario value $L_6(M_\eta) = (0.0 \pm 0.3)10^{-3}$. This translates into

$$\Sigma(3) = \Sigma(2)[1 - 0.54 \pm 0.27], \quad (111)$$

where the central value indicates that the condensate decreases by a factor of two when one decreases the strange mass from its physical value down to zero but the uncertainties are large enough to give

marginal consistency with the standard scenario. The correlator Π has been recalculated on more general grounds in [359]. It is particularly interesting to look at the m_s dependence of $\Sigma(N_f)$ obtained in this analysis. This is shown on Fig. 23 where the so-called Gell-Mann-Oakes-Renner ratio

$$X(N_f) = \frac{2\hat{m}\Sigma(N_f)}{F_\pi^2 M_\pi^2} \quad (112)$$

is displayed as a function of m_s/m . For more details see ref. [359].

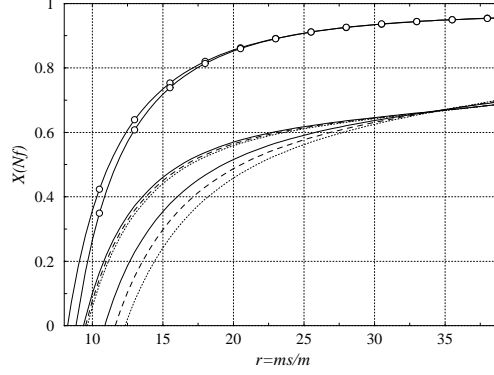


Figure 23: Upper and lower bounds for $X(3)$ as a functions of $r = m_s/m$ for $F = 85$ MeV with the T-matrix model of Ref. [360]. The allowed range for $X(2)$ is also shown (line with an open circle). Figure taken from [359]

More work on the theory side, for example three dynamical flavors lattice calculations with quark masses as close as possible to their physical values, as well as more experimental informations are needed in order to precisely determine the condensates.

In the baryon sector the $SU(3)$ case has been much less studied. Here I will first present the status of calculations done in standard CHPT. I will then discuss shortly proposal to modify the expansion considering the perturbative expansion as not justified. There are also interesting questions like for example what is the structure of some strange states like the $\Lambda(1405)$ or the $S_{11}(1535)$ where a unitary extension of CHPT has to be used. This is a nice tool which has been developped by [361–366]. I won't have space to discuss all this here, I refer the interested reader to the early review [367].

Before going to the applications let me briefly sketch the straightforward modifications which have to be done when going from $SU(2)$ to $SU(3)$. The effective meson-baryon Lagrangian is now expressed in terms of the baryon octet

$$B = \begin{pmatrix} \frac{1}{\sqrt{2}}\Sigma^0 + \frac{1}{\sqrt{6}}\Lambda & \Sigma^+ & p \\ \Sigma^- & -\frac{1}{\sqrt{2}}\Sigma^0 + \frac{1}{\sqrt{6}}\Lambda & n \\ \Xi^- & \Xi^0 & -\frac{2}{\sqrt{6}}\Lambda \end{pmatrix}, \quad (113)$$

and pseudoscalar Goldstone fields ($\phi = \pi, K, \eta$) collected in a now 3×3 unimodular, unitary matrix $U(\phi)$,

$$U(\phi) = u^2(\phi) = \exp\{i\phi/F\}. \quad (114)$$

In the case of isospin breaking the neutral pion and the η mix, so that the physical fields are related to the pure $SU(3)$ components via a mixing angle ε with

$$\tan 2\varepsilon = \frac{\sqrt{3}}{2R}, \quad R = \frac{m_s - \hat{m}}{m_d - m_u} \quad (115)$$

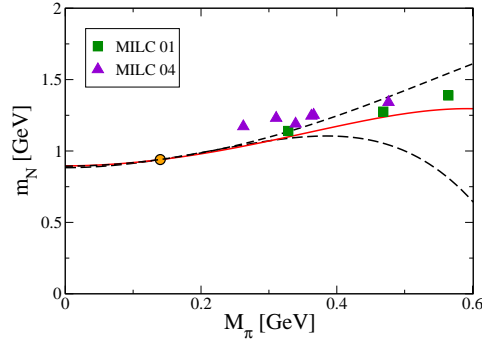


Figure 24: $SU(3)$ analysis of the nucleon mass. The solid line gives the best fit and the dashed line the theoretical uncertainty under the constraint that the nucleon mass takes its physical value for the physical quark masses. The square/triangle are the MILC 2001 [171] / 2004 [374] data.

with $\hat{m} = (m_u + m_d)/2$. The value of R has been determined in [368], leading to the usually quoted result $R = 40.8 \pm 3.2$. Note that in the determination of R enters a quantity denoted Q^2 which is taken in [368] to be equal to 22.7 ± 0.8 using the difference between the charged and neutral kaon masses and the partial width $\eta \rightarrow \pi^+ \pi^- \pi^0$. However a smaller value of this quantity was obtained in [369] leading to smaller values of R . The value of R has never been tested experimentally. In fact R could be obtained by looking at the ratio of charged and neutral K_{l3} decay, see [370]. The complete and minimal chiral effective meson-baryon Lagrangian at third order can be found in [371], see also [372]. As compared to the $SU(2)$ case one has more fields and more operator structures in the EFT and consequently more LECs. For example the dimension one Lagrangian reads:

$$\mathcal{L}_{MB}^{(1)} = \langle \bar{B} [i \not{\nabla}, B] \rangle - \tilde{m}_0 \langle \bar{B} B \rangle + \frac{D}{2} \langle \bar{B} \{ \psi \gamma_5, B \} \rangle + \frac{F}{2} \langle \bar{B} [\psi \gamma_5, B] \rangle , \quad (116)$$

with \tilde{m}_0 the average octet mass in the chiral limit and $D \simeq 0.81$ and $F \simeq 0.46$, two axial-vector coupling constants which can be determined from hyperon beta decays. The leading symmetry breakers within $SU(2)$ and $SU(3)$ are:

$$c_1 \bar{\psi}_N \langle \chi_+ \rangle \psi_N \rightarrow b_0 \langle \bar{B} B \rangle + b_D \langle \bar{B} \{ \chi_+, B \} \rangle + b_F \langle \bar{B} [\chi_+, B] \rangle . \quad (117)$$

A certain amount of LECs could be determined using lattice data. Also, the various operators in $SU(2)$ and $SU(3)$ are related by matching conditions which are important constraints that should be implemented in any $SU(3)$ analysis. The full matching conditions to fourth order in the chiral expansion have been derived in [373]. To leading order, one has for example:

$$\tilde{m}_0 = m_0 [1 + \mathcal{O}(m_s)], \quad g_A = D + F + \mathcal{O}(m_s), \quad c_1 = b_0 + \frac{1}{2}(b_D + b_F) + \mathcal{O}(\sqrt{m_s}) . \quad (118)$$

7.2 Baryon masses and Chiral Extrapolation

Explicit expressions for the baryon masses in terms of the quark masses to one loop order with isospin breaking can be found in [373]. They are very lengthy and contain a large number of LECs. For illustration I will just give the expression up to third order $\sim m_q^{3/2}$:

$$m_B = \tilde{m}_0 + \left(\gamma_{1,B} + \tilde{\gamma}_{1,B} \frac{\varepsilon}{\sqrt{3}} \right) B \hat{m} + \left(\gamma_{2,B} + \tilde{\gamma}_{2,B} \frac{\varepsilon}{\sqrt{3}} \right) B m_s$$

$$\begin{aligned}
& + \left(\delta_{1,B} + \tilde{\delta}_{1,B} \frac{\varepsilon}{\sqrt{3}} \right) \frac{\sqrt{2} B^{3/2}}{4\pi F_\pi^2} \hat{m}^{3/2} + \delta_{2,B} \frac{B^{3/2}}{4\pi F_\pi^2} (\hat{m} + m_s)^{3/2} \\
& + \left(\delta_{3,B} + \tilde{\delta}_{3,B} \frac{\varepsilon}{\sqrt{3}} \right) \frac{\sqrt{2} B^{3/2}}{4\sqrt{3}\pi F_\pi^2} (\hat{m} + 2m_s)^{3/2} + \tilde{\delta}_{4,B} \frac{\varepsilon}{\sqrt{3}} \frac{B^{3/2}}{4\pi F_\pi^2} (\hat{m} - m_s)(\hat{m} + m_s)^{1/2} ,
\end{aligned} \tag{119}$$

where $\gamma_{I,B}$ are functions of the symmetry breakers b_0, b_D and b_F , $\delta_{I,B}$ are combinations of F and D and ε is the mixing angle defined in Eq. (115). This expression is clearly of the same form as its SU(2) counterpart, Eq. (49) in the isospin limit.

With these expressions fits to the MILC 2001 data have been performed [375] based on two different regularization schemes (cut-off and dimensional regularization) and with the constraint that the physical value of the nucleon mass is obtained for the physical quark mass. In these fits the dimension two LECs were taken from [225] and the dimension four LECs were determined from a best description of the lattice data, see the solid line on Fig. 24. It turns out that the later MILC 2004 data at lower quark masses are too high compared to this best fit due to the constraint at the physical value. Taking into account also the kaon mass dependence of the nucleon mass and the uncertainty due to the MILC 2004 data, the following ranges for various (isoscalar) quantities have been obtained:

$$710 \text{ MeV} \lesssim \tilde{m}_0 \lesssim 1070 \text{ MeV} , \quad 39.5 \text{ MeV} \lesssim \sigma(0) \lesssim 46.7 \text{ MeV} , \quad 0.07 \lesssim y \lesssim 0.22 , \tag{120}$$

where the $\pi N \sigma$ term, $\sigma(0)$, and the strangeness fraction of the proton, y , have been defined in Section 3.1.

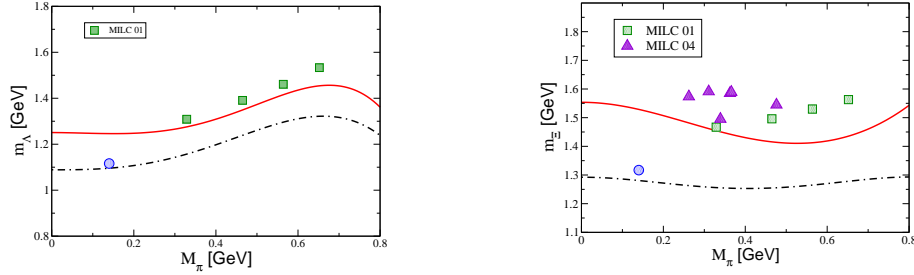


Figure 25: Pion mass dependance of the Λ mass (left panel) and the Ξ mass (right panel).

Once the nucleon has been fitted one can predict the masses of the other octet members. While the Σ mass is well reproduced the Λ and Ξ masses come about 10 – 15% too high. Predictions for the pion mass dependence of the Λ are shown in Fig.25 in comparison to the MILC data, see the upper solid line. For comparison the lower dot-dashed line is the result when the dimension four LECs are taken from [225], where in that case the masses at the physical pion mass are well reproduced. Interestingly the Ξ pion mass dependence is much flatter than what one would expect from the MILC data. One in fact expects the Ξ to be less sensitive to variations in the pion mass since it contains only one valence light quark and the MILC result is a mystery to be resolved.

7.3 Baryon Electromagnetic Properties

I will restrict myself here due to lack of space to the discussion of the nucleon form factors. Calculations of the magnetic moments of the whole octet can be found in [376]. There are three independent diagonal vector currents in SU(3):

$$J_\mu^{(i)} = \bar{q} \frac{\lambda^i}{2} \gamma_\mu q \quad i = 3, 8, 0 \tag{121}$$

which are proportional to the isovector and isoscalar electromagnetic currents and the baryon number current, respectively. In Eq. (121), $\lambda^{3,8}$ are the usual Gell-Mann matrices and $\lambda^0 = \sqrt{2/3} \text{ I}$. The

Table 5: Predictions for the electric radii $\langle r_E^2 \rangle$ [fm²]. The errors for the relativistic fourth order predictions display the uncertainty due to two order 2 LECs taken from the best fit to the magnetic moments at fourth order. The errors for the experimental Σ^- radius values refer to statistical (first) and systematic (second) errors.

	HB		IR		
	$\mathcal{O}(p^3)$	$\mathcal{O}(p^4)$	$\mathcal{O}(p^3)$	$\mathcal{O}(p^4)$	exp.
Σ^+	0.59	0.72	0.63	0.60 ± 0.02	—
Σ^0	-0.14	-0.08	-0.05	-0.03 ± 0.01	—
Σ^-	0.87	0.88	0.72	0.67 ± 0.03	$0.61 \pm 0.12 \pm 0.09$ [378]
Ξ^0	0.36	0.08	0.15	0.13 ± 0.03	—
Ξ^-	0.67	0.75	0.56	0.49 ± 0.05	—

electromagnetic J_μ^{EM} and the strangeness J_μ^s currents are linear combinations of these. I will discuss the first current here and the second in the following section. One has:

$$J_\mu^{\text{EM}} = J_\mu^{(3)} + \frac{1}{\sqrt{3}} J_\mu^{(8)} . \quad (122)$$

Extension of the SU(2) calculations of the em form factors presented in Section 5.1 has been done in [377]. I will mainly discuss here the difference between the HBCHPT and the IR results specially for the convergence of the chiral series in the case of the electric radii $\langle r_E^2 \rangle$ as shown on Table 5. For more details on the Q^2 dependence of the form factors and the magnetic radii, see this reference. The table shows the predictions for $\langle r_E^2 \rangle$ for the third and fourth order in both formalisms. The IR scheme yields overall considerable improvement over the HBCHPT scheme, especially for Λ , Σ^+ , and Ξ^0 . Also it shows the hierarchy in the size of the electric radii expected from naive quark model considerations, $\langle (r_E^p)^2 \rangle > \langle (r_E^{\Sigma^\pm})^2 \rangle > \langle (r_E^{\Xi^\pm})^2 \rangle$. Furthermore the experimental Σ^- radius given by the SELEX collaboration [378] is in very good agreement with the calculated IR value.

7.4 Strange form factors of the nucleon

One particularly interesting question which we have already touched upon in the context of the $\pi N \sigma$ term and which is connected to the violation of the OZI rule is: what is the strangeness content in the nucleon? There has been a lot of work done on this subject both from theory and experiment. The question of the spin content of the proton for example has been widely studied. Also it was pointed out a long time ago [379] that the dispersion theoretical analysis of the nucleon's electromagnetic form factors allows one to get bounds on the violation of the OZI rule. It was found there that the ratio of the vector coupling constants to the nucleon of the ϕ and of the ω which is almost entirely due to the coupling of $\bar{s}s$ to the nucleon is fairly large ~ -0.4 indicating a strong violation of the Zweig's rule. Interesting quantities in this context are the strange form-factors. Jaffe showed [380], see also [381], that under certain assumptions the information encoded in the isoscalar nucleon form factors could be used to extract strange matrix elements and that the strange form factor $F_1^{(s)}$ thus obtained was rather large in magnitude due to the strong coupling of the ϕ to the nucleon in dispersion theoretical analysis. However a realistic isoscalar spectral function including the $\rho\pi$ exchange led to sizeably reduced values for the strange magnetic moment and radius [382]. To determine the strange form factor experimentally one measures parity violating (PV) asymmetries in PV electron scattering from nucleons and nuclei. There is a whole experimental program dedicated to such measurements with on going experiments from the G0 [383], HAPPEX [384] (for the nucleon) and [385] (for ^4He), Mainz A4 [386] and SAMPLE [387]

collaborations with, at present, no strong evidence for the presence of strange-quark effects in the nucleon. ${}^4\text{He}$ is particularly interesting since due to the spin-parity of this nucleus it can lead to a direct determination of the strangeness electric form factor provided that other effects like isospin symmetry breaking or meson exchange contributions to the charge operators are negligible. Recently values for the strange magnetic moment μ_s and the strange electric radius $\langle r_{E,s}^2 \rangle$ have been extracted from a complete world set of the data obtained by these collaborations up to $Q^2 \sim 0.3 \text{ GeV}^2$ leading to [388]

$$\langle r_{E,s}^2 \rangle = (0.014 \pm 0.096 \mp 0.00) \text{ fm}^2, \quad \mu_s = 0.12 \pm 0.55 \pm 0.07. \quad (123)$$

Let us look in more detail at these strange form factors. They are defined in terms of the strangeness current:

$$J_\mu^s = \sqrt{\frac{2}{3}} J_\mu^{(0)} - \frac{2}{\sqrt{3}} J_\mu^{(8)}, \quad (124)$$

in complete analogy to what is done in the electromagnetic case. They have been calculated in lattice simulations as well as hadron models. I will concentrate here on CHPT. As can be seen the baryon number current enter Eq. (124). Thus one expects that LECs will contribute which do not appear in any other known processes. It was thus claimed [389] that CHPT would not be able to say anything about these form factors. However with the advent of experimental results which could be used to fix some of these LECs, one hoped to be able to predict for example the anomalous magnetic moment. At present an $\mathcal{O}(q^4)$ calculation of the radius and the magnetic moment has been done [390] in HBCHPT (note that here the definition of the radius does not involve the normalization factor as it is usually the case for the em radii). It leads to

$$\begin{aligned} \mu_s &= 1.2 + 2.5(b_s(\lambda = 1\text{GeV}) + 0.6b_8(\lambda = 1\text{GeV})) , \\ \langle r_{M,s}^2 \rangle &= -0.16 + [0.12 + 0.3b_s^r(\lambda = 1\text{GeV})] \text{ fm}^2 . \end{aligned} \quad (125)$$

In this formula b_s , b_s^r and b_8 are undetermined singlet LECs. The contributions ~ 1.2 and ~ 0.12 arise from loop graphs and LECs which were obtained from measured octet baryon magnetic moments [391]. The first number on the r.h.s. of the expression for $\langle r_{M,s}^2 \rangle$ corresponds to the $\mathcal{O}(q^3)$ result. It has been first obtained in [392] and shown to satisfies a Low Energy Theorem:

$$\langle r_{M,s}^2 \rangle = -\frac{5D^2 - 6DF + 9F^2}{48\pi F_K^2} \frac{m}{M_K} + \mathcal{O}(M_K^0). \quad (126)$$

Using this $\mathcal{O}(q^3)$ parameter free prediction together with an extrapolation of the SAMPLE result at $Q^2 = 0.1 \text{ GeV}^2$ down to zero Q^2 a determination of the strange magnetic moment has been made. Unfortunately as can be seen from Eq. (125) there is a large cancellation between the $\mathcal{O}(q^3)$ and some of the $\mathcal{O}(q^4)$ terms making the strange radius very sensitive to the unknown LEC b_1^r . Thus neither the magnitude nor the size of the magnetic radius can be determined in a model independent manner. The value of b_1^r and $b_s(\lambda = 1\text{GeV}) + 0.6b_8(\lambda = 1\text{GeV})$ have been obtained in [390] by a matching with dispersion relations and found to be -1.1 and -0.6 respectively in nice agreement with the expectation from dimensional analysis. This leads to $\langle r_{M,s}^2 \rangle \sim 0.34 \text{ fm}^2$ and $\mu_s = -0.36$. This last quantity is within the error bars of the best fit Eq. (123). A quenched lattice calculation of $G_M^{(s)}(q^2)$ at five different kinematic points [393] is in agreement with the value of μ_s but in disagreement with the one of $\langle r_{M,s}^2 \rangle$.

While the SAMPLE collaboration measures the strange magnetic form factor, the other collaborations which have chosen different kinematics measure a combination of the strange electric and magnetic form factor. Combining the SAMPLE and the HAPPEX results in order to fix two unknown LECs the Q^2 dependence of the strange electric form factor has been determined to $\mathcal{O}(q^3)$ [394], leading to a strange electric radius fairly small and positive:

$$\langle r_{E,s}^2 \rangle = (0.05 \pm 0.09) \text{ fm}^2 \quad (127)$$

to be compared with Eq. (123). Few things have to be stressed with respect to this number. First this calculation uses the strange magnetic moment to $O(q^3)$. Its central value is found to be $\mu_s = 0.18$ not in agreement with the central value discussed above. Second the experimental values have been updated since the calculation has been done. Third, a $O(q^4)$ calculation should of course be performed to evaluate the $1/m$ corrections which can, in some cases, be non negligible.

Up to now the experimental results concerning the strange form factors seem to give rather small values. It was pointed out [395] that the inequality of up and down quarks produces in fact effects that mimic the strange form factors and thus could be of importance for a precise determination of these form factors. Isospin violation in the vector form factors of the nucleon have thus been recently calculated in two flavor CHPT with extraction of some LECs from resonance saturation [395]. Some upper limits have been obtained $G_M^{u,d}(t) < 0.05$ and $G_E^{u,d}(t) < 0.01$, for more details see that reference. As we have previously said, the knowledge of isospin symmetry breaking effects are also of utmost importance for the measurements on ${}^4\text{He}$. They have been determined in a very recent paper [396] and found to be of comparable magnitude to those associated with strangeness components in the nucleon electric form factor at the low momentum transfers of interest.

More low- t data on the nucleon's strange vector form factors will clearly be extremely useful in getting a better understanding of these quantities.

7.5 Kaon-Nucleon scattering

Since the review [7] has been written not much work has been done on the subject of kaon-nucleon scattering in pure CHPT. In fact there is a big difference between the strangeness $S=1$ and the $S=-1$ channels. While the first one is purely elastic at low energies, the second one involves inelastic channels. Especially the isospin 0 $\bar{K}N$ channel is completely dominated by the nearby subthreshold $\Lambda(1405)$ resonance. It thus seems difficult to explain this channel in pure CHPT.

I will briefly report on a calculation by Kaiser [397] of the threshold T-matrix of kaon-nucleon and antikaon-nucleon scattering to one loop order in HBCHPT. The following empirical values have been obtained [398] from a combined dispersion relation analysis of $\bar{K}N$ and KN scattering data.

$$\begin{aligned} T_{KN}^{(0)} &= 0.4 \text{ fm} , & T_{KN}^{(1)} &= -6.3 \text{ fm} , \\ T_{\bar{K}N}^{(0)} &= (-32.6 + 13.0i) \text{ fm} , & T_{\bar{K}N}^{(1)} &= (7.1 + 11.5i) \text{ fm} . \end{aligned} \quad (128)$$

Using the KN empirical values to fix the two LECs entering the calculation, Kaiser predicted the $\bar{K}N$ threshold T-matrices:

$$T_{\bar{K}N}^{(0)} = (30.4 + 6.2i) \text{ fm} , \quad T_{\bar{K}N}^{(1)} = (7.1 + 10.4i) \text{ fm} . \quad (129)$$

The complex valued isospin-1 amplitude is in very good agreement with the corresponding empirical value, whether, as expected, CHPT fails completely in the case of the isospin 0. It is interesting to look at the chiral expansion of these quantities. One has: $T_{KN}^{(0)} = (0 + 2.29 - 1.87) \text{ fm}$, $T_{KN}^{(1)} = (-7.63 + 7.83 - 6.54) \text{ fm}$ and $T_{\bar{K}N}^{(1)} = (3.81 + 5.06 - 1.74 + 10.39i) \text{ fm}$. It shows a pattern which seems generic for the $SU(3)$ baryon CHPT calculations namely the cancellations of large contributions at second and third chiral order, see for example the baryon masses and their magnetic moments [225,376].

In order to be able to describe the $S=-1$ channel one has to employ non-perturbative methods [361–366] which will allow for example to generate the $\Lambda(1405)$ as a quasi-bound $\bar{K}N$ state from the lowest order attractive chiral meson-baryon interaction in this channel. Recent calculations have been made within unitarized CHPT in [399,400]. These studies are very important in view of the kaonic atoms measurement at DEAR [401] (analog to the pionic atoms measurement described in Section 4.1.2) which allow to measure the $\bar{K}N$ threshold amplitude to a very good accuracy. There is also a foreseen

even better determination by the DEAR/SIDDHARTA Collaboration [402]. The pertinent formula for the energy shift and decay width in terms of the scattering amplitudes has been obtained in [403] in the framework of effective field theory, that accounts for a systematic expansion in isospin breaking effects. Let me just briefly summarize what is the present status. It was pointed out in [403] that the scattering lengths obtained within unitarized CHPT are in disagreement with the DEAR measurement [404], statement which was confirmed in [399]. However some recent papers [400, 405] show that it is in fact possible to obtain fits compatible both with DEAR and K^-p scattering data. For a thorough discussion of these issues, see [406].

7.6 Kaon-Photoproduction

We have been discussing in section 5.3 pion photo- and electroproduction. In fact some kaon photoproduction data have also been taken at the electron stretcher ring ELSA (Bonn) over a wide energy range. An exploratory study of the reactions $\gamma p \rightarrow \Sigma^+ K^0, \Lambda K^0$ and $\Sigma^0 K^+$ has thus been done within HBCHPT in [407] to third order. Clearly as discussed in the case of the pion a full scale q^4 calculation would be necessary, however as stressed in [407] it is first necessary to see whether the method is applicable in view of the not that small expansion parameter in $SU(3)$ as discussed previously.

The calculation goes as in the $SU(2)$ case except that now one has to take into account kaon and η loops. Also more LECs, 13, contribute. One combination is fixed from the nucleon axial radius while the others are determined within resonance saturation. One immediate outcome is the investigation of the effect of such loops on the $SU(2)$ predictions. As expected, they are small, e.g. for neutral pion photoproduction off protons, $E_{0+, \text{thr}}^K = (eF M_\pi^3)/(96\pi^2 F_\pi^3 M_K) = 0.14 \cdot 10^{-3}/M_{\pi^+}$ which is just 1/10th of the empirical value and considerably smaller than the pion contribution.

For the reaction $\gamma p \rightarrow K^0 \Sigma^+$ no data points exists in the first 100 MeV above threshold. In [407] a prediction is made for the electric dipole amplitude $E_{0+, \text{thr}}(K^0 \Sigma^+) = 1.07 \cdot 10^{-3}/M_\pi$. An interesting observation is that in that case the leading P -wave multipoles are very sensitive to the yet unmeasured magnetic moment of the Σ^0 because it is enhanced by the coupling constant ratio $g_{pK\Lambda}/g_{pK\Sigma^0} = (D + 3F)/\sqrt{3}(F - D) \simeq -5$. Results of the calculation for the reactions $\gamma p \rightarrow K^+ \Lambda$, and $\gamma p \rightarrow K^+ \Sigma^0$ [407] have been compared to the available data [408]. While the total cross section for the second reaction agrees with the two data points, the lowest bin from ELSA is slightly bigger than the calculation. The predicted recoil polarization comes out generally too small except for the forward angles for the reaction $\gamma p \rightarrow K^+ \Lambda$, however the shape is well described. Also the important sign difference between the recoil polarization of the two reactions is well reproduced. It stems from an intricate interference of the complex S - and P - wave multipoles.

Results are encouraging but clearly more work has to be done on the theory side, e.g. inclusion of higher order effects and higher partial waves as well as a better handle on the various coupling constants. On the experimental side one would need data closer to threshold together with finer energy binning. Note that here also unitarized CHPT calculations have been done [409].

7.7 Proposals for improved chiral expansion

As we have seen the strange mass is not that small and in some processes one can question the validity of the standard perturbative expansion, see for example [115] for a discussion of such processes and also some of the one discussed here. Let me discuss some proposals to improve on the chiral expansion. There are two different ways to proceed. Either the strange quark is treated on equal footing with the up and down quarks following the standard scenario or not. In the first case different methods of regularizations can be proposed to improve on the convergence (one should keep in mind the remark already done in Section 2.3.5 that the resulting physics should be independent of the choice of the regularization scheme. However at a given order one choice might be more efficient than another

one). We have already seen in the previous sections that the IR regularization can lead to improved convergence compared to HBCHPT. Another regularization named long distance regularization has been proposed first by Donoghue and Holstein [114]. On the other hand, A. Roessl [410] proposed a different way of treating the kaon making use of the fact that M_π/M_K is not that large. This is the so-called Heavy Kaon CHPT (HKCHPT). Note that the approach [29] is somewhat different. There only the two first orders in the chiral expansion in the meson sector are questioned due to the possible small value of the condensate in SU(3), the series is then supposed to be well converging. I will here briefly summarize HKCHPT and the long distance regularization.

7.7.1 Heavy kaon CHPT

Roessl's idea [410] is to consider the kaon as a heavy source in much the same way as the nucleon in HBCHPT (a closely related work applying reparameterization invariance instead of the reduction of relativistic amplitude is presented in [411]). Since the kaons appear now as matter fields, the chiral Lagrangian for pion-kaon interactions decomposes into a string of terms with a fixed number of kaons field. One has

$$\mathcal{L}_{\text{HKCHPT}} = \mathcal{L}_\pi + \mathcal{L}_{\pi KK} + \mathcal{L}_{\pi KKKK} + \dots \quad (130)$$

where the first term is the conventional pion effective Lagrangian. Then each term of the string is chirally expanded. Similarly to the baryons the Lagrangian for processes with at most one kaon in the in/out states contains terms with an odd number of derivatives and the power counting has to be modified due to the new large mass scale M_K . Matching conditions allow to fix the LECs of HKCHPT from the ones based on the standard chiral expansion with light kaons. This framework has been applied for example to the calculation of the pion-kaon sigma terms [412].

7.7.2 long distance regularization

Donoghue and Holstein [114] observed that the large corrections from one-loop graphs found in some processes arised to a large extent from propagation at short distances—smaller than the physical size of baryons—where the EFT cannot represent the correct physics. Using a cut-off regularization instead of dimensional regularization enables to remove this short-distance physics. The method thus introduces an additional parameter Λ and a cutoff function. Λ has to be chosen not too low as to remove any truly long distance physics and not too large as not to include spurious short distance physics. It is assumed to be of the order of $\Lambda \gg 1/r_B \sim 300 - 600$ MeV, where r_B is the size of the baryon. The loop integrals will usually give rise to strong dependence in the cutoff in the form Λ^3 , Λ^2 , Λ and $\ln \Lambda$. These are absorbed into renormalized values of the LECs.

This regularization has been used in the calculation of different processes without [115, 413] and with decuplets degrees of freedom [413, 414]. It was shown to greatly improve on the convergence of the chiral series. It amounts to multiplying the dimensional regularized quantity by a cut-off dependent function. In the case of the strange magnetic radius [413], for example one has using a dipole regulator:

$$\langle r_{M,s}^2 \rangle_{\text{cutoff}} = \langle r_{M,s}^2 \rangle_{\text{dim.reg}} X(\Lambda/M_K) = -0.162 \text{ fm}^2 X(\Lambda/M_K), \quad X(x) = \frac{x^3(x^2 + 14x/5 + 1)}{(x+1)^5}. \quad (131)$$

The function $X(x)$ is an increasing function of x such that $X(\infty) = 0$. For $\Lambda = 300 \dots 600$ MeV the strange magnetic moment is sizeably reduced compared to the dimensionally regularized result. One has $\langle r_{M,s}^2 \rangle_{\text{cutoff}} = -0.01 \dots -0.032 \text{ fm}^2$. This calculation is formally $\mathcal{O}(p^3)$ though the long distance portion of the one-loop integral contains higher order pieces.

There are, however, some drawbacks with this regularization. It involves one additional parameter, the cut-off Λ which might not be so easily determined. Also chiral symmetry is by no means guaranteed. Furthermore, the analytic structure can be screwed up, additional unphysical poles and/or cuts can be

produced. Note also that contrary to IR regularization it does not solve the problems of possible large $1/m$ corrections. Also up to now only $\mathcal{O}(p^3)$ calculations have been performed. It would be interesting to have full one loop results within this scheme.

8 Conclusion

Understanding the implications of spontaneous symmetry breaking, the symmetry which governs the strong interactions at low energies, on baryon properties is a difficult task. It has become possible on the theory side with the development of effective theories and particularly the model-independent framework, CHPT, as well as with the progress of lattice QCD. One of the big advantages of CHPT is that it allows for a precise determination of the theoretical uncertainties. On the experimental side much more precise data have become available due to the advent of CW machines and the possibility of having polarized targets as well as polarized beams. Some successes have been obtained as we have seen in this review. Also Baryon CHPT has been refined in the last decade with the development of new regularization schemes. Chiral extrapolations have been performed and studies of generalized parton distribution are actually developed, I unfortunately did not have the space to report on it here. However, work remains to be done to further sharpen our understanding of QCD at low energies. Particularly the Δ degree of freedom has still to be better understood for some processes. Also calculations in the resonance region have to be generalized. Chiral extrapolations have to be pursued, specially the study of unstable particles. Isospin breaking effects have also to be well under control considering the degree of accuracy reached in many processes. $SU(3)$ calculations have to be continued so as to understand better the mechanism of chiral symmetry breaking.

Acknowledgments

I would like to thank Ulf-G. Meißner, S. R. Beane, N. Fettes, J. Gasser, T. Hemmert, N. Kaiser, B. Kubis, J. Kambor, H. Krebs, T.-S. H. Lee, A. Rusetsky and J. Stern with whom I had enjoyable and enriching collaboration. I am particularly grateful to Ulf-G. Meißner for many useful comments and careful reading of the manuscript. I would also like to thank O. Pène and H. Wittig for sharing their insights on lattice QCD and reading carefully the part of the review related to it. This work was supported in part by the EU Integrated Infrastructure Initiative Hadron Physics Project (contract number RII3-CT-2004-506078) and the EU Contract No. MRTN-CT-2006-035482, “FLAVIANet”.

References

- [1] G. Ecker, Lectures given at the 2005 European School of High-Energy Physics, Kitzbühel, Austria, Aug. 21 - Sept. 3, 2005; to appear in the *Proceedings (CERN Yellow Report)*
- [2] E. Epelbaum, *Prog. Part. Nucl. Phys.* 57 (2006) 654
- [3] J. F. Donoghue, *Presented at Int. School of Low-Energy Antiprotons, Erice, Italy, Jan 25-31, 1990*, CERN-TH-5667-90
- [4] U.-G. Meißner, *Rept. Prog. Phys.* 56 (1993) 906
- [5] H. Leutwyler, *hep-ph/9406283*
- [6] G. Ecker, *Prog. Part. Nucl. Phys.* 35 (1995) 1
- [7] V. Bernard, N. Kaiser and U.-G. Meißner, *Int. J. Mod. Phys. E* 4 (1995) 193
- [8] A. Pich, *Rept. Prog. Phys.* 58 (1995) 563
- [9] A. Pich, “Effective Field Theory”, in *Les Houches Summer School in Theoretical Physics, Session 68: Probing the Standard Model of Particle Interactions*

- [10] J. Gasser, *Nucl. Phys. Proc. Suppl.* 86 (2000) 257
- [11] H. Leutwyler, *hep-ph/0008124*.
- [12] S. Scherer, *Adv. Nucl. Phys.* 27 (2003) 277
- [13] J. Gasser, *Lect. Notes Phys.* 629 (2004) 1
- [14] V. Bernard and U.-G. Meißner, to appear in *Ann. Rev. Nucl. Part. Sci.* 57 (2007) 33, *hep-ph/0611231*
- [15] C. McNeile, *Phys. Lett. B* 619 (2005) 124
- [16] J. Gasser and H. Leutwyler, *Ann. Phys. (N.Y.)* 158 (1984) 142
- [17] J. Goldstone, *Nuovo Cim.* 19 (1961) 154; J. Goldstone, A. Salam and S. Weinberg, *Phys. Rev.* 127 (1962) 965
- [18] S. Weinberg, *Physica* 96A (1979) 327
- [19] J. Gasser and H. Leutwyler, *Nucl. Phys. B* 250 (1985) 465
- [20] H. Leutwyler, *Ann. Phys. (N.Y.)* 235 (1994) 165
- [21] S. Weinberg, *hep-ph/9412326*
- [22] T. Appelquist and J. Carazzone, *Phys. Rev. D* 11 (1975) 2856
- [23] T. Banks and A. Casher, *Nucl. Phys. B* 169 (1980) 103
- [24] H. Leutwyler and A. Smilga, *Phys. Rev. D* 46 (1992) 5607
- [25] J. Stern, *hep-ph/9801282*
- [26] J. Stern, H. Sazdjian and N. H. Fuchs, *Phys. Rev. D* 47 (1993) 3814; M. Knecht and J. Stern, “Generalized Chiral Perturbation Theory”, contribution to the Second DAΦNE Physics Handbook, L. Maiani, N. Paver and G. Pancheri, eds, May 1995; *hep-ph/9411253*; M. Knecht B. Moussallam and J. Stern, *Nucl. Phys. B* 429 (1994) 125
- [27] B. Moussallam, *Eur. Phys. J. C* 14 (2000) 111; *JHEP* 0008 (2000) 005
- [28] S. Descotes-Genon, L. Girlanda and J. Stern, *JHEP* 0001 (2000) 041
- [29] S. Descotes-Genon, L. Girlanda and J. Stern, *Eur. Phys. J. C* 27 (2003) 115; S. Descotes-Genon, N. H. Fuchs, L. Girlanda and J. Stern, *Eur. Phys. J. C* 34 (2004) 201
- [30] L. Masetti [NA48 collaboration], Talk at the 33rd International Conference on High Energy Physics (ICHEP 06), *hep-ex/0610071*
- [31] G. Colangelo, J. Gasser and H. Leutwyler, *Phys. Lett. B* 488 (2000) 261
- [32] G. Colangelo, J. Gasser and H. Leutwyler, *Nucl. Phys. B* 603 (2001) 125
- [33] M. Mojžiš and J. Kambor, *Phys. Lett. B* 476 (2000) 344
- [34] J. Bijnens, *Prog. Part. Nucl. Phys.* 58 (2007) 521
- [35] N. Fettes, U.-G. Meißner, M. Mojžiš and S. Steininger, *Ann. Phys. (N.Y.)* 283 (2000) 273
- [36] S. Weinberg, *Phys. Rev.* 112 (1958) 1375
- [37] M. Morita, R. Morita and K. Koshigiri, *Nucl. Phys. A* 577 (1994) 387c
- [38] G. Colangelo and S. Dürr, *Eur. Phys. J. C* 33 (2004) 543
- [39] J. Bijnens, G. Colangelo, G. Ecker, J. Gasser and M. E. Sainio, *Nucl. Phys. A* 508 (1997) 263
- [40] G. Ecker and M. Mojžiš, *Phys. Lett. B* 365 (1996) 312
- [41] J. Gasser, M. E. Sainio and S. Svarc, *Nucl. Phys. B* 307 (1988) 779
- [42] U.-G. Meißner, G. Müller and S. Steininger, *Ann. Phys. (N.Y.)* 279 (2000) 1
- [43] J. Gasser, M. A. Ivanov, E. Lipartia, M. Mojžiš and A. Rusetsky, *Eur. Phys. J. C* 26 (2002) 13

- [44] H. Neufeld, J. Gasser and G. Ecker, *Phys. Lett. B* 438 (1998) 106; H. Neufeld, *Eur. Phys. J. C* 7 (1999) 355
- [45] J. F. Donoghue and B. R. Holstein, *Phys. Rev. D* 46 (1992) 4076
- [46] B. Moussallam, *Eur. Phys. J. C* 6 (1999) 681
- [47] B. Ananthanarayan, P. Büttiker and B. Moussallam, *Eur. Phys. J. C* 22 (2001) 133
- [48] J. Bijnens, *Phys. Rep.* 265 (1996) 369
- [49] V. Bernard, N. Kaiser and U.-G. Meißner, *Phys. Lett. B* 309 (1993) 421
- [50] V. Bernard, N. Kaiser and U.-G. Meißner, *Nucl. Phys. A* 615 (1997) 483
- [51] J. F. Donoghue, C. Ramirez and G. Valencia, *Phys. Rev. D* 39 (1989) 1947
- [52] G. Ecker, J. Gasser, A. Pich and E. de Rafael, *Nucl. Phys. B* 321 (1989) 311;
- [53] G. Ecker, J. Gasser, H. Leutwyler, A. Pich and E. de Rafael, *Phys. Lett. B* 223 (1989) 425
- [54] M. Bando, T. Kugo and K. Yamawaki, *Phys. Rep.* 164 (1988) 217; U.-G. Meißner, *Phys. Rep.* 161 (1988) 213
- [55] V. Cirigliano, G. Ecker, M. Eidemüller, R. Kaiser, A. Pich and J. Portoles, *Nucl. Phys. B* 753 (2006) 139
- [56] G. 't Hooft, *Nucl. Phys. B* 72 (1974) 461
- [57] M. Knecht and A. Nyffeler, *Eur. Phys. J. C* 21 (2001) 651
- [58] V. Cirigliano, G. Ecker, M. Eidemüller, R. Kaiser, A. Pich and J. Portoles, *JHEP* 0504 (2005) 006
- [59] V. Cirigliano, G. Ecker, M. Eidemüller, A. Pich and J. Portoles, *Phys. Lett. B* 596 (2004) 96
- [60] I. Rosell, J. J. Sanz-Cillero and A. Pich, *JHEP* 0408 (2004) 042
- [61] O. Catà and S. Peris, *Phys. Rev. D* 65 (2002) 056014
- [62] I. Rosell, J. J. Sanz-Cillero and A. Pich, *JHEP* 0701 (2007) 039
- [63] K. Kampf and B. Moussallam, *Eur. Phys. J. C* 47 (2006) 723
- [64] E. Epelbaum, U.-G. Meißner, W. Glöckle and C. Elster, *Phys. Rev. C* 65 (2002) 044001
- [65] Ph. Boucaud *et al.* [ETM Collaboration], *hep-lat/0701012*
- [66] Del Debbio, L. Giusti, M. Lüscher, R. Petronzio and N. Tantalo, *hep-lat/0610059*
- [67] C. Bernard *et al.* [MILC Collaboration], *Proceedings of Science (Lattice 2006)* (2006) 163; *hep-lat/0611024*
- [68] Particle Data Group, *J. Phys. G: Nucl. Part. Phys.* 33 (2006) 1
- [69] W. J. Marciano and A. Sirlin, *Phys. Rev. Lett.* 95 (2005) 081601
- [70] J. Stern, *hep-ph/0611127*
- [71] E. Blucher and W. J. Marciano, Particle Data Group, *J. Phys. G: Nucl. Part. Phys.* 33 (2006) 1
- [72] M. Suzuki, Particle Data Group, *J. Phys. G: Nucl. Part. Phys.* 33 (2006) 1
- [73] Y. Ishikawa *et al.* [CP-PACS Collaboration], *PoS LAT2006 (2006)* 181
- [74] C. Allton *et al.* [RBC+UKQCD Collaboration], *hep-lat/0701013*
- [75] S. R. Beane, P. F. Bedaque, K. Orginos and M. J. Savage, *hep-lat/0606023*
- [76] T. Kaneko, talk at the Kaon 2007 conference
- [77] N. Fettes and U.-G. Meißner, *Nucl. Phys. A* 676 (2000) 311
- [78] T. Becher and H. Leutwyler, *JHEP* 0106 (2001) 017
- [79] V. Bernard, N. Kaiser and U.-G. Meißner, *Nucl. Phys. B* 457 (1995) 147
- [80] P. Büttiker and U.-G. Meißner, *Nucl. Phys. A* 668 (2000) 97

- [81] U.-G. Meißner, *PoS LAT2005 (2005) 009*
- [82] M. C. M. Rentmeester, R. G. E. Timmermans and J. J. de Swart, *Phys. Rev. C* 67 (2003) 044001
- [83] J. Gasser, H. Leutwyler and M. E. Sainio, *Phys. Lett. B* 253 (1991) 253; *ibid Phys. Lett. B* 253 (1991) 260
- [84] S. Ando and H. W. Fearing, *Phys. Rev. D* 75 (2007) 014025
- [85] N. Fettes, V. Bernard and U.-G. Meißner, *Nucl. Phys. A* 669 (2000) 269
- [86] J. L. Goity, R. Lewis, M. Schvellinger and L. Zhang, *Phys. Lett. B* 454 (1999) 115
- [87] J. J. de Swart, M. C. Rentmeester and R. G. E. Timmermans, *PiN Newslett.* 13 (1997) 96
- [88] V. V. Abaev, P. Metsä and M. E. Sainio, *hep-ph/0704.3167*
- [89] E. Jenkins and A. V. Manohar, *Phys. Lett. B* 255 (1991) 558
- [90] V. Bernard, N. Kaiser, J. Kambor and U.-G. Meißner, *Nucl. Phys. B* 388 (1992) 315
- [91] T. Becher, PhD thesis, “The low Energy Structure of the Pion Nucleon interaction”, T. Becher and H. Leutwyler, *Eur. Phys. J. C* 9 (1999) 643
- [92] G. Höhler and E. Pietarinen, *Phys. Lett. B* 53 (1975) 471
- [93] W. R. Frazer and J. Fulco, *Phys. Rev.* 117 (1960) 1603
- [94] V. Bernard, N. Kaiser and U.-G. Meißner, *Nucl. Phys. A* 611 (1996) 429
- [95] T. Becher, *hep-ph/0011079*
- [96] N. Kaiser, *Phys. Rev. C* 68 (2003) 025202
- [97] H.-B. Tang, *hep-ph/9607436*
- [98] P. J. Ellis and H.-B. Tang, *Phys. Rev. C* 57 (1998) 3356
- [99] B. Kubis, “Strong Interactions and Electromagnetism in low energy Hadron Physics”, PhD thesis Bonn 2002, Jülich Report 4007
- [100] M. Procura, T. R. Hemmert and W. Weise, *Phys. Rev. D* 69 (2004) 034505
- [101] J. L. Goity, D. Lehmann, G. Prezeau and J. Saez, *Phys. Lett. B* 504 (2001) 21
- [102] P. C. Bruns and U.-G. Meißner, *Eur. Phys. J. C* 40 (2005) 97
- [103] J. Gegelia and G. Japaridze, *Phys. Rev. D* 60 (1999) 114038
- [104] T. Fuchs, J. Gegelia, G. Japaridze and S. Scherer, *Phys. Rev. D* 68 (2003) 056005
- [105] J. Gegelia, G. Japaridze and K. S. Turashvili, *Theor. Math. Phys.* 101 (1994) 1313
- [106] M. R. Schindler, J. Gegelia and S. Scherer, *Phys. Lett. B* 586 (2004) 258
- [107] M. R. Schindler, J. Gegelia and S. Scherer, *Nucl. Phys. B* 682 (2004) 367
- [108] T. Fuchs, J. Gegelia, G. Japaridze and S. Scherer, *Phys. Lett. B* 575 (2003) 11
- [109] C. Hacker, N. Wies, J. Gegelia and S. Scherer, *Phys. Rev. C* 72 (2005) 055203
- [110] D. Lehmann and G. Prezeau, *Phys. Rev. D* 65 (2002) 016001
- [111] C. Itzykson and J.-B. Zuber, *Quantum Field Theory* (McGraw-Hill, New York, 1980)
- [112] J. Gasser, *Ann. Phys. (N.Y.)* 136 (1981) 62
- [113] D. Espriu and J. Matias, *Nucl. Phys. B* 418 (1994) 494
- [114] J. F. Donoghue and B. R. Holstein, *Phys. Lett. B* 436 (1998) 331
- [115] J. F. Donoghue, B. R. Holstein and B. Borasoy, *Phys. Rev. D* 59 (1999) 036002
- [116] R. D. Young, D. B. Leinweber and A. W. Thomas, *Prog. Part. Nucl. Phys.* 50 (2003) 399
- [117] D. B. Leinweber, A. W. Thomas and R. D. Young, *Phys. Rev. Lett.* 92 (2004) 242002
- [118] V. Bernard, T. R. Hemmert and U.-G. Meißner, *Nucl. Phys. A* 732 (2004) 149

- [119] D. Djukanovic et al, *Phys. Rev. D* 72 (2005) 045002
- [120] J. Gasser and A. Zepeda, *Nucl. Phys. B* 174 (1980) 445
- [121] E. Jenkins and A. V. Manohar, *Phys. Lett. B* **259** (1991) 353 and “Baryon Chiral Perturbation Theory” in “Effective Field Theories of the Standard Model,” ed. U.-G. Meißner, World Scientific, Singapore (1992).
- [122] T. R. Hemmert, B. Holstein and J. Kambor, *Phys. Lett. B* 395 (1997) 89
- [123] T. R. Hemmert, “Heavy Baryon Chiral Perturbation Theory with Light Deltas”, Ph. D. thesis, University of Massachusetts, Amherst (1997).
- [124] T. R. Hemmert, B. Holstein and J. Kambor, *J. Phys. G: Nucl. Part. Phys.* 24 (1998) 1831
- [125] K. Torikoshi and P. J. Ellis, *Phys. Rev. C* 67 (2003) 015208
- [126] V. Bernard, T. R. Hemmert and U.-G. Meißner, *Phys. Lett. B* 565 (2003) 137
- [127] M. R. Schindler, J. Gegelia and S. Scherer, *Phys. Lett. B* 586 (2004) 258
- [128] K. G. Wilson, *Phys. Rev. D* 10 (1974) 2445
- [129] P. H. Ginsparg and K. G. Wilson, *Phys. Rev. D* 25 (1982) 2649
- [130] S. Chandrasekharan and U.-J. Wiese, *Prog. Part. Nucl. Phys.* 52 (2004) 373
- [131] K. Symanzik, in *Recent Developments in Gauge Theories*, G. t’Hooft et al. (Eds), Plenum, New York, 313; *Nucl. Phys. B* 226 (1983) 187
- [132] J. B. Kogut and L. Susskind, *Phys. Rev. D* 11 (1975) 395
- [133] S. R. Sharpe, *Lectures given at TASI 94, Boulder, CO, USA, May29-June24*, hep-ph/9412243
- [134] M. Golterman and J. Smit, *Nucl. Phys. B* 255 (1985) 328
- [135] R. Frezzotti, P. A. Grassi, S. Sint and P. Weisz, *JHEP* 0108 (2001) 058
- [136] D. B. Kaplan, *Phys. Lett. B* 288 (1992) 342
- [137] Y. Shamir, *Nucl. Phys. B* 406 (1993) 90
- [138] H. Neuberger, *Phys. Lett. B* 417 (1998) 141; 427 (1998) 353
- [139] D. B. Renner et al. (LHPC), *Nucl. Phys. Proc. Suppl.* 140 (2005) 255
- [140] S. Beane, P. F. Bedaque, K. Orginos and M. J. Savage, *hep-lat/0607036*
- [141] S. R. Sharpe, *hep-lat/0607016*
- [142] S. R. Sharpe and R. J. Singleton, *Phys. Rev. D* 58 (1998) 074501
- [143] W.-J. Lee and S. R. Sharpe, *Phys. Rev. D* 60 (1999) 114503
- [144] O. Bär, *hep-lat/0409123*
- [145] O. Bär, G. Rupak and N. Shoresh, *Phys. Rev. D* 70 (2004) 034508
- [146] G. Colangelo, *Nucl. Phys. Proc. Suppl.* 140 (2005) 120
- [147] P. H. Damgaard, *hep-lat/0310037*
- [148] J. Gasser and H. Leutwyler, *Phys. Lett. B* 184 (1987) 83; H. Leutwyler, *Phys. Lett. B* 189 (1987) 197
- [149] J. Gasser and H. Leutwyler, *Nucl. Phys. B* 307 (1988) 763
- [150] L. Giusti, P. Hernandez, M. Laine, P. Weisz and H. Wittig, *JHEP* 0404 (2004) 013
- [151] W. Bietenholz, T. Chiarappa, K. Jansen, K. I. Nagai and S. Shcheredin, *JHEP* 0402 (2004) 023
- [152] P. Bedaque, H. Griebhammer and G. Rupak, *Phys. Rev. D* 71 (2005) 054015
- [153] S. R. Beane, *Nucl. Phys. B* 695 (2004) 192
- [154] W. Detmold and M. Savage, *Phys. Lett. B* 599 (2004) 32
- [155] W.J. Lee and S. R. Sharpe, *Phys. Rev. D* 60 (1999) 114503

- [156] C. Aubin and C. Bernard, *Phys. Rev. D* 68 (2003) 034014, 074011
- [157] C. Bernard, *hep-lat/0603011*
- [158] C. Aubin et al. (MILC collaboration), *Phys. Rev. D* 70 (2004) 114501
- [159] J. A. Bailey and C. Bernard, *PoSLAT2005* (2005) 047
- [160] O. Bär, C. Bernard, G. Rupak and N. Shores, *Phys. Rev. D* 72 (2005) 054502
- [161] S. Myint and C. Rebbi, *Nucl. Phys. B* 421 (1994) 241
- [162] I. A. Shushpanov and A. V. Smilga, *Phys. Rev. D* 59 (1999) 054013
- [163] B. Borasoy, R. Lewis and P.-P. A. Ouimet, *hep-lat/0310054*
- [164] A. C. Irving, C. McNeile, C. Michael, K. J. Sharkey and H. Wittig [UKQCD Collaboration], *Phys. Lett. B* 518 (2001) 243
- [165] G. T. Fleming, D. R. Nelson and G. W. Kilcup, *Nucl. Phys. Proc. Suppl.* 119 (2003) 245
- [166] F. Farchioni, C. Gebert, L. Montvay, E. Scholz and L. Scorzato [qq+q Collaboration], *Phys. Lett. B* 561 (2003) 102
- [167] J. A. Mc Govern and M. C. Birse, *Phys. Rev. D* 74 (2006) 097501
- [168] S. Steininger, U.-G. Meißner and N. Fettes, *JHEP* 09 (1998) 008
- [169] J. Kambor and M. Mojžiš, *JHEP* 9904 (1999) 031
- [170] M. Schindler, D. Djukanovic, J. Gegelia and S. Scherer, *hep-ph/0612164*
- [171] C. W. Bernard et al., *Phys. Rev. D* 64 (2001) 054506
- [172] CP-PACS collaboration, Ali Khan et al., *Phys. Rev. D* 65 (2002) 054505
- [173] S. Aoki et al., *Phys. Rev. D* 68 (2003) 054502
- [174] C. R. Allton et al., *Phys. Rev. D* 65 (2002) 054502
- [175] Ali Khan et al., *Nucl. Phys. B* 689 (2004) 175
- [176] M. Göckeler, *hep-lat/0412013*
- [177] V. Bernard, T. R. Hemmert and U.-G. Meißner, *Phys. Lett. B* 622 (2005) 141
- [178] M. Procura, B. U. Musch, T. Wollenweber, T. R. Hemmert and W. Weise, *Phys. Rev. D* 73 (2006) 114510
- [179] D. B. Leinweber, A. W. Thomas and R. D. Young, *Nucl. Phys. A* 755 (2005) 59 and references therein
- [180] V. Pascalutsa and M. Vanderhaeghen, *Phys. Lett. B* 636 (2006) 31
- [181] R. D. Young, D. B. Leinweber and A. W. Thomas, *Prog. Part. Nucl. Phys.* 50 (2003) 399
- [182] S. Aoki et al. [JLQCD Collaboration], *Phys. Rev. D* 68 (2003) 054502
- [183] G. Colangelo, A. Fuhrer and C. Haefeli, *Nucl. Phys. Proc. Suppl.* 153 (2006) 41
- [184] M. Lüscher, *Commun. Math. Phys.* 104 (1986) 177
- [185] A. Fuhrer, The nucleon in finite volume (master thesis, univ. Bern)
- [186] G. Colangelo, S. Dürr and C. Haefeli, *Nucl. Phys. B* 721 (2005) 136
- [187] V. Bernard, L. Elouadrhiri and U.-G. Meißner, *J. Phys. G* 28 (2002) R1
- [188] R. G. Edwards et al, *Phys. Rev. Lett.* 96 (052001) 2006
- [189] A. A. Khan et al, *Nucl. Phys. Proc. Suppl.* 140 (2005) 408
- [190] S. Sasaki et al., *Nucl. Phys. Proc. Suppl.* 106 (2002) 302
- [191] D. Dolgov et al., *Phys. Rev. D* 66 (2002) 034506
- [192] M. Göckeler, private communication; QCDSF collaboration, to be published
- [193] T. R. Hemmert, M. Procura and W. Weise, *Phys. Rev. D* 68 (2006) 075009

- [194] V. Bernard and U.-G. Meißner, *Phys. Lett. B* 639 (2006) 278
- [195] S. R. Beane and M. J. Savage, *Phys. Rev. D* 70 (2004) 074029
- [196] B. R. Holstein, V. Pascalutsa and M. Vanderhaegen, *Phys. Rev. D* 72 (2005) 094014
- [197] B. Kubis and U.-G. Meißner, *Nucl. Phys. A* 679 (2001) 698
- [198] B. Borasoy, P. C. Bruns, U.-G. Meißner and R. Lewis, *Phys. Lett. B* 641 (2006) 294
- [199] N. Mathur et al., *Phys. Lett. B* 605 (2005) 137
- [200] D. Guadagnoli, M. Papinutto and S. Simula, *Phys. Lett. B* 604 (2004) 74
- [201] V. Bernard, U.-G. Meißner and A. Rusetsky, *hep-lat/0702012*
- [202] M. Lüscher, *Commun. Math. Phys.* 105 (1986) 153; *Nucl. Phys. B* 354 (1991) 531; *Nucl. Phys. B* 364 (1991) 237; *DESY-88-156 Lectures given at Summer School 'Fields, Strings and Critical Phenomena', Les Houches, France, Jun 28 - Aug 5, 1988*
- [203] U.-J. Wiese, *Nucl. Phys. Proc. Suppl.* 9 (1989) 609
- [204] K. Rummukainen and S. A. Gottlieb, *Nucl. Phys. B* 450 (1995) 397
- [205] N. H. Christ, C. Kim and T. Yamazaki, *Phys. Rev. D* 72 (2005) 114506
- [206] C. H. Kim, C. T. Sachrajda and S. R. Sharpe, *Nucl. Phys. B* 727 (2005) 218
- [207] G. Höhler, in *Landolt-Börnstein, vol.9 b2, Ed. H. Schopper (Springer, Berlin)*
- [208] M. Mojžiš, *Eur. Phys. J. C* 2 (1998) 181
- [209] A. Datta and S. Pakvasa, *Phys. Rev. D* 56 (1997) 4322
- [210] N. Fettes, U.-G. Meißner and S. Steininger, *Nucl. Phys. A* 640 (1998) 199
- [211] K. Torikoshi and P. J. Ellis, *Phys. Rev. C* 67 (2003) 015208
- [212] R. Koch, *Nucl. Phys. A* 448 (1986) 707
- [213] E. Matsinos, *Phys. Rev. C* 56 (1997) 3014
- [214] SAID on-line program, R. A. Arndt et al., see website <http://gwdac.phys.gwu.edu/>.
- [215] H. Denz et al. (CHAOS Collaboration), *Phys. Lett. B* 633 (2006) 209
- [216] R. Meier et al., *Phys. Lett. B* 588 (2004) 155
- [217] J. Breitschopf et al., *nucl-ex/0605027*
- [218] R. A. Arndt, W. J. Briscoe, I. I. Strakovsky and R. L. Workman, *Phys. Rev. C* 74 (2006) 045205
- [219] N. Fettes and U.-G. Meißner, *Nucl. Phys. A* 679 (2001) 629
- [220] N. Fettes and U.-G. Meißner, *Nucl. Phys. A* 693 (2001) 693
- [221] T. P. Cheng and R. Dashen, *Phys. Rev. Lett.* 26 (1971) 594
- [222] L. S. Brown, W. J. Pardee and R. D. Peccei, *Phys. Rev. D* 4 (1971) 2801
- [223] V. Bernard, N. Kaiser and U.-G. Meißner, *Phys. Lett. B* 389 (1996) 144
- [224] S. Weinberg, *Phys. Rev. Lett.* 17 (1966) 616
- [225] B. Borasoy and U.-G. Meißner, *Ann. Phys. (N.Y.)* 254 (1997) 192
- [226] R. Koch, *Z. Phys. C* 15 (1982) 161
- [227] J. Gasser, H. Leutwyler, M. P. Locher and M. E. Sainio, *Phys. Lett. B* 213 (1988) 85
- [228] M. Olsson, *Phys. Lett. B* 482 (2000) 50
- [229] S. Weinberg, *Trans. N. Y. Acad. of Sci* 38 (1997) 185
- [230] S. Weinberg, in *"Chiral Dynamics: Theory and Experiment", A. M. Bernstein and B. R. Holstein (eds.), Springer Verlag, Berlin, 1995.*
- [231] R. Urech, *Nucl. Phys. B* 433 (1995) 234

- [232] H. Neufeld and H. Rupertsberger, *Z. Phys. C* 68 (1995) 91
- [233] R. Bauer, J. Kambor and D. Wyler, *Nucl. Phys. B* 460 (1996) 127
- [234] M. Knecht and R. Urech, *Nucl. Phys. B* 519 (1998) 329
- [235] U.-G. Meißner, G. Müller and S. Steininger, *Phys. Lett. B* 406 (1997) 154, (E) *ibid B* 407 (1997) 434
- [236] U.-G. Meißner and S. Steininger, *Phys. Lett. B* 419 (1998) 403
- [237] G. Müller and U.-G. Meißner, *Nucl. Phys. B* 556 (1999) 265
- [238] U.-G. Meißner, U. Raha and A. Rusetsky, *Phys. Lett. B* 639 (2006) 478
- [239] V. E. Lyubovitskij, T. Gutsche, A. Faessler and R. Vinh Mau, *Phys. Rev. C* 65 (2002) 025202
- [240] J. Gasser, A. Rusetsky and I. Scimeni, *Eur. Phys. J. C* 32 (2003) 97
- [241] N. Fettes, U.-G. Meißner and S. Steininger, *Phys. Lett. B* 451 (1999) 233
- [242] A. M. Bernstein, *Phys. Lett. B* 442 (1998) 20
- [243] N. Fettes and Ulf-G. Meißner, *Phys. Rev. C* 63 (2001) 045201
- [244] W. R. Gibbs, Li Ai and W. B. Kaufmann, *Phys. Rev. Lett.* 74 (1995) 3740; E. Matsinos, *Phys. Rev. C* 56 (1997) 3014
- [245] J. Gasser, A. Rusetsky and J. Schacher, *HadAtom03, hep-ph/0401204*
- [246] D. Chatellard et al., *Nucl. Phys. A* 625 (1997) 855; P. Hauser et al., *Phys. Rev. C* 58 (1998) 1998
- [247] S. Deser, M. L. Goldberger, K. Baumann and W. Thirring, *Phys. Rev.* 96 (1954) 774
- [248] V. E. Lyubovitskij and A. Rusetsky, *Phys. Lett. B* 494 (2000) 9
- [249] S. R. Beane, V. Bernard, E. Epelbaum, U.-G. Meißner and D. R. Phillips, *Nucl. Phys. A* 57 (2003) 399
- [250] U.-G. Meißner, U. Raha, and A. Rusetsky, *Eur. Phys. J. C* 41 (2005) 213
- [251] S. Weinberg, *Phys. Lett. B* 295 (1992) 114
- [252] N. Kaiser, *Phys. Rev. C* 65 (2002) 057001
- [253] M. Döring, E. Oset and M. J. Vicente Vacas, *Phys. Rev. C* 70 (2004) 045203
- [254] B. Borasoy and H. W. Griebhammer, *Int. J. Mod. Phys. E* 12 (2003) 65
- [255] S. R. Beane and M. Savage, *Nucl. Phys. A* 717 (2003) 104
- [256] E. Epelbaum, W. Glöckle and U.-G. Meißner, *Nucl. Phys. A* 671 (2000) 295
- [257] D. Sigg, A. Badertscher, P. F. A. Goudsmit, H. J. Leisi and G. C. Oades, *Nucl. Phys. A* 609 (1996) 310
- [258] H. C. Schröder et al., *Eur. Phys. J. C* 21 (2001) 473
- [259] P. Hauser et al., *Phys. Rev. C* 58 (1998) 1869; D. Chatellard et al., *Nucl. Phys. A* 625 (1997) 855
- [260] D. Gotta (Pionic Hydrogen Collaboration), *Int. J. Mod. Phys. A* 20 (2005) 349
- [261] A. Nogga and C. Hanhart, *Phys. Lett. B* 634 (2006) 210
- [262] K. Brückner, *Phys. Rev.* 98 (1955) 769
- [263] I. R. Afnan and A. W. Thomas, *Phys. Rev. C* 10 (1974) 109; D. S. Koltun and T. Mizutani, *Ann. Phys. (N.Y.)* 109 (1978) 1
- [264] T. E. O. Ericson, B. Loiseau and A. W. Thomas, *Phys. Rev. C* 66 (2002) 014005
- [265] V. Lensky, V. Baru, J. Haidenbauer, C. Hanhart, A. Kudryavtsev and U.-G. Meißner, *Phys. Lett. B* 648 (2007) 46
- [266] T. D. Cohen, J. L. Friar, G. A. Miller and U. van Kolck, *Phys. Rev. C* 53 (1996) 2661

- [267] C. Hanhart, U. van Kolck and G. A. Miller, *Phys. Rev. Lett.* 85 (2000) 2905; C. Hanhart and N. Kaiser, *Phys. Rev. C* 66 (2002) 054005
- [268] C. Hanhart, *Phys. Rep.* 397 (2004) 155
- [269] D. Gotta et al., *PSI experiment R-06.03*
- [270] A. W. Thomas and R. H. Landau, *Phys. Rep.* 58 (1980) 121
- [271] T. Eden et al., *Phys. Rev. C* 50 (1994) R1749; M. Meyerhoff et al., *Phys. Lett. B* 327 (1994) 201 ; C. Herberg et al., *Eur. Phys. J. A* 5 (1999) 131; I. Passchier et al., *Phys. Rev. Lett.* 82 (1999) 4988; M. Ostrick et al., *Phys. Rev. Lett.* 83 (1999) 276 ; J. Becker et al., *Eur. Phys. J. A* 6 (1999) 329
- [272] C. F. Perdrisat, V. Punjabi and M. Vanderhaegen, *hep-ph/0612014*
- [273] M. A. B. Bég and A. Zepeda, *Phys. Rev. D* 6 (1972) 2912
- [274] H. W. Fearing, R. Lewis, N. Mobed and S. Scherer, *Phys. Rev. D* 56 (1997) 1783
- [275] T. Fuchs, J. Gegelia and S. Scherer, *J. Phys. G* 30 (2004) 1407
- [276] M. R. Schindler, J. Gegelia and S. Scherer, *Eur. Phys. J. A* 26 (2005) 1
- [277] V. Bernard, H. W. Fearing, T. R. Hemmert and U.-G. Meißner, *Nucl. Phys. A* 642 (1998) 563
- [278] V. Bernard, N. Kaiser and U.-G. Meißner, *Phys. Rev. Lett.* 67 (1991) 1515
- [279] V. Bernard, N. Kaiser, A. Schmidt and U.-G. Meißner, *Phys. Lett. B* 319 (1993) 269 and *Z. Phys. A* 348 (1994) 317
- [280] S. R. Beane, M. Malheiro, J. A. McGovern, D. R. Phillips and U. van Kolck, *Phys. Lett. B* 567 (2003) 200; *Nucl. Phys. A* 747 (2005) 311; J. McGovern, *Phys. Rev. C* 63 (2001) 064608, [Erratum *ibid C*66 (2002) 039902]
- [281] T. R. Hemmert, B. R. Holstein and J. Kambor, *Phys. Rev. D* 55 (1997) 5598
- [282] J. Tonnison, A. M. Sandorfi, S. Hoblit and A. M. Nathan, *Phys. Rev. Lett.* 80 (1998) 4382
- [283] V. Olmos de León et al., *Eur. Phys. J. A* 12 (2001) 231
- [284] G. Galler et al., *Phys. Lett. B* 503 (2001) 245
- [285] D. Drechsel, B. Pasquini and M. Vanderhaeghen, *Phys. Rep.* 378 (2003) 99
- [286] G. C. Gellas, T. R. Hemmert and U.-G. Meißner, *Phys. Rev. Lett.* 85 (2000) 14
- [287] K. B. Vijaya Kumar, J. A. McGovern and M. C. Birse, *Phys. Lett. B* 479 (2000) 167
- [288] H. W. Griedhammer and T. R. Hemmert, *Phys. Rev. C* 65 (2002) 045207
- [289] R. P. Hildebrandt, H. W. Griedhammer, T. R. Hemmert and B. Pasquini, *Eur. Phys. J. A* 20 (2004) 293
- [290] H. Arenhövel and D. Drechsel, *Nucl. Phys. A* 233 (1974) 153
- [291] P. A. M. Guichon, G. Q. Liu and A. W. Thomas, *Nucl. Phys. A* 591 (1995) 606; P. A. M. Guichon and M. Vanderhaeghen, *Prog. Part. Nucl. Phys.* 41 (1998) 125
- [292] D. Drechsel, G. Knöchlein, A. Metz and S. Scherer, *Phys. Rev. C* 55 (1997) 424; D. Drechsel, G. Knöchlein, A. Yu Korchin, A. Metz and S. Scherer, *Phys. Rev. C* 57 (1998) 941
- [293] N. d'Hose, *Eur. Phys. J. A* 28, s01 (2006) 117
- [294] C.-W. Kao, B. Pasquini and M. Vanderhaeghen, *Phys. Rev. D* 70 (2004) 114004
- [295] T. R. Hemmert, B. R. Holstein, G. Knöchlein and D. Drechsel, *Phys. Rev. D* 62 (2000) 014013
- [296] J. P. Chen, Proceedings of 5th international Workshop on Chiral Dynamics, *nucl-ex/0611024*
- [297] D. Drechsel, S. S. Kamalov and L. Tiator, *Phys. Rev. D* 63 (2001) 114010
- [298] S. B. Gerasimov, *Sov. J. Nucl. Phys.* 2 (1965) 598; S. D. Drell and A. C. Hearn, *Phys. Rev. Lett.* 16 (1966) 908

- [299] K. Helbing, in press at *Prog. Part. Nucl. Phys.*
- [300] X. Ji and J. Osborne, *J. Phys. G* 27 (2001) 127
- [301] J. R. Ellis and R. L. Jaffe, *Phys. Rev. D* 9 (1974) 1444
- [302] H. Burkhardt and W. N. Cottingham, *Ann. Phys. (N.Y.)* 56 (1970) 453
- [303] V. Bernard, T. R. Hemmert and U.-G. Meißner, *Phys. Rev. D* 67 (2003) 076008
- [304] X. Ji, C. Kao and J. Osborne, *Phys. Lett. B* 472 (2000) 1
- [305] V. D. Burkert, *Phys. Rev. D* 63 (2001) 097904
- [306] C. W. Kao, T. Spitzenberg and M. Vanderhaeghen, *Phys. Rev. D* 67 (2003) 016001
- [307] V. Bernard, T. R. Hemmert and U.-G. Meißner, *Phys. Lett. B* 545 (2002) 105
- [308] W. Bartel *et al.*, *Phys. Lett. B* 28 (1968) 148; S. Galster *et al.*, *Phys. Rev. D* 5 (1972) 519; V. Burkert and Z.-J. Li, *Phys. Rev. D* 47 (1993) 46
- [309] R. Fatemi *et al.*, *Phys. Rev. Lett.* 91 (2003) 222002
- [310] V. Pascalutsa, M. Vanderhaeghen and Shin Nan Yang, *Phys. Rep.* 437 (2007) 125
- [311] T. Fuchs and S. Scherer, *Phys. Rev. C* 68 (055502) 2003
- [312] A. I. Vainsthein and V. I. Zakharov, *Nucl. Phys. B* 36 (1972) 589
- [313] P. de Baenst, *Nucl. Phys. B* 24 (1970) 633
- [314] V. Bernard, N. Kaiser, J. Gasser and U.-G. Meißner, *Phys. Lett. B* 268 (1991) 291
- [315] V. Bernard, N. Kaiser and U.-G. Meißner, *Nucl. Phys. B* 383 (1992) 442
- [316] G. Ecker and U.-G. Meißner, *Comments Nucl. Part. Phys.* 21 (1995) 347.
- [317] V. Bernard, N. Kaiser and U.-G. Meißner, *Z. Phys. C* 70 (1996) 483
- [318] V. Bernard, N. Kaiser and U.-G. Meißner, *Phys. Lett. B* 378 (1996) 337
- [319] M. Fuchs *et al.*, *Phys. Lett. B* 368 (1996) 20
- [320] J. C. Bergstrom *et al.*, *Phys. Rev. C* 53 (1996) R1052; *Phys. Rev. C* 55 (1997) 2016
- [321] A. Schmidt *et al.*, *Phys. Rev. Lett.* 87 (2001) 232501
- [322] A. M. Bernstein *et al.*, *Phys. Rev. C* 55 (997) 1509
- [323] A. M. Bernstein, *πN Newsletter* No.11, 1995; Proceedings of the PANIC Conference, C. E. Carlson, J. J. Domingo (Eds), World Scientific, Singapore, 1996.
- [324] V. Bernard, N. Kaiser and U.-G. Meißner, *Eur. Phys. J. A* 11 (2001) 209
- [325] T. P. Welch *et al.*, *Phys. Rev. Lett.* 69 (1992) 2761
- [326] H.B. van den Brink *et al.*, *Phys. Rev. Lett.* 74 (1995) 3561; *Nucl. Phys. A* 612 (1997) 391
- [327] M. O. Distler *et al.*, *Phys. Rev. Lett.* 80 (1998) 2294
- [328] V. Bernard, T.-S.H. Lee, N. Kaiser and U.-G. Meißner, *Phys. Rep.* 246 (1994) 315
- [329] V. Bernard, N. Kaiser and U.-G. Meißner, *Nucl. Phys. A* 607 (1996) 379
- [330] H. Merkel *et al.*, *Phys. Rev. Lett.* 88 (2002) 012301
- [331] M. Weis *et al.*, 0705.3816 [*nucl-ex*]
- [332] the MAID Collaboration, <http://www.kph.uni-mainz.de>
- [333] J. Garcia Llongo, *Diploma Thesis, in preparation*
- [334] D. Crabb *et al.* (BigBite Collaboration), “Precision Measurement of Electroproduction of π^0 near Threshold: A Test of Chiral QCD Dynamics”, approved CEBAF experiment E01014.
- [335] S. Fubini, G. Furlan and C. Rosetti, *Nuovo Cimento* 40 (1965) 1171
- [336] B. Pasquini, D. Drechsel and L. Tiator, *Eur. Phys. J. A* 23 (2005) 279

- [337] V. Bernard, B. Kubis and U.-G. Meißner, *Eur. Phys. J. A* 25 (2005) 419
- [338] B. Pasquini, D. Drechsel and L. Tiator, *Eur. Phys. J. A* 27 (2006) 231
- [339] S. R. Beane, V. Bernard, T.-S.H. Lee, U.-G. Meißner and U. van Kolck, *Nucl. Phys. A* 618 (1997) 381
- [340] J. C. Bergstrom et al., *Phys. Rev. C* 57 (1998) 3203
- [341] H. Krebs, V. Bernard and U.-G. Meißner, *Nucl. Phys. A* 713 (2003) 405; *Eur. Phys. J. A* 22 (2004) 503
- [342] N. Fettes, V. Bernard and U.-G. Meißner, *Nucl. Phys. A* 669 (2000) 269
- [343] V. Bernard, N. Kaiser, U.-G. Meißner and A. Schmidt, *Nucl. Phys. A* 580 (1994) 475
- [344] V. Bernard, N. Kaiser and U.-G. Meißner, *Phys. Lett. B* 382 (1996) 19
- [345] M. Wolf et al., *Eur. Phys. J. A* 9 (2000) 5
- [346] M. Kotulla et al, *Phys. Lett. B* 578 (2004) 63
- [347] M. Kotulla and F. Zehr, private communication
- [348] V. Bernard, N. Kaiser and U.-G. Meißner, *Phys. Rev. D* 50 (1994) 6899
- [349] V. Bernard, N. Kaiser and U.-G. Meißner, *Phys. Rev. Lett.* 69 (1992) 1877
- [350] N. Kaiser, *Phys. Rev. C* 67 (2003) 027002
- [351] G. Bardin et al., *Phys. Lett. B* 104 (1981) 320
- [352] G. Jonkmans et al., *Phys. Rev. Lett.* 77 (1996) 4521; D. H. Wright et al., *Phys. Rev. C* 57 (1998) 373
- [353] T. Meissner, F. Myhrer and K. Kubodera, *Phys. Lett. B* 416 (1998) 36
- [354] S.-I. Ando and D.-P. Min, *Phys. Lett. B* 417 (1998) 177
- [355] V. Bernard, T. R. Hemmert and U.-G. Meißner, *Nucl. Phys. A* 686 (2001) 290
- [356] S.-I. Ando, F. Myhrer and K. Kubodera, *Phys. Rev. C* 63 (2000) 015203; *Phys. Rev. C* 65 (2002) 048501
- [357] V. A. Andreev et al., 0704.2072 [nucl-ex]
- [358] A. Czarnecki, W. Marciano and A. Sirlin, 0704.3968 [hep-ph]
- [359] S. Descotes and J. Stern, *Phys. Lett. B* 488 (2000) 274
- [360] J. A. Oller, E. Oset and J. R. Pelaez, *Phys. Rev. D* 59 (1999) 074001
- [361] N. Kaiser, P. B. Siegel and W. Weise, *Phys. Lett. B* 362 (1995) 23
- [362] N. Kaiser, P. B. Siegel and W. Weise, *Nucl. Phys. A* 594 (1995) 325
- [363] E. Oset and A. Ramos, *Nucl. Phys. A* 635 (1998) 99
- [364] J. A. Oller and U.-G. Meißner, *Phys. Lett. B* 500 (2001) 263
- [365] M. F. M. Lutz and E. E. Kolomeitsev, *Nucl. Phys. A* 700 (2002) 193
- [366] D. Jido, J. A. Oller, E. Oset, A. Ramos and U.-G. Meißner, *Nucl. Phys. A* 725 (2003) 181
- [367] J. A. Oller, E. Oset and A. Ramos, *Prog. Part. Nucl. Phys.* 45 (2000) 157
- [368] H. Leutwyler, *Phys. Lett. B* 378 (1996) 313
- [369] G. Amoros, J. Bijnens and P. Talavera, *Nucl. Phys. B* 602 (2001) 87
- [370] J. Stern, talk at Flavianet mini workshop 2007, see also talks at the Kaon 2007 conference
- [371] M. Frink and U.-G. Meißner, *Eur. Phys. J. A* 29 (2006) 255
- [372] A. Krause, *Helv. Phys. Acta* 63 (1990) 3; J. A. Oller, M. Verbeni and J. Prades, *JHEP* 0609 (2006) 079 ; ibid *hep-ph/0701096*
- [373] M. Frink and U.-G. Meißner, *JHEP* 0407 (2004) 028

- [374] C. Aubin et al. (MILC collaboration), *Phys. Rev. D* 70 (2004) 094505
- [375] M. Frink, U.-G. Meißner and I. Scheller, *Eur. Phys. J. A* 24 (2005) 395
- [376] U.-G. Meißner and S. Steininger, *Nucl. Phys. B* 499 (1997) 349
- [377] B. Kubis and U.-G. Meißner, *Eur. Phys. J. C* 18 (2001) 747
- [378] I. Eschrich et al. [Selex collaboration], *Phys. Lett. B* 522 (2001) 233
- [379] H. Genz and G. Höhler, *Phys. Lett. B* 61 (1976) 389
- [380] R. L. Jaffe, *Phys. Lett. B* 229 (1989) 275
- [381] H.-W. Hammer, U.-G. Meißner and D. Drechsel, *Nucl. Phys. A* 596 (1996) 367
- [382] U.-G. Meißner, V. Mull, J. Speth and J. W. van Orden, *Phys. Lett. B* 408 (1997) 381
- [383] D. S. Amstrong et al. *Phys. Rev. Lett.* 95 (2005) 092001
- [384] K. A. Aniol et al., *Phys. Rev. Lett.* 82 (1999) 1096; *Phys. Lett. B* 509 (2001) 211; *Phys. Rev. C* 69 (2004) 065501; *Phys. Lett. B* 635 (2006) 275
- [385] K. A. Aniol et al., *Phys. Rev. Lett.* 96 (2006) 022003; A. Acha et al., *Phys. Rev. Lett.* 98 (2007) 032301
- [386] F. E. Maas et al., *Phys. Rev. Lett.* 93 (2004) 022002; *Phys. Rev. Lett.* 94 (2005) 152001
- [387] D. T. Spayde et al., *Phys. Lett. B* 583 (2004) 79; T. M. Ito et al., *Phys. Rev. Lett.* 92 (2004) 102003
- [388] R. D. Young, J. Roche, R. D. Carlini and A. W. Thomas, *Phys. Rev. Lett.* 97 (2006) 102002
- [389] M. J. Ramsey-Musolf and H. Ito, *Phys. Rev. C* 55 (1997) 3066
- [390] H. W. Hammer, S. J. Puglia, M. J. Ramsey-Musolf and S.L. Zhu, *Phys. Lett. B* 562 (2003) 208
- [391] S. J. Puglia and M.J. Ramsey-Musolf, *Phys. Rev. D* 62 (2000) 034010
- [392] T. R. Hemmert, U.-G. Meißner and S. Steininger, *Phys. Lett. B* 437 (1998) 184
- [393] S. J. Dong, K. F. Liu and A. G. Williams, *Phys. Rev. D* 58 (1998) 074504
- [394] T. R. Hemmert, B. Kubis and U.-G. Meißner, *Phys. Rev. C* 60 (1999) 045501
- [395] B. Kubis and R. Lewis, *Phys. Rev. C* 74 (2006) 015204
- [396] M. Viviani et al., *nucl-th/0703051*
- [397] N. Kaiser, *Phys. Rev. C* 64 (2001) 045204
- [398] A. D. Martin, *Nucl. Phys. B* 179 (1981) 33
- [399] B. Borasoy, R. Nissler and W. Weise, *Phys. Rev. Lett.* 94 (2005) 213401
- [400] J. A. Oller, J. Prades and M. Verbeni, *Phys. Rev. Lett.* 95 (2005) 172502
- [401] R. Baldini et al. [DEAR collaboration], “DAPHNE exotic atom research: The DEAR proposal”, LNF-95-055-IR
- [402] D. L. Sirghi and F. Sirghi, (DEAR/SIDDHARTA Collaboration), http://www.lnf.infn.it/esperimenti/dear/DEAR_RPR.pdf
- [403] U.-G. Meißner, U. Raha and A. Rusetsky, *Eur. Phys. J. C* 35 (2004) 349
- [404] G. Beer et al. [DEAR Collaboration], *Phys. Rev. Lett.* 94 (2005) 212302
- [405] J. A. Oller, *Eur. Phys. J. A* 28 (2006) 63
- [406] B. Borasoy, U.-G. Meißner and R. Nissler, *Phys. Rev. C* 74 (2006) 055201
- [407] S. Steininger and U.-G. Meißner, *Phys. Lett. B* 391 (1997) 446
- [408] M. Bockhorst et al., *Z. Phys. C* 63 (1994) 37
- [409] N. Kaiser, T. Waas and W. Weise, *Nucl. Phys. A* 612 (1997) 297
- [410] A. Roessl, *Nucl. Phys. B* 555 (1999) 507

- [411] S. M. Ouellette, *hep-ph/0101055*
- [412] M. Frink, B. Kubis and U.-G. Meißner, *Eur. Phys. J. C* 25 (2002) 259
- [413] J. F. Donoghue and B. R. Holstein, *Fizika* 14 (2005) 217
- [414] B. Borasoy, B. R. Holstein, R. Lewis and P.-P. A. Ouimet, *Phys. Rev. D* 65 (2002) 114023